

**DEVELOPMENT OF SINGLE STEP PRESSURE REDUCTION SYSTEM
FOR NGVM**

***(PEMBANGUNAN SISTEM PENURUN TEKANAN SEPERINGKAT BAGI
NGVM)***

**ASSOC. PROF. Dr. RAHMAT MOHSIN
ZULKIFLI ABD MAJID
PROF. Dr. ZULKIFLI YAACOB
ASSOC. PROF. ZULKAFLI HASSAN
SHAMEED ASHRAF
ABU SAMAH NASIR
MOHD REDHUAN RAMLEE**

**RESEARCH VOT NO:
74169**

**GAS TECHNOLOGY CENTRE (GASTEG)
FAKULTI KEJURUTERAAN KIMIA DAN
KEJURUTERAAN SUMBER ASLI
UNIVERSITI TEKNOLOGI MALAYSIA**

ACKNOWLEDGEMENT

Sincere appreciation is dedicated to the Management of the Faculty of Chemical & Natural Resources Engineering (FKKKSA), UTM for their continual support and useful advice. The technical staffs of Gas and Petroleum Engineering department are also greatly acknowledged for their continuous efforts, technical supports that they have shown throughout.

Full accreditation is addressed to the Research Management Centre (RMC), UTM for their advices, support and kind services rendered, mainly to the Director, Prof. Dr. Arifin Samsuri and RMC's staff. The Ministry of Science Technology and Innovations (MOSTI) is highly acknowledged for providing financial support through the research Vot 74169.

Finally, the appreciation goes to researchers whom had directly and indirectly contribute to the success of this project.

ABSTRACT

The objective of this study is to design, fabricate and test a single step pressure regulation system for the natural gas motorcycle. The pressure regulator prototype design was based upon the fundamental principles of the pressure regulator. The aid of Computational Fluid Dynamic (CFD), pressure vessel code and threaded fastener standards were implied to design the pressure regulator prototype. The commercially available CFD code FLUENT™ was used to analyse and optimize the flow within the regulator. The structural design was based on the American Society of Mechanical Engineer (ASME) pressure vessel code. The Society of Automotive Engineers (SAE) and American Society of Testing and Materials (ASTM) served as reference for threaded fasteners selection. The material selection achieved for the prototype design consists of stainless steel 304, Teflon™ and 3 ply elastomer as the selected material of choice. The final CFD evaluation provided an optimum opening of 3 mm between the obturator and valve seat. The pressure regulator base has a wall thickness of 7.5 mm while the bonnet cap has 11.5 mm thickness. The loading element spring selected was a helical grounded type with 10 active coils and a wire diameter of 3 mm. The prototype designed was fabricated using Computer Numerical Configuration (CNC) machining as it is the best economically viable solution. The prototype performance was evaluated using the specially designed pressure regulator test bench equipped with data acquisition and high pressure gas supply system. Outlet gas flow rates were steadily controlled from 5 to 25 litres per minute and the outlet pressure was found to be steady at 4.5 bar. It is clearly proven that the developed pressure regulator is capable of providing the downstream components with natural gas at 4.5 bar up to 25 litres per minute. The single step pressure regulation developed, can be used on the Kriss Modenas 110cc or any small engines with similar fuel requirement.

ABSTRAK

Objektif utama kajian ini adalah untuk merekabentuk, meghasil dan menguji pengatur tekanan seperingkat untuk kegunaan motorsikal gas asli. Rekabentuk prototaip pengatur tekanan in adalah berasaskan prinsip asas pengatur tekanan. Dengan bantuan Dinamik Bendalir Berkomputer (CFD), kod baling bertekanan dan pendedap berbebenang, reka bentuk pengatur tekanan seperingkat dicapai. Kod perisian CFD FLUENT™ telah digunakan untuk menganalisa aliran gas di dalam pengatur tekanan seperingkat. Rekabentuk diasaskan kepada kod balang bertekanan Persatuan Jurutera Mekanikal Amerika (ASME) dan pendedap berbebenang berasaskan oleh Persatuan Jurutera Otomobil (SAE) dan Persatuan Pengujian Bahan Amerika (ASTM). Bahan asas yang dipilih untuk pengatur tekanan seperingkat terdiri dari keluli tanpa karat 304, Teflon™ dan elastomer 3-lapis. Keputusan simulasi Dinamik Bendalir Berkomputer memberikan pembukaan optima sebesar 3 mm pada bukaan injap. Dinding tapak pengatur tekanan mempunyai ketebalan 7.5 mm manakala ketebalan penutup adalah 11.5 mm. Elemen pembeban yang dipilih adalah dari jenis helikal dengan 10 lingkaran aktif dan mempunyai ketebalan rod wayar 3 mm. Pembuatan prototaip pengatur tekanan seperingkat dihasilkan dengan menggunakan mesin Konfigurasi Numerikal Berkomputer (CNC) yang dipilih berasaskan keberkesanannya. Prestasi prototaip diuji dengan menggunakan kemudahan pengujian pengatur tekanan yang direka khas serta dilengkapi dengan sistem pengumpulan data dan bekalan gas bertekanan tinggi. Aliran keluar gas dikawal dari 5 hingga 25 liter seminit dengan tekanan keluaran mantap setinggi 4.5 bar. Ini membuktikan keberkesanan rekabentuk prototaip untuk membekalkan gas pada 4.5 bar dengan kadar alir setinggi 25 liter seminit. Pengatur tekanan seperingkat yang terhasil ini boleh digunakan untuk injin Modenas Kriss 110cc atau sebarang injin kecil lain yang mempunyai keperluan yang sama.

TABLE OF CONTENTS

CHAPTER	TITLE	PAGE
	TITLE	i
	DECLARATION	ii
	ACKNOWLEDGEMENT	iii
	ABSTRACT	iv
	ABSTRAK	v
	TABLE OF CONTENT	vi
	LIST OF TABLES	xi
	LIST OF FIGURES	xii
	LIST OF APPENDICES	xv
1	1.0 INTRODUCTION	1
	1.1 Motivation of Study	2
	1.2 Research Problem Statement	3
	1.3 Research Objective	4
	1.4 Scope of Work	4
	1.5 Contribution of the Study	5
2	2.0 INTRODUCTION	
	2.1 Natural Gas Vehicles	6
	2.1.1 Development of Natural Gas Vehicles	7
	2.1.2 Advantages of Natural Gas Vehicles	8
	2.1.3 NGV Technology	11

2.2	Global Implementation of NGV	12
2.2.1	NGV in the United States of America	14
2.2.2	NGV in Canada	15
2.2.3	NGV in Latin America and Caribbean	15
2.2.4	NGV in Europe	16
2.2.5	NGV in India	17
2.3	Vehicle Manufacturers Resolution to NGV	18
2.4	Implementation of NGV in Malaysia	19
2.5	Natural Gas Vehicle Fuel System	20
2.6	Natural Gas Motorcycle	24
2.6.1	Natural Gas Motorcycle Performance And Emission Test	26
2.6.2	Natural Gas Motorcycle Lubrication Oil Test	27
2.7	Natural Gas Motorcycle Second Generation Fuel System	30

3 3.0 PRESSURE REGULATOR

3.1	Pressure Regulation System	33
3.1.1	Pressure Regulator Component	34
3.1.2	Pressure Regulator Body	36
3.1.3	Pressure Regulator Valve Trim	36
3.1.4	Pressure Regulator Actuator	38
3.2	Basic Operating Element of Pressure Regulator	40
3.2.1	Loading Mechanism	40
3.2.2	Sensing Element	40
3.2.3	Control Element	40
3.3	Operation of Pressure Regulator	41
3.4	Principle of Pressure Regulator Operation	43

3.4.1	Single Stage Design	44
3.4.2	Double Stage Design	44
3.5	Natural Gas Vehicle (NGV) Pressure Regulator	45
3.5.1	Typical NGV Regulator System	45
3.6	Pressure Regulator Type	46

4 DESIGN AND DEVELOPMENT

4.0	Introduction	49
4.1	Pressure Regulation System Bi-Fuel Study	51
4.1.1	Lesson Learned from the Bi- Fuel Engine Test Skid	51
4.2	Parameter Selection and Boundary Condition	53
4.3	Regulator Prototype Design	53
4.3.1	Regulator Restriction Design	54
4.3.2	Computational Fluid Dynamics Evaluation	57
4.3.3	Regulator Actuation Design	61
4.4	Compression Spring	62
4.4.1	Compression Spring Principles	64
4.5	Valve Body Wall Thickness	68
4.5.1	Minimal Wall Thickness of Shell Under Internal Pressure	69
4.5.2	Minimal Wall Thickness of Unstayed Flat Heads	70
4.5.3	Minimal Wall Thickness of Unstayed Covers	71
4.6	Regulator Loading Element Design	72
4.7	Regulator Body Design	75
4.7.1	Threaded Fastener	76
4.8	Regulator Material Selection	77

4.9	Regulator Prototype Fabrication	79
4.10	Regulator Prototype Testing	80
4.11	Regulator Prototype and Test Bench Testing	83
4.11.1	Pressure Regulator Test Bench Operation	84

5 REFINEMENT OF PRESSURE REGULATOR DESIGN

5.0	Introduction	86
5.1	AUTOCAD (v2004) Model Drawing	89
5.2	SOLIDWORKS (v 2005) Model Drawing	89
5.3	MSC PATRAN (v 2005r1)	91
5.3.1	Database Creation	91
5.3.2	Model Preferences Specification	92
5.3.3	Importing Geometry Model	93
5.3.3.1	Geometry Creation	94
5.4	Finite Element Model Creation	95
5.4.1	Loads and Boundary Condition Application	98
5.4.2	Material Property Models Creation	103
5.4.3	Elements Properties Creation	105
5.5	Running the Analysis	107
5.6	Retrieving the Analysis Result	108
5.6.1	Numerical Result Visualization	109
5.7	Analysis and Discussion	111

6 RESULTS AND DISCUSSIONS

6.0	Introduction	112
6.1	Regulator Restriction Results	113
6.2	Regulator Actuation Results	117

6.3	Regulator Body Results	119
6.4	Regulator Prototype End Product	120
6.5	Pressure Regulator Performance Results	121
6.6	Refinement of Previous Product	123
6.7	Two Dimensional Modeling	123
6.8	Solidified Modeling	125
6.9	MSC PASTRAN/NASTRAN Analysis	127
6.9.1	Simulation Data for Single Stage Regulator	128
6.9.2	Comparison on MSC/PASTRAN Simulation Results	132
6.10	Comparison on Material Selection	141
7	CONCLUSION	146
	REFERENCES	148
	APPENDIX	

LIST OF TABLES

TABLE NO.	TITLE	PAGE
2.1	Comparison of Natural Gas Characteristic	9
2.2	Combustion Related Properties of Gasoline & CNG	10
2.3	Natural Gas Vehicle Population Worldwide	12
2.4	Conversion Kit Component	21
2.5	Natural Gas Composition	26
2.6	Petrol Specification	27
2.7	Engine Oil Properties and Standard Testing Method	28
6.1	Simulation Data for Part A Using SS304	128
6.2	Simulation Data for Part A Using Aluminium Cast Alloy	128
6.3	Simulation Data for Part A Using Brass	129
6.4	Simulation Data for Part B Using SS304	129
6.5	Simulation Data for Part B Using Aluminium Cast Alloy	130
6.6	Simulation Data for Part B Using Brass	130
6.7	Yield Strength for Each Material	131
6.8	Material Design Stress	132
6.9	Optimise Thickness of Each Material Selection	132
6.10	Material Strength Preliminary Analysis for Part A	142
6.11	Material Strength Preliminary Analysis for Part B	143

6.12	Material Strength Preliminary Analysis for New Prototype	
	Model	144
6.13	Gross Material Cost of Regular New Prototype	145
7.1	Result Summary	147

LIST OF FIGURES

FIGURE NO.	TITLE	PAGE
2.1	Natural Gas Vehicle Bi-Fuel System Components and Layout	21
2.2	Schematic Diagram of Bi-Fuel Mechanism	23
2.3	Natural Gas Motorcycle First Generation Fuel System Schematic Diagram.	30
2.4	Natural Gas Motorcycle Second-Generation Fuel System Schematic Diagram	31
3.1	Components of Typical Spring Loaded Pressure Regulator	35
3.2	Schematic Diaphragm of Open Restricting Element	42
3.3	Schematic Diagram of Closed Restricting Element	43
3.4	Typical Stage Regulator	44
3.5	TN I SIC Regulator produced by Landirenzo	47
4.1	Methodology Flow Diagram of Study	50
4.2	Compress Natural Gas Fuel Line	55
4.3	Open and Close Position of the Restricting Element	57
4.4	The Meshed Geometry Used for CFD Simulation	58
4.5	3 Dimensional Fluid Flow Pattern Around the Restricting Element	58
4.6	2-Dimensional Fluid Flow Pattern Around the Restricting Element.	59
4.7	Obturator positioning simulated by CFD software	60
4.8	Mechanical Linkage Relating All Three Elements	62

4.9	Single Coil of a Helical Compression Spring	64
4.10	The twisting moment on the spring coils	65
4.11	Pictorial Description of Longitudinal and Circumferential Stress	70
4.12	Types of Unstayed Flat Heads and Covers	70
4.13	Schematic Drawing of the Pressure Regulator Test Bench	83
4.14	Pressure Regulator Test Bench	85
5.1	Methodology Process Flow	88
5.2	SOLIDWORK IGES File Save Format	90
5.3	Creating New Database	92
5.4	New Model Preferences Form	93
5.5	MSC.NASTRAN Import IGES File Format	94
5.6	Geometry Application Form	95
5.7	Finite Element Model Creation	97
5.8	Geometry Model after Meshing	99
5.9	Load/BCs Application Form for Displacement Force	100
5.10	LBC Select Application Region Subform for Displacement Force	101
5.11	Region of Displacement Force Application (Red Line)	101
5.12	Region of Pressure Force Application (Red Line)	102
5.13	Geometry Model after Displacement and Pressure Force Applied	102
5.14	Material Property Models Application Form	104
5.15	Element Properties Application Form	106
5.16	Analysis Application Form	107
5.17	Common Prompt Window	108
5.18	Access Result Application Form	109
5.19	Result Visualization	110
6.1	3-Dimensional Fluid Flow Pattern around the Restricting Element	114
6.2	2-Dimensional Fluid Flow Pattern around the	

	Restricting Element	114
6.3	Velocity Magnitude of Each Cross-Sectional Plane	115
6.4	Total Pressure Profile of One Cross-Sectional Plane	115
6.5	CFD Simulation Results Comparing Mass Flow Rate and Obturator Distance of Opening.	116
6.6	Final Loading Element Design	118
6.7	Pressure Regulator Body Dimensions	119
6.8	Bonnet Cap Dimensions	120
6.9	Fabricated Pressure Regulator Prototype	121
6.10	Performance Plot of the Pressure Regulator Prototype Evaluated Using the Pressure Regulator Test Bench	122
6.11	Two Dimensional Drawing of Part A and Part B	124
6.12	Evolution of Structural Design Modification via SOLIDWORK	126
6.13	Part A and Part B of New Design via SOLIDWORK	127
6.14	Stress Tensor Analysis Result for New Model of Part A Using SS304	133
6.15	Deformation Analysis Result for New Model of Part A Using SS304	133
6.16	Stress Tensor Analysis Result for New Model of Part A Using Brass	134
6.17	Deformation Analysis Result for New Model of Part A Using Brass	135
6.18	Stress Tensor Result for New Model of Part A Using Aluminium Cast Alloy	136
6.19	Deformation Analysis Result for New Model of Part A Using Aluminum Cast Alloy	136
6.20	Stress Tensor Result for New Model of Part B Using SS304	138
6.21	Deformation Analysis Result for New Model of Part B Using SS_304	138

6.22	Stress Tensor Result for New Model of Part B Using Brass	139
6.23	Displacement Result for New Model of Part B Using Brass	139
6.24	Stress Tensor Result for New Model of Part B Using Aluminum Cast Alloy	140
6.25	Deformation Analysis Result for New Model of Part B Using Aluminum Cast Alloy	140

CHAPTER 1

INTRODUCTION

Energy has proven to be the prerequisite and basis for life and mobility. We owe the wealth and prosperity of today's society to the use of fossil energies. Petroleum products derived from fossil fuel have physical and chemical properties that make them very desirable as transportation fuels. This combination of attractive properties and affordability has resulted in more than 95% of the world's transportation system being fuelled by petroleum products. With all the conventional oil we have discovered, and all we think awaits discovery, this source of virtually all of the world's transportation fuels will be forced to relinquish. This is estimated within perhaps 10 to 40 years as oil demand continues to grow while world crude oil production will begin an inevitable decline. The proportional depletion of supply has also caused the rise in oil price. Among all human activities, driving motor vehicles produces the most regulated air pollutants such as lead, hydrocarbons, oxides of nitrogen (NO_x), carbon monoxide, and particulate matter.

The increase in price and heavy pollution caused by the use of petrol and diesel conventional fuel indicates we can no longer rely exclusively on it. This supports the need for an alternative fuel source that would diversify the dependency on mainstream petroleum fuel and help mitigate the pollution problem. Compressed Natural Gas (CNG) is relatively well tested and is currently the cleanest and most widely used alternative fuel in the world. The number of natural gas vehicle (NGV) is currently about 4.6 million units worldwide as depicted in Table 2.3. Anyone who desires to effectively contribute to the saving of our resources and the reduction of

emissions should resort to the use of natural gas. Natural gas as a fuel helps to save oil resources and reduces emissions effectively.

1.1 Motivation of Study

Any vehicle operated by an internal combustion engine can be powered by natural gas. Vehicles may operate solely on natural gas (mono-fuel), operate on natural gas or other fuel as desired by user (bi-fuel) or operate on fuel mixture containing natural gas and another fuel (dual-fuel). This diversity has caused various vehicles, such as buses, trailers, forklifts, cars, tricycles, mopeds and even motorcycles to be converted to NGV. Gas Technology Centre (GASTEG) of Universiti Teknologi Malaysia is the pioneering local body to implement natural gas as motorcycle fuel since 1997. This prototype Natural Gas Motorcycle (NGM) uses a locally made Modenas Kriss 110cc.

The successful testing results of the first generation natural gas fuel system are comprehensively described in Chapter 2. As a whole, the first generation natural gas fuel system implied on this motorcycle begins at the Compressed Natural Gas (CNG) storage cylinder and ends at the fuel-metering device that prepares the air fuel mixture to be combusted by the engine. Between these two components lies the pressure regulator that moderates the storage pressure to meet the requirement of the fuel-metering device. Each component of the first generation natural gas fuel system suits the Modenas Kriss 110cc motorcycle. The Natural Gas Vehicle – Motorcycle (NGM) Research Group under GASTEG also carried out studies on an advance storage system which employs Adsorption Natural Gas (ANG) which provides two third of the gas volume storage capacity of CNG at one sixth of the current 3000 psi operating pressure. A dedicated mixer was designed and fabricated to provide the Kriss 110 a homogenous air-fuel mixture of 10:1 air fuel ratio.

The valuable experience and lesson learned from the development of the first generation system has lead to the development of the improved second-generation

natural gas fuel system for the same motorcycle. The second-generation fuel system further improves the carburetion fuel metering system by utilising an electronically controlled injection system that provides better air-fuel mixing which in return provides better fuel efficiency, power output and enhances fuel economy. This current study completes part of the second-generation fuel system development.

1.2 Research Problem Statement

The implementation of the injection system (fuel-metering device) on the second generation fuel system requires the pressure regulator to provide higher outlet pressure compared to the carburetion system. The first generation system had the storage cylinders charged with 1800 psi of pressure causing lighter loads on the regulator. The actual charging pressure from the compressed natural gas (CNG) refuelling station would provide 3000 psi of pressure that may cause severe loading on the first generation pressure regulator, which may lead to regulator failure. The first generation carburetion fuel system requires the pressure regulator to provide an output of 5 psi. The vast pressure reduction requires the first generation pressure regulation system to have two pressure regulators to reduce the pressure. The second-generation fuel system that uses injection system requires the regulator to provide higher output pressure. This higher pressure requirement has potentials to employ only one stage of pressure reduction. The previous regulator was readily available in the market and it is primarily design for common utility gas use. The natural gas regulator is governed by various standards that cover gaseous fuels use on automotive vehicles that needs to be addressed.

This generates the need to develop a dedicated pressure regulator that would suit the second-generation fuel system. The regulator understudy will be designed to comply with related standards and to work onboard the motorcycle where the space

is a major constraint. The outlet pressure and flow rate would be designed to meet the requirement of the engine.

1.3 Research Objective

The aim of this study is to design, fabricate and test a single step pressure regulation system prototype to provide constant pressure output at varying flow demands dedicated for natural gas motorcycle Modenas Kriss 110cc Natural Gas Motorcycle (NGM) second generation fuel system and to designed new prototype of NGVM and to gain the optimize thickness of this designed prototype of NGVM pressure regulator via the assistance of finite element analysis (FEA).

1.4 Scope of Work

The scopes of study are as follows:

- i. To establish basic understanding on the design criteria required for a NGV pressure regulator.
- ii. To formulate a pressure regulation mechanism that incorporates restricting, loading and measuring elements of the pressure regulator.
- iii. To utilize Computational Fluid Dynamic as design aid.
- iv. To develop a final operational prototype natural gas pressure regulator that would suite the operational conditions.
- v. To design and develop basic performance test bench for the NGM pressure regulator system equipped with data acquisition system.
- vi. Understand the basic concept and function of NGVM pressure regulator.
- vii. Develop of a 3D model of the existing prototype using AutoCAD and SolidWorks

- viii. Simulate the process model using finite element analysis (FEA) system known as NASTRAN / PATRAN.
- ix. Analyze the simulation results in terms of material selection, wall thickness and stress analysis of the regulator
- x. Optimize the pressure regulator in terms of spacing to be fitted into NGVM

1.5 Contribution of the Study

The successful design, fabrication and testing of the current work would provide a comprehensive method to produce a pressure regulator in general. The dedicated prototype pressure regulator would compliment the second-generation fuel system by providing appropriate gas flow and pressure from the storage tank to the fuel-metering device. The bi-fuel engine test skid provides an overall understanding of the natural gas fuel system for carburetion engines in general. The pressure regulator test bench would be a suitable facility to conduct basic pressure regulation testing for other pressure regulators in the future. The current work also provides an overall method on the development of the test bench. Calibration and data acquisition that includes flow, pressure and temperature monitoring is covered within this scope of study. Safety issues that relate high pressure and flammable gas handling concerning all designs are addressed accordingly.

CHAPTER 2

NATURAL GAS VEHICLE

2.0 Introduction

This section begins with the natural gas vehicle introduction that covers its benefits and the global implementation of it. The support of the vehicle manufacturers on natural gas vehicle is also discussed. This discussion is then lead to the implementation of natural gas vehicle (NGV) in Malaysia. Interest is then diverted to the NGV fuel system by the description of the entire fuel system. This discussion then cascades to the previous work on the natural gas motorcycle followed by the intended improved second generation fuel system. The pressure regulation system is elaborated in terms of its types. The regulator components and their functions are expressed in Chapter 3. As for the pressure regulator operation is illustrated in Chapter 3 graphically too. The final part of chapter reviews the natural gas vehicle pressure regulator.

2.1 Natural Gas Vehicle

The use of natural gas as a transportation fuel can offer emissions and environmental benefits, energy diversity and security. Relative to petrol, this fuel reduces the particulate matter of up to 10 microns in size (PM_{10}) significantly and the unburned hydrocarbons to substantial degrees. Compressed Natural Gas (CNG) generally costs less than petrol and many countries are making CNG economically favorable. The natural gas distribution infrastructure in many countries increases the availability of

natural gas. CNG vehicles emit reduced amount of carbon monoxide than petrol or methanol vehicles because CNG mixes better with air than do liquid fuels and requires less enrichment for engine start-up. Greater energy and heat efficiency can be obtained (11,000 kilocalories per cubic meter) due to the higher octane number (130) of natural gas that permits internal combustion engines to operate at higher compression ratios. The use of natural gas over petrol reduces carbon monoxide (CO) by 97%, unburned hydrocarbon (HC) by 72%, nitrogen dioxide (NO_x) by 39%, and carbon dioxide (CO₂) by 25% of the emission content. The absence of benzene or aromatic hydrocarbon in natural gas ensures minimal harmful emissions from natural gas-powered engines².

2.1.1 Development of Natural Gas Vehicles

The first natural gas engine was built in 1860, before the development of the gasoline engine. Compressed Natural Gas (CNG) has been used in vehicles since 1930's and the current worldwide NGV population is more than 4.5 million according to the International Association for Natural Gas Vehicle (IANGV) statistics and this figure is fast increasing everyday.

Natural gas vehicles have been used with much success in the United States since the 1960s and in Europe for nearly 50 years. Natural gas as a vehicle fuel has a long and established record in Europe, Canada, New Zealand, Australia, and in the U.S.A. In fact, there are currently more than 30,000 natural gas vehicles on U.S. roads and over 700,000 worldwide. The use of natural gas as vehicular fuel is growing more popular by the hour, as it is demonstrated by the fact that more than 60 countries have chosen this alternative fuel. In Malaysia, the number of registered vehicles is 12 million with 51% of them are using gasoline (Ministry of transport, Malaysia' 2002) and there are only 15,600 conventional NGV (July' 2005), which are mainly taxi.

There are two main reasons why countries chose to implement NGV projects, mainly due to ecology and economic factors. The advantages of NGV from these two different perspectives may initially be considered conflicting, but that in fact has an

intimate connection. Natural gas is chosen as a means of drastically reducing social health costs due to the reduction in polluting emissions, mainly particulates, benzene and ground level ozone. At the other hand NGV is chosen as an economic instrument, by taking advantage of its low cost in order to motorize expansion through cheap freights and increased savings for large sectors of society; at the same time exportable surplus of oil and fuels generate solid incomes to the nation (Diego Goldin and Santiago Manconi, 2004)

2.1.2 Advantages of Natural Gas Vehicles

Natural gas is the cleanest-burning fossil fuel available. Natural gas vehicles can achieve up to a 93 percent reduction in carbon monoxide emissions, 33 percent reduction in nitrogen oxides emissions and a 50 percent reduction in reactive hydrocarbons in comparison with gasoline vehicles as reported by Washington Gas NGV Holding (1999). Natural gas vehicles emit virtually no carcinogenic particulate matter. Therefore, it becomes a strong force in improving the nation's air quality.

NGVs operate so cleanly because the fuel is inherently clean. Natural gas is generally composed of at least 90 percent methane and may contain other hydrocarbons in small amounts including ethane, propane and butane. Table 2.1 showed the composition of Natural Gas characteristic by Gas Malaysia (2003). Because the methane is relatively pure component, the emissions of hydrocarbon, carbon monoxide and in some cases nitrogen dioxide can be significantly less from the NGV than from a gasoline or diesel vehicle. Per unit of energy, natural gas contains less carbon than any other fossil fuel, and thus lower carbon monoxide (CO₂) emissions per vehicles mile traveled. In addition, natural gas has an octane rating of 130, which means it has an efficiency advantage over gasoline (Rashidi, 2001)

Table 2.1: Composition of Natural Gas Characteristic

COMPONENT	MOL %
Methane, C ₁	92.73
Butane, C ₂	4.07
Propane, C ₃	0.77
Isobutane, iC ₄	0.08
n-butane, nC ₄	0.06
Other Hydrocarbon	0.01
Nitrogen, N ₂	0.45
Carbon Monoxide, CO ₂	1.83
Compressibility	0.9977
Specific Gravity	0.61
Density	0.7478 kg/m ³
Molecular Weight	17.4518
Gross Caloric Value	9530 Kcal/Sm ³
Burning Velocity (m/s)	0.3
Upper Flammability Limit	15.4
Lower Flammability Limit	4.5
Auto Ignition Temperature (°C)	640
Theoretical Air Requirement (m ³ /m ³)	9.74

(Source: <http://www.gasmalaysia.com>)

Compared to the base petrol engine, CO and HC reduction of between 40–50% and 35–50%, respectively, were achieved. Kalam et al. also presented the difference in performance and emissions for a modified spark ignited natural gas engine. It showed 15% power loss, 15–18% less BSFC and 10% higher efficiency revealed by CNG compared to gasoline. CO and HC emissions were reduced by 90 and 12%, respectively, and NO_x emissions were increased by 30% compared to gasoline engine.

Recently Hamid and Ahmad (2002) presented a comparison of the NGV and gasoline base engine performance where they found the volumetric efficiency of the

NGV engine is reduced by about 15% and overall performance lowered by circa 9% at maximum torque and maximum power conditions.

The substantial advantage that CNG has in anti knock quality is related to the higher auto ignition temperature and higher octane number compared to that of gasoline as shown in Table 2.2. Due to such antiknock properties, dedicated SI CNG engines could potentially be designed with compression ratio (CR) as high as 13:1 (Thomas J.F., Staunton R.H., 1999).

Table 2.2: Combustion Related Properties of Gasoline & CNG

Properties	Gasoline	CNG
Motor octane number	80 -90	120
Molar mass (kg/mol)	110	16.04
Carbon weight fraction (mass %)	87	75
(A/F) _x	14.6	16.79
Stoichiometric mixture density (kg/m ³)	1.38	1.24
Lower heating value (MJ/kg)	43.6	47.377
Lower heating value of stoic. mixture (MJ/kg)	2.83	2.72
Flammability limits (vol% in air)	1.3-7.1	5-15
Spontaneous ignition temperature (°C)	480-550	645

Note: (A/F)_x = Stoichiometric air fuel ratio

Natural gas has a high ignition temperature, about 1,200 ° F, compared with about 600 ° F for gasoline. It also has a narrow range of flammability that is, in concentrations in air below about 5% and above about 15%, natural gas will not burn. The high ignition temperature and limited flammability range make accidental ignition or combustion of natural gas unlikely. An American Gas Association study reported o injuries or fatalities after more than a half billion miles driven with natural gas vehicles.

In addition, natural gas vehicle also much safer compared to gasoline-powered vehicles. The fuel storage cylinders used in NGVs are much stronger than gasoline fuel

tanks. The design of NGV cylinders subjected to a number of federally required “severe abuse” tests such as heat and pressures extremes, gunfire, collisions and fires. NGV fuel systems are “sealed” which prevents any spills or evaporative losses. Even if a leak were, occur in an NGV fuel system, the natural gas would dissipate into the atmosphere instead of forming a spreading pool or vapor cloud on the ground, as other fuels do because it is lighter than air.

Natural gas is an economical fuel because the use of natural gas is no exception to that economic rule. In addition, because natural gas is an inherently clean fuel, it reduces engine wear. Therefore, use of natural gas as a vehicle fuel extends engine life as well as reduces engine maintenance. Finally, natural gas fuel use decreases the federal trade deficit. Currently, over 50 percent of the oil currently used comes from imports. Approximately 90 percent of the natural gas used produced in the United States. It has been projected that there is an ample supply of Natural Gas and that it will last approximately 150 years or more as reported by [A.J. Taormina](#) (2005).

2.1.3 NGV Technology

There are some recent important advances in NGV technology that will keep the industry on track with the most advanced technologies being produced by the major automotive manufacturers. NGVs now are compatible with computerized fuel injected engines. They are superior to carbureted vehicles because natural gas is injected directly into the combustion chamber in its gaseous state without having to go through a special gas/air mixer. This makes the changeover instantaneous from gasoline to natural gas and back again.

The newest systems are 'closed loop'; they are part of the systems that include oxygen sensors in the vehicle tailpipe, and provide feedback to the engine control systems to alter the fuel/air ratio depending upon the requirements of a vehicle's performance at any given time (Rashidi, 2005). Dedicated natural gas heavy-duty engines are based on diesel technology, but the engines include spark plugs since natural gas, unlike diesel fuel, does not combust under pressure. A great deal of development is under

way to improve the efficiencies of heavy-duty natural gas engines, and improvements are occurring rapidly.

Some heavy duty natural gas engines also have used a mixture of 80% natural gas to about 20% diesel as a 'pilot' fuel that causes ignition under the normal 'heat-of-compression' common in the diesel cycle engine. The dual fuel approach which is principally used as retrofit systems, have not seen widespread acceptability in countries where emissions standards are increasingly strict, but the vehicles do perform in such a mode.

2.2 Global Implementation of NGV

The successful implementation of alternative fuels throughout the world can be clearly seen from the natural gas vehicle population according to country as shown in the Table 2.3 below. In some countries, vehicles have been operated on natural gas for over twenty years without technical problems, as the technology is simple and mature. Even at this moment, the number of vehicle operating on natural gas is increasing. Apart from this, the following sub topics that follow describe some examples of the advances, policies and strategies taken by countries and regions across the planet.

Table 2.3: Natural Gas Vehicle Population Worldwide

Country	Vehicles*	Refuelling Stations	VRA**	Last Updated
Argentina	1,439,527	1,402	32	Apr 05
Brazil	1,018,163	1158		Oct 05
Pakistan	800,000	740		Jul 05
Italy	382,000	509		May 05
India	204,000	198		Apr 04
USA	130,000	1,340	3,331	Dec 04
China	97,200	355		Jan 05
Ukraine	67,000	147		May 05
Egypt	62,150	90		Sep 05
Colombia	60,000	90		May 05
Iran	48,029	72		Aug 05

Bangladesh	44,534	106	8	Nov 05
Venezuela	44,146	149		Apr 04
Russia	41,780	213	15	May 05
Bolivia	38,855	63		Sep 05
Armenia	38,100	60		Feb 05
Germany	27,200	558	779	Apr 05
Japan	25,000	289	686	Sep 05
Canada	20,505	222	3,258	Sep 03
Malaysia	14,900	39	1	May 05
Tajikistan	10,600	53		May 05
Ireland	9,780	10	6	Jul 04
France	7,400	105	209	Jan 05
Sweden	6,709	86		Nov 05
Indonesia	6,600	17		Jul 05
Korea	6,487	170		Feb 05
Thailand	5,500	34		Aug 05
Bielorussia	5,500	24		May 05
Chile	5,500	12		May 05
Moldova	4,500	8		May 05
Bulgaria	4,177	9		May 05
Trinidad & Tobago	4,000	13		Apr 05
Myanmar (Burma)	4,343	14		Nov 05
Mexico	3,037	6		Mar 04
Switzerland	1,346	56	89	Jul 05
Australia	895	12	55	Aug 01
Great Britain	875	34	40	Jul 03
Spain	797	28	21	Jan 05
Poland	771	28	18	Apr 05
United Kingdom	543	31	115	Nov 04
Austria	500	68	58	May 05
New Zealand	471	12		Jun 04
Turkey	400	5		Aug 04
Czech Republic	390	16	6	May 05
Netherlands	348	8	394	Jun 04
Latvia	310	4	5	Oct 04
Belgium	300	5	60	Aug 04
Slovakia	250	7		Sep 04
Portugal	242	5		Jan 05
Hungary	202	13		Feb 05
Norway	147	4		Apr 05
Algeria	125	3		Oct 04
Croatia	100	1		May 05
Serbia	92	2		Dec 04
Finland	84	3	4	Mar 05
Yugoslavia	81	1		Jul 03

Nigeria	60	2		May 05
Iceland	45	1		May 05
Cuba	45	1		Feb 01
Greece	40			May 03
U.A.E	35			Dec 05
Macedonia	32	1		Jan 05
Luxembourg	32	3		Jul 04
Liechtenstein	26	1		Sep 04
South Africa	22	1	4	Jan 00
Uruguay	20			Dec 01
Philippines	12	1		Jul 04
Singapore	7	1		May 05
Denmark	5	1	3	Feb 00
Taiwan	4	1		Apr 05
North Korea	4	1		Aug 00
Bosnia	1		1	Apr 05
TOTALS	4,696,881	8,722	9,198	

* Includes both OEM and converted NGVs

** VRA = Number of Vehicle Refueling Appliances

Source: www.langv.org

2.2.1 NGV in the United States of America

The Department of commerce (DOC) has issued mandatory guidelines in February 27, 2003, to all the department bureaus requiring that all light-duty petroleum fuelled vehicles due for replacement be replaced with alternative fuel vehicles as this would ensure compliance with Environmental Protection Act and Executive Order 13149. The department of transportation in the final report on “Fuel options for reducing green house gas emission from motor vehicles” in year 2003 has highlighted the prospect of alternative fuels within the near-term time horizon. One of these alternative fuels is the compressed natural gas (CNG), which can be used in both bi-fuel (vehicles that can operate on either petrol or CNG) and dedicated vehicles (which operate only on CNG). The exhaust emission reduction by replacing 25% of petrol with CNG would amount to 5-6% when emissions during both vehicle use and fuel production are accounted.

The Alternative Fuel News published by the department of energy of the U.S., pointed out that the Natural gas buses emit 40 to 86 % less particulate matter and 38 to 58

% less nitrogen oxide than diesel buses. According to “bus features”, natural gas is “virtually toxic-free, while diesel exhaust contains more than 40 toxic constituents, about half of which are known or suspected carcinogens.” There are approximately 2,675 alternative fuel school buses operated by nearly 130 school districts across the country. Majority is located in California, with large number also in Texas, Oklahoma, Indiana, and Pennsylvania. Several standards and rating systems for green vehicles have been developed. The Clean Car Campaign, for example, defines a green vehicle as one that is 1.5 times more fuel efficient than the average in its class. This clean car should comply with the California's super-ultra-low-emission vehicle (SULEV) tailpipe emissions standards and must be manufactured using non-toxic, recyclable materials.

2.2.2 NGV in Canada

The Ontario's green energy strategy carried out by the Ontario Government under the Ministry of Energy, Science and Technology has highlighted the goals of maximizing energy conservation and the generating capacity for green energy in Ontario. It also plans to create viable conservation and green energy industry in Ontario to provide consumers with access to affordable conservation measures and green power options. Reduction in emission is also a prime target similar to the Kyoto target of a 6% reduction in greenhouse gases by 2012. Another program that curbs the emission is the Anti Smog Action Plan target of 45% reduction in nitrogen oxides (NOx) and volatile organic compound (VOCs) by 2015.

2.2.3 NGV in Latin America and Caribbean

Latin America and The Caribbean (LAC) is among the most urban of the world's developing country regions. Indeed, three of the world's largest cities are found in this region: Mexico City, Rio de Janeiro, and Sao Paulo. In these cities, motor vehicles account for virtually all of the carbon monoxide emissions, anywhere from 50 to 90 % of hydrocarbons, at least three-quarters of nitrogen oxides, and as much as 40 % of

suspended particulate matter. The impact on human health of these pollutants is substantial, especially when they exceed recommended maximum limits. A recent study by World Resources Institute has found that the level of total suspended particulate is a major contributor to lung problems in Mexico City, Rio de Janeiro and Sao Paulo. In addition, both Mexico City and Rio de Janeiro violate World Health Organization (WHO) air concentration guidelines for sulphur dioxide and nitrogen oxides. Apart from being the major source of local air pollution in cities, motor vehicles are also the most rapidly growing source of greenhouse gas emissions in the region, including carbon dioxide, chlorofluorocarbons, nitrous oxide, and carbon monoxide. The use of natural gas as a vehicular fuel in Latin America was introduced in Argentina in 1984. With decades of experience in the industrial and domestic use of natural gas, Argentine companies soon developed the new market. Chile has an ongoing NGV program, looking for an answer to the very serious air pollution in Santiago. Bolivia, Colombia, Venezuela, Mexico have also introduced NGVs. Integration will bring many benefits, but mainly, it will allow NGV users to move around the area with a clean and inexpensive domestic fuel.

2.2.4 NGV in Europe

The Commission of European Committees sees three main potential alternative fuels namely biofuels, natural gas and hydrogen to have high volume potential that could each be developed up to the level of 5% or more of the total automotive fuel market by 2020. In Italy, 400,800 vehicles run on natural gas provided through a network of 463 refueling points. In addition, 50,000 more vehicles throughout Europe operate on natural gas. These vehicles normally operate in a limited geographical area and refuel at one or a few dedicated points. Natural gas has great potential in principle as a motor fuel. It is a cheap alternative fuel, has a high octane number, is clean and has no problem in meeting existing and future emission standards. It offers potential for a 20-25% lower CO₂-emission than the energy equivalent amount of petrol, although no significant CO₂ advantage over the more efficient diesel engine. When used in buses, natural gas offers a

most welcome noise reduction in cities. Increased use of natural gas would move the dependency away from the oil market, normally is seen as an advantage.

2.2.5 NGV in India

The significant implications of vehicle emissions have led to control regulations in conjunction with environment-friendly technologies to reduce vehicle pollution. The emission norms are being aligned with Euro Standards and vehicular technology is being upgraded accordingly. Vehicle manufactures are also working towards bridging the gap between Euro Standards and Indian Emission Norms. Due to the directions from Supreme Court of India, New Delhi was the first city in India to introduce CNG as a fuel for all public transports such as buses, taxis and three wheelers. This effort is going to be implemented in Mumbai followed by Chennai, Baroda, Surat and Kolkata. The demand for the natural gas engine is tremendous and taking the example of Mumbai market alone, each bus manufactures can sell on the average 700 to 800 buses per annum for the next 10 years there. India's leading commercial vehicle manufacturers and gas distribution agency are working with Canadian firms in acquiring conversion technology including developing natural gas engines and the latest dispensing infrastructure to suit the Indian conditions. A study conducted by Bose from the Tata Energy Research Institute of India to predict the automotive energy use and emission control for Indian metropolis shows the increase in the use of alternative fuels based on business as usual prediction by year 2010. The following assumptions related to alternative fuels were made based on business as usual assumption on the model generated:

- a) The share of 4-stroke engines in Delhi, Calcutta and Mumbai would increase from 11%–12% to 50%, while that in Bangalore would increase from 20% to 25% with a view to phase out 2-stroke technologies.
- b) It is predicted that 15% of auto rickshaws (tricycle) would run on propane and 10% would run on electricity (battery operated vehicles).

- c) The share of cars fitted with three-way catalytic converters using unleaded petrol, battery operated electric cars, and cars that use compressed natural gas (CNG) cars would increase whereas, the share of old model petrol and diesel cars would decrease.
- d) The share of CNG-powered taxis would increase whereas, that of diesel-powered ones would decrease, and all taxis using petrol would be fitted with three-way catalytic converters.
- e) The share of CNG-powered and battery operated buses would increase.
- f) Sulphur content in petrol and diesel would be reduced to 0.05% and 0.25%, respectively.

2.3 Vehicle Manufacturers Resolution to NGV

Strong reasons for car manufacturers to embark on alternative fuel strategy is that it truly mitigates environmental matters such as reduced emission, the technology is commercially available, it has hand in hand market and technology development and it is well accepted by customers. In conjunction with this, many vehicle manufacturers have added models that are readily available to operate on CNG to existing range of models. The introduction of the “316G Compact” model in December 1995 by BMW became Europe’s first car maker to add an Original Equipment Manufacturer (OEM) produced natural-gas powered passenger car to its model program. Volvo Car Corporation has the S80, V70 and S60 models available in the bi-fuel NGV form and has sold 3500 units in year 2002¹⁶. These models are made right from the beginning on the assembly line causing no after market adaptation.

The potential of a NGV as Environmentally Enhanced Vehicle (EEV) is proven by The Honda Research & Development Department with there Honda Civic GX¹⁷. This model can meet the Super-Ultra-Low-Emission Vehicle (SULEV) emission standard in California and also meet the future European & Japanese emission standards. Car maker,

DaimlerChrysler now configures many of its vans and ever-popular minivans for natural gas flex fuelling. The Dodge Ram Van and Ram Wagon are designed to use dedicated CNG-powered 5.2 liter V8 engines that produces 200 horsepower. Ford's half-ton pickups F-150 are produced with CNG-dedicated, CNG bi-fuel and even LPG bi-fuel power. These are only a fraction of the car makers that included alternative fuel models in their product line, as they are many other car makers doing the same.

2.4 Implementation of NGV in Malaysia

The implementation of NGV in Malaysia is strongly supported by the Department of Environment (DOE) whom has been encouraging the use of natural gas as alternative fuel for motor vehicles, especially by the public service vehicles in urban areas where piped natural gas is available and where air quality is deteriorating mainly due to motor vehicle exhaust emission. Other factors that directly contribute to the implication of NGV in Malaysia are the infrastructure of the Peninsular Gas Utilization (PGU) networks that supplies natural gas throughout Peninsular Malaysia. The government has introduced various incentives to boost the number of vehicles by relieving tax on the conversion kit. The bi-fuel (able to operate on both petrol or gas separately) and dual fuel (operates with a mixture of natural gas and other fuel) vehicles operating with natural gas are given 25% road tax reduction, while mono-fuel vehicles that operate solely on natural gas are given 50% road tax reduction.

Existing pipeline systems ensures full coverage and steady supply of natural gas in most industrial countries especially Malaysia. Natural Gas which composed mainly of methane is odorized to have a pungent smell using odorizing agent (mercaptans) to ease detection of its presence. Natural Gas processed by the PETRONAS Gas Processing Plant (GPP) in Kerteh is sent via the Natural Gas Distribution System (NGDS) to the conventional NGV refueling stations. The gas is then compressed to 3600psi via three stage compressors to increase the packing density. It is then stored in a cascading storage

bank system before being transferred to the vehicles storage cylinders. The storage pressures in these cylinders are at 3000psi, giving a pressure gradient of 600psi between the dispenser and the cylinder for speedy refueling.

The Compressed Natural Gas (CNG) is discharged in two types of stations; one being the mother stations while the other is called the daughter station. The mother station has the natural gas supplied via pipeline and it has a three-stage compressor to convert the natural gas into CNG. The CNG is then stored in the cascading bulk storage system prior to being sold to the NGV owners. The portable CNG cascading bulk storage system is charged in the mother station and freighted to the daughter station. This enables the daughter station to operate without the supply of natural gas via pipeline and compressor.

2.5 Natural Gas Vehicle Fuel System

There are two types of Natural Gas Vehicle. The first type is specifically designed to operate on natural gas while the other is a petrol-powered vehicle fitted with a conversion kit enabling petrol or gas operation with the ease of a switch. Malaysia has 14,900 NGV as up to May 2005 consisted mostly of the second type. A typical petrol powered vehicle is fitted with a conversion kit to enable the bi-fuel operation that provides the user with fuel options of either petrol or natural gas with the ease of a switch. NGV in Malaysia mostly consists of bi-fuel taxis having a 1500cc carburetion petrol engine. The bi-fuel NGV conversion kit used on the 1500cc carburettor petrol engines consists of a fuel selector switch, a spark advancer, air fuel mixer, pressure regulator, CNG solenoid valve, petrol solenoid valve and a storage cylinder.

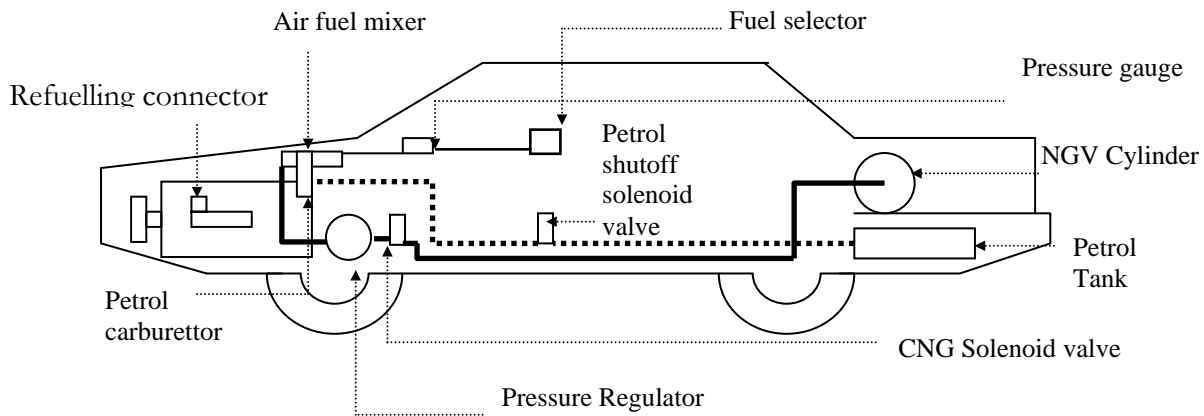


Figure 2.1: Natural Gas Vehicle Bi-Fuel System Components and Layout²⁰

Figure 2.1 shows the position of the various NGV components where the storage cylinder is placed in the rear trunk while the other components are in the front engine compartment. A detailed schematic diagram of the bi-fuel system is shown in Figure 2.2. On the other hand, Table 2.4 shows the description of conversion kit components that can be found in the NGV fuel system. The fuel pressure regulator, mounted on the fuel rail, is used to maintain a constant pressure drive from the fuel rail to the intake manifold. In the case of CNG, the pressure regulator regulates the CNG from the storage cylinder according to the engine requirement and sends it to the mixer. In the carburetion fuel system, this natural gas then enters the air-fuel mixer where it forms a combustible mixture with air²³.

Table 2.4: Conversion Kit Components

COMPONENTS	DESCRIPTIONS
The cylinder	The cylinder used to store CNG at a working pressure of 200bars. It is fitted with a shut-off valve and a safety burst disc.
The Vapor Bag	Fitted onto the cylinder, the Vapor Bag used to enclose the cylinder valve and the pipes connecting it and vented out of the car.
The High Pressure Solenoid	Allows gas to flow through only when the engine is running and the switch is in the gas position.
The High Pressure Pipe	This high pressure pipe connects the refueling valve to the CNG cylinder and pressure regulator
The Refueling Valve	The refueling valve is used to refuel the CNG Cylinder
The Pressure Regulator	The Pressure Regulator has a Solenoid Valve to shut-off gas supply to the engine. The CNG stored at a high pressure in the cylinder reduced to just below atmospheric pressure by this unit. This negative pressure is also a safety feature that will not allow gas to pass through when the engine is not running.
The Gas Air –Mixer	The air/fuel mixer constantly maintained at a stoichiometric ratio and continually adapts the rate flow of gas to engine by means of the linear electromechanical actuator to ensure optimum carburetion in terms of driving, consumption and emission.
The Petrol Solenoid Valve	The Petrol Solenoid Valve is used to cut off petrol supply to the engine when it is run on CNG.
The Selector Switch	The Selector switch is fitted at the dashboard enabling the driver to choose either the CNG mode or the petrol mode of operation. The electronics built into this unit also ensures safety by switching off the gas solenoid whenever the engine is switched off.

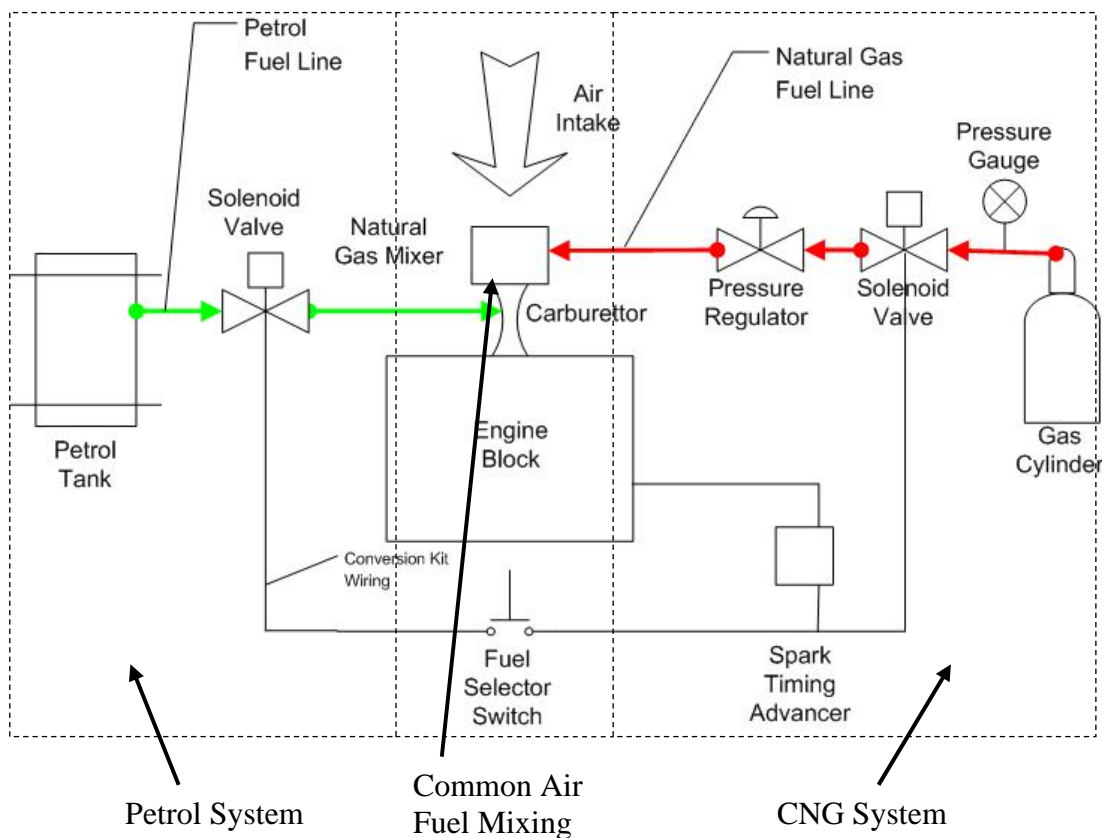


Figure 2.2: Schematic Diagram of Bi-Fuel Mechanism

During normal petrol operation, the petrol solenoid valve is left open while the CNG solenoid is held shut. This restricts the natural gas from entering the common carburetion system as shown in Figure 2.2. When the fuel selector switch is turned to natural gas, the petrol solenoid valve blocks the flow of the petrol to the carburettor while the current is supplied to the NGV solenoid valve that in turn permits natural gas to flow into the pressure regulator. The natural gas supplied to the engine is proportional to the vacuum pressure generated by the air flow through the mixer. The air fuel mixer's fuel passage is normally closed and opens at the actuation of a vacuum signal from the engine cranking or running. This again is a desirable safety feature because if the engine stops or is turned off, the fuel flow automatically stops.

When the mixer receives the desired vacuum signal from the engine, it draws a metered amount of natural gas from the pressure regulator and blends it with air at the proper ratio to achieve peak engine performance over the complete operating range. This vacuum signal generated by the mixer geometry acts on the third stage diaphragm of the pressure regulator to ensure suitable supply of natural gas according to the engine speed. The high pressure fuel line between the storage tank and high pressure regulator is fitted with a quarter turn valve which serves as an emergency shut-off. The high pressure regulator is equipped with a solenoid valve that permits gas flow only when the ignition of the vehicle is turned on. The spark advancer is activated during natural gas operation to alter the spark angle.

The only major difference between a gasoline vehicle and an NGV system is the fuel system. When natural gas powers the engines, it leaves the storage cylinders, passes through a master manual shut-off valve, travels through stainless steel lines, and goes to the engine compartment through a high-pressure pipe, which is also connected to the refueling system.

2.6 Natural Gas Motorcycle

A prototype model of the natural gas motorcycle was designed and developed by the Natural Gas Motorcycle (NGM) Research Group under Gas Technology Center (GASTEG) of UTM back in 1997. The Modenas Kriss 110cc was selected, as it was the most widely used motorcycle that is made locally. The four stroke natural gas prototype motorcycle was prepared for testing with a new set of conversion kit that includes a mixer, a regulator, a storage tank, related control elements and measuring apparatus. The CNG storage cylinder and pressure regulator were purchased to meet the operating condition of the new fuel system, while a dedicated air fuel mixer was designed and fabricated to provide air fuel mixture within the natural gas flammability limit. After the preparation stage of developing the prototype NGVM Modenas KRISS 110cc

motorcycle, the vehicle was evaluated by several tests to attain the engine's performance, exhaust emission and the lubrication oil quality in order to conduct a comparison between the natural gas and petrol operations.

The power output of the engine and exhaust emission data was successfully recorded using the CycleDyn Pro SF 250 chassis dynamometer and Horiba MEXA 324J emission analyzer at the Modenas assembly plant in Gurun, Kedah. Physical and chemical testing on the lubrication oil was conducted in the Laboratory Service Unit (UNIPEM) of Universiti Teknologi Malaysia. UNIPEM is an accredited laboratory under SAMM (Sijil Akreditasi Makmal Malaysia) (ISO/IEC G25) scheme Exhaust emission test was conducted at constant speed using the standard procedure from ISO 3929. The physical and chemical testing of the lubrication oil were based on ASTM standards as outlined in the following section. The results of both tests together with the methods that were taken to conduct these tests are described in depth in the following sections. In general, the NGM offers great advantages over petrol operation in terms of emission where the carbon monoxide (CO) is reduced by 99.7% while the unburned hydrocarbon (HC) emitted is reduced by 79.3% compared to petrol operation. The degradation of the engine oil after operating for a distance of 2500 km, favors the natural gas over petrol. However, power is reduced by 15% at high engine speeds due to the gaseous medium of the natural gas displacing the amount of air induced.

The power loss disadvantage of natural gas operation (that may be altered by modifications) is compensated with advantages in emission and lubrication oil quality as both tests favors natural gas operation. Various modifications could be made to improve the natural gas operation. This includes the ignition spark advancement to compensate the slow flame speed of natural gas combustion. The compression ratio could be increased to suite the natural gas combustion. The air fuel mixture could be modified between lean and rich to suite the engine power requirement. The injection system is also a simple way to enhance performance of the natural gas fuel system.

2.6.1 Natural Gas Motorcycle Performance and Emission Test

The performance test was previously conducted to obtain the maximum engine power output and the vehicle velocity. The results obtained at wide-open throttle with manufacturer ignition timing setting showed that the natural gas operation had 10 to 15 % power loss at high engine RPM compared to the petrol operation. The top speed of 105 km/hr achieved during petrol operation decreases to 92 km/hr during natural gas operation. The engine operating at maximum speed was supplied with 24 liters/ min of natural gas supplied at 5 psi. This performance depletion is caused by the gaseous phase of the fuel which displaces the amount of air induced at high engine velocity. This is not experienced during the petrol operation as the petrol is in liquid form. Other contributing factor towards the performance drop of the natural gas operation is slower flame speed compared to petrol. The octane rating of natural gas is 130 whereas the petrol has 92-98 RON rating. This requires the natural gas to operate at a compression ratio of 16:1 while the engine under study has a compression ratio of 9.3:1. The specification of PETRONAS Primax PX2 petrol and the natural gas used for the testing are given in the Tables 2.5 and 2.6 as provided by PETRONAS.

Table 2.5: Natural Gas Composition

Component	Mol%
C ₆₊	0.07
C ₃	0.90
iC ₄	0.29
nC ₄	0.13
iC ₅	0.07
N ₂	0.68
C ₁	93.07
CO ₂	1.10
C ₂	3.70
Density	0.7404 kg/sm ³
Relative Density	0.6042
Molecular Weight	17.4663
Gross Calorie Value	39.20 MJ/sm ³

Table 2.6: Petrol Specification

Description	Value
Density @ 15°C, kg/l	0.733
Research Octane Number (RON)	97.0
Lead Content, kPa	0.008
Reid Vapour Pressure, % wt	62
Total Sulphur	Trace
Distillation	
50% evaporated, °C	105
90% evaporated, °C	152
Colour	Yellow

The exhaust emission for both petrol and natural gas were analysed at idle and average speeds of 40 to 90km/hr. This emission analysis is in accordance with the ISO 3929 test procedure. The motorcycle evaluated on a chassis dynamometer at various constant speeds: idle, 40 to 90km/hr, respectively using the Horiba MEXA 324J infrared emission analyzer. The carbon monoxide (CO) emission analysis at idle speed shows that the natural gas powered motorcycle releases an average of 0.02% volume compared to 3.99% volume for petrol operations giving 99.7% reductions over petrol operation this is due to the complete combustion of natural gas with air. The amount of unburned hydrocarbon (HC) emitted by natural gas motorcycle detected was 79.3% lower than petrol powered motorcycle, which is equivalent to 48.875 ppm volume at idle speed.

2.6.2 Natural Gas Motorcycle Lubrication Oil Test

Locally produced engine oil, PETRONAS Sprinta 4XT, was used for the test. After running at a constant speed of 4265rpm for a distance of 2500km using natural gas and petrol, respectively, the engine oil was tested for its physical and chemical properties using ASTM Standards as shown in Table 2.4. The stable engine oil temperature after certain duration of operation at 4265rpm was attained at 85.5°C for petrol while natural gas operation was at 57.8°C. These operation temperatures are known to influence the deterioration and the quality of the engine oil. The cooler temperature during natural gas

operation is due to the lower calorific value of the air fuel mixture. Table 2.7 represents the quality of engine oil after running 2500km on both fuels.

The sulphated ash content test result provides the chemical characteristic changes to the physic of the engine oil. The test is important because an increase in ash content of used oil usually indicates combustion chamber deposits and top ring wear problem or a build-up of contaminants. Build-up contaminants are commonly contributed by dust, dirt, wear debris and possibly other contaminations such as lead salts, which are derived from the combustion of the leaded petrol in internal combustion engines. This study showed that the ash content in the lubricant oil operated with natural gas increases only by 2.06% while petrol caused an increment of 6.89% compared to the unused lubricant oil.

Table 2.7: Engine Oil Properties and Standard Testing Method

Test	Standard		
Sulphated	ASTM 874 -92		
Carbon Residue content (MCRT method)	ASTM D 4530 – 30		
Kinematic Viscosity	ASTM D 455- 94		
Colour (ASTM Colour Scale)	ASTM D 1500 -91		
Flash Point (Cleveland Open Cup)	ASTM D 92 – 90		
Pour Point	ASTM D 97 – 93		
Density, Specific Gravity, API Gravity	ASTM D 1298 – 85		
Properties	Engine Oil Samples		
	Unused	Used With Natural Gas	Used With Petrol
Ash Content (wt%)	1.45	1.48	1.55
Carbon Residue (wt%)	1.09	1.19	1.30
Cloud point (°C)	-5.88	-5.83	-6.21
Colour ASTM	L4	D8	D8
Density	893.8	893.8	894.8
Specific Gravity	0.8943	0.8943	0.8953
API gravity	26.83	26.83	26.66
Flash Point	248	258	246
Water content	0	0	0
Kinematic Viscosity (40°C), cSt	151.3	129.2	122.1
Kinematic Viscosity (100°C), cSt	16.57	14.79	14.31

The carbon residue of lubricating oil is the amount of deposit left after evaporation and pyrolysis of the oil under prescribed conditions. In an internal combustion engine, carbon is deposited on the cylinder head and piston crown. This carbon is from the incomplete combustion of the fuel as well as the carbonizing of the engine oil carried over by the piston rings into the combustion chamber. The increase of carbon contamination in the lubricant oil will decrease the viscosity of the oil. The carbon residue is increased by 8.4% for the natural gas operation while the petrol operation caused an increase of 19.3% compared to the unused engine oil.

Since both density and specific gravity change with temperature, determinations are made at a controlled temperature and then corrected to a standard temperature by using special tables. However for the used lubricant oil, a decrease in specific gravity (increase in API gravity) may indicate that the fuel is diluted, whereas an increase in specific gravity might indicate the presence of contaminants such as fuel soot or oxidized materials. The API gravity value based on the ASTM D1298-85(90) for the oil used with natural gas shows no changes compared to the unused oil, whereas the oil operated with petrol shows a decrease of 0.6%.

The viscosity of any fluid changes with temperature where the decrease in temperature will increase the viscosity and vice versa. Two temperatures most often used for reporting viscosity are 40°C and 100°C. Plotting these points on special viscosity temperature chart developed by ASTM would provide linear correlation between these points. The kinematic viscosity conducted at 40°C for the natural gas operated engine oil decreased by 14.6% while the petrol operated engine oil decreased by 19.3%. Similar patterns are observed in the kinematic viscosity test conducted at 100°C. The ability of the engine oil to lubricate the engine component depletes proportionally to the degradation of its kinematic viscosity. The success of the NGM is clear at this point. The fuel system implied on board the NGM is described to provide the reader with an overall picture to enhance understanding.

2.7 Natural Gas Motorcycle Second Generation Fuel System

The successful testing elaborated in Section 2.7 uses the standard Modenas Kriss 110cc carburetion system fitted with a natural gas and air mixer as shown in Figure 2.3. The air fuel mixer was supplied with 5psi of natural gas that was regulated from a storage supply of 1800psi by two regulators. This first mixer was then again modified with the aid of computational fluid dynamics to obtain better mixing. After all the optimisation done on the carburetion system the only way to further improve the air fuel mixing system is to introduce the fuel injection system. There are generally two types of fuel metering devices employed on internal combustion engines being the carburetion system or a fuel injection system.

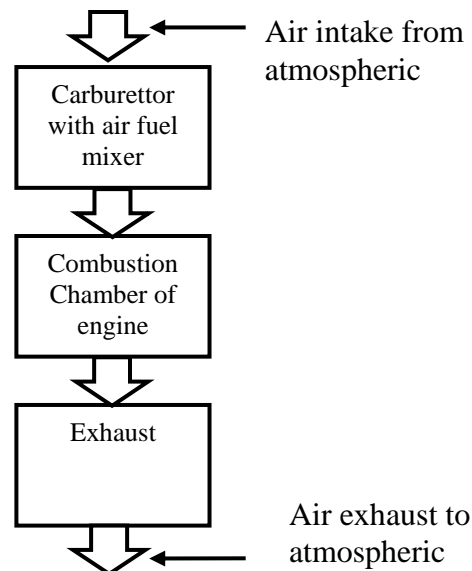


Figure 2.3: Natural Gas Motorcycle First Generation Fuel System Schematic Diagram.

The fuel metering device for the carburetion system is called an air fuel mixer. This device is pneumatically operated where the air entering the carburettor generates strong static pressure vacuum based on the venturi effect. This pressure vacuum acts on the final stage of the pressure regulator to draw more natural gas to mix with the increasing amount of air entering the carburettor.

The injection system on the other hand is electronically controlled to provide precise control of fuel metering which was not possible with the carburetion system. This proper control of air fuel metering is known to provide better power output, better emission quality and fuel economy. The fuel injection system as depicted in Figure 2.4 uses various sensors such as the oxygen sensor in the exhaust line, the engine rpm, ambient and air temperature. This information is sent to the electronic control unit (ECU), which does the necessary calculations to actuate the injector to provide the precise amount of fuel to optimise the combustion process. This in return optimises fuel efficiency, exhaust emission, fuel consumption and various other added benefits. The air fuel must be within the flammable limit of natural gas which lies between 5 to 15 % of natural gas. The non combustible mixture prepared out of this narrow range would be effect the environment as methane is a strong green house gas. This injection type fuel-metering device is being developed under the name of second-generation fuel system for the NGM.

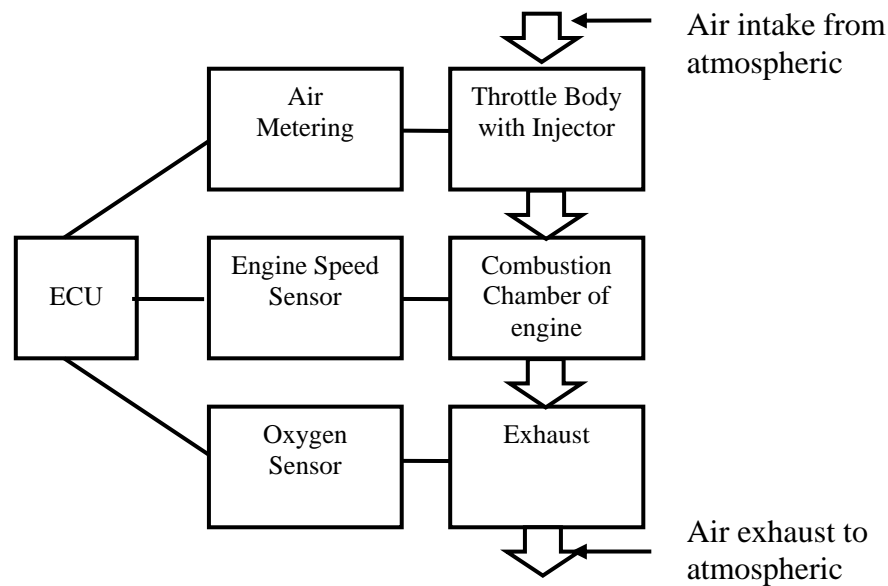


Figure 2.4: Natural Gas Motorcycle Second-Generation Fuel System
Schematic Diagram.

The supply of natural gas to the fuel-metering device regardless of types requires attention as it depicts the density and energy of the gas supply. This is a crucial criterion on the fuel metering devices performance. The key component that links the storage and the fuel-metering device is the pressure regulator. The previous pressure regulator used with the first generation fuel system provided 5 psi of pressure to the air fuel mixer attached to the carburettor. This pressure would not be sufficient for the second-generation fuel system, as the injector requires operating on a choke condition that requires greater supply pressure from the pressure regulator.

CHAPTER 3

PRESSURE REGULATOR

3.1 Pressure Regulation System

Fluids are generally divided into liquid and gas, where the compressibility of gas significantly improves the packing density compared to liquid. For this reason, gas is generally stored and distributed in the compressed form. A pressure regulator is required to reduce the pressure of the compressed state of the gas to a lower desired pressure regardless of the demand posed on the line. This clearly indicates that a regulator is required to reduce and maintain downstream pressure regardless of upstream conditions. A number of examples of pressure regulator encountered in our life are elaborated in the paragraphs below. Open source systems such as gas transmission pipelines transport natural gas from one place to another, usually over long distances. Control valves, pilot-operated regulators, and relief valves are used to control the pressure and flow of gas through these pipelines. Fuel gas regulators are used to control the gas pressure to a burner. Accurate pressure control is a vital factor that affects the efficiency of the burner. The regulator must maintain the pressure within a specified range regardless of flow to ensure perfect combustion of the fuel. The ideal mixing pattern of air and fuel will give the desired energy output from the burner.

Although the duty of the regulator in every application is deemed similar, the regulator requirements relatively differ. Regulators used for LPG gas regulation has certain standard that it should meet as the gas is flammable. The regulator truly is the heart of any LPG installation system. It must compensate for variations in tank pressure

from as low as 8 psi to 220 psi and still has an ability to deliver a steady flow of LPG at 11" w.c. to the consuming appliances.

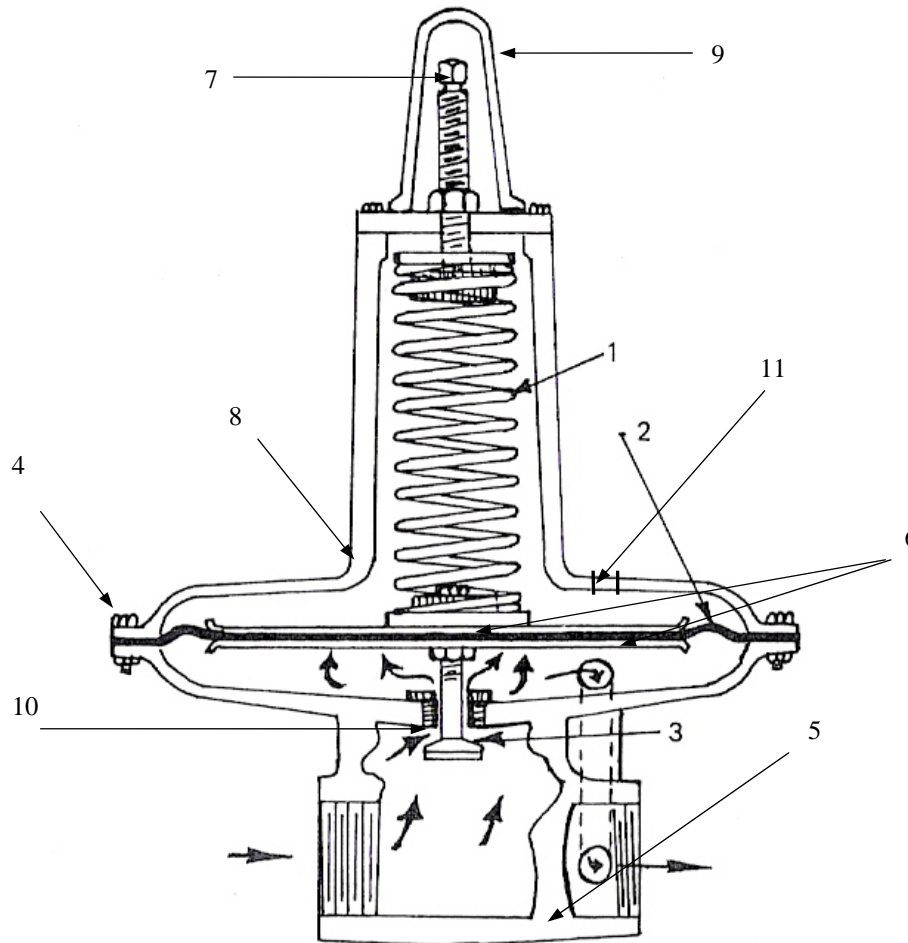
Regulators used with oxygen lines also have designated standards that cover its appropriate application. The application determines the design and shape of the regulator whereas the flow rate and pressure variation depicts the size. High flow rate pressure regulators used in the natural gas city gates are very large in size while the regulators used with the domestic LPG tanks are relatively small in size. The components within this device that are designed and arranged to perform its precise task will be elaborated within this chapter.

3.1.1 Pressure Regulator Components

Pressure regulators are produced in many sizes and configurations, but all are bounded to three basic components namely the regulator body, the regulator trim and the actuator. These components can be further described in terms of elements that are the restricting, loading and measuring. The regulator trim is the restricting element, while the actuator is a combination of the loading and measuring element. Each part of the pressure regulator components is described in greater depth in the following sections. Figure 3.1 describes the position of these components. It clearly shows that the spring that is the loading element is seated against the diaphragm. This loading element exerts force against the measuring element that is the diaphragm.

The spring permits the gas to enter the regulator compartment while the diaphragm restricts the entrance of gas. Both these loading and measuring element controls the restricting element. The restricting element consists of the valve seat and valve pad or obturator. Other supporting elements are added to aid this mechanism. This includes the support disc that supports the diaphragm, set point screw that varies the spring force, vent that enables the movement of air from the compartment above the diaphragm. The cap secures the set point screw from unwanted adjustments, while the

regulator bonnet cover combined with the pressure regulator body houses all the components that form a pressure regulator.



No	Component Name	No	Component Name
1	Spring	2	Diaphragm
3	Obturator	4	Threaded Fastener
5	Regulator	6	Support Disk
7	Set Point Screw	8	Bonnet Cover
9	Cap	10	Valve Seat
11	Breather Vent		

Figure 3.1: Components of Typical Spring Loaded Pressure Regulator

3.1.2 Pressure Regulator Body

The regulator body in this context refers to the structure that houses the valve trim and actuator. It provides support to all the other components and ensures that the fluid flow is leak tight. Regulator bodies are frequently designed with a bonnet or top closure piece to ease maintenance and assembly. The bonnet of the valve body serves as a guide to the spring that actuates the valve movement. Careful packing and adjustment is required particularly when the valve is fitted with a spring and diaphragm actuator. This is to ensure the clearances between the relevant components are properly set. The bonnet or upper part of the valve body generally contains the means for mounting the spring which pairs with the diaphragm to actuate the valve.

Sealing gasket maintains pressure tightness. The types and selection of sealing gasket largely depend on the conditions of service. Suitable threaded fasteners are used to ensure the bonnet is fastened on the body against various internal forces. The external geometry of the pressure regulator body requires various design considerations that having prime focus on the regulator body minimum wall thickness and the required threaded fasteners to hold the bonnet cover in position.

3.1.3 Pressure Regulator Valve Trim

Valve trim refers to those internal parts controlling the flow and in physical contact with the line fluid, comprises of plugs or disc, seat(s), bushes, guides, cages and stem. The valve trim of the actuator control portion generally includes an obturator and seat. The movement of the plug or disc relative to the seat regulates the amount of fluid passing, which may be linear or rotary, depending on the type of valve being considered.

There are five basic designs of valves, which are distinguished by the operation motion of their closure device (obturator) and the direction of flow in the seating area.

- 1) Gate Valve: A valve where the closure device moves in a straight line and, in the seating area, across (at right angles to) the direction of flow. This sliding method causes the closure member to slide across the valve seat face to open or close the valve.
- 2) Globe valve: A valve in which the closure device moves in a straight line and, in the seating area, longitudinally (parallel) to the direction of flow. This closing method causes the closure member to move away from or towards the valve seat to open or close the valve. Closure is achieved by abutment against the seat face or by projection into the seat orifice.
- 3) Plug and Ball valves: Valves that has the closure device which rotates about an axis at right angles to the direction of flow and, in the open position the flow passes through it.
- 4) Butterfly valve: A valve wherein the closure device rotates about an axis at right angles to the direction of flow and, in the open position, the flow passes around it.
- 5) Diaphragm (pinch) valve: A valve in which the closure device is provided by the deformation of a flexible diaphragm or tube. This implies the flexing method where the opening and closing is achieved by flexure of a resilient membrane within the valve body.

Many types of valves have been used as control valves, with varying degrees of success, but for many years the most commonly used and supplied type was the globe style. The most suitable restricting method to be employed in the regulating valve design would be the globe valve type³⁶. This valve is designed to regulate or stop the flow of fluid and can be applied in all positions between fully open and fully closed. The globe type valve has high flow resistance that frequently creates turbulence, resulting in a significant pressure drop.

3.1.4 Pressure Regulator Actuator

An actuator provides the force necessary to move the plug or disc and maintain it in the desired position against the fluid line forces. Pneumatically operated control valve actuators are the most popular type in use, but electric, hydraulic, and manual actuators can also be used. The spring and diaphragm pneumatic actuator is commonly specified because of its dependability and its simplicity of design. The net output thrust is the difference between the diaphragm force and the opposing spring force. Molded diaphragms are used to provide linear performance and increase the traveling distance. The size of diaphragm actuator dependence on the output thrust required and the availability of pressure supplied. They are simple, dependable and economical to use. Electric and electro-hydraulic actuators are considered as more complex and relatively expensive than pneumatic actuators. The pneumatic system requires pressured air supply to actuate the pressure regulator accordingly to maintain the downstream pressure. The diaphragm spring type offers advantage over the pneumatic system where no air supply is available, where low ambient temperatures could freeze condensed water, in pneumatic supply lines, or where unusually large stem forces are needed.

The study will focus on the diaphragm and spring combination as the actuating system due to its advantages over other methods. It also suits the condition under study best. The designs of the most popular actuator styles for pressure regulators are diaphragm and spring. The diaphragm actuator is pressure operated which is done by tapping the downstream pressure that is sensed by the diaphragm. The diaphragm then retracts the actuator stem or vice versa to ensure the downstream pressure is at the set point level.

The diaphragm under development would also play the role of a gasket that is placed between the regulator body and its bonnet cover. For this reason the material that is selected must be of a suitable type to serve as a gasket as well as a diaphragm. One of the most widely used materials for such condition would be the three ply fabric inserted elastomer. This diaphragm's prime duty is to convert the pressure of the fluid in terms of

movement that would be balanced by the spring to actuate the obturator. Circular shapes are preferred to ensure proper force distribution of the fluid onto the diaphragm. This proper force distribution ensures the stability and workability of the components within the regulator.

The need of a loading element is to provide force to the restricting element to open and to provide resistance to the closure by the measuring element according to the set point pressure. This indeed proves that the loading element should be of an elastic type of design. The spring is the best candidate for the job. Springs are often considered to be one of the most important yet most difficult items to design. In many cases the spring is considered the most troublesome part of a machine or mechanism. This applies great responsibility on the product manufacturer and the spring manufacturer to produce a reliable system that ensures proper workability. Both parties would benefit if the designer devotes a little more time on investigating the wide variety of materials and the simplified design procedures available.

Comprehensive evaluation on the design requirement during the preliminary design stage would help minimizing trouble, reduce breakage and extend fatigue life. The springiness of metals is related in a general way to their hardness. Lead, for example, is a soft, with virtually no 'spring' properties, and extreme hardness. On the other hand, results in lack of spring properties, as the material is brittle rather than 'elastic'. The range of suitable spring materials should combine suitable hardness with elasticity. Springs come in various forms that in general can be categorized into three groups, compression, extension and torsion. The compression type is the most widely used type as it has several benefits (discussed later) over the other types.

3.2 Basic Operating Element of Pressure Regulator

There are three basic operating element of pressure regulator, which is:

- i. Loading Mechanism
- ii. Sensing Element
- iii. Control Element

3.2.1 Loading Mechanism

Loading mechanism is used to determine the setting of the regulator delivery pressure. Spring normally used as the loading mechanism. When the regulator hand knob is turned, the spring is compressed. Force that is placed on the spring is communicated to the sensing element and the control element to achieve the outlet pressure.

3.2.2 Sensing Element

Sensing element senses the force placed on the spring to set the delivery pressure. Most regulators used a diaphragm as the sensing element. The diaphragm may be constructed of elastomers or metal. The sensing element communicates this change in force to the control element.

3.2.3 Control Element

In this control element, valve normally used to accomplish the reduction of inlet pressure to the outlet pressure. When the regulator hand knob is turned, the spring (loading mechanism) is compressed. The spring displaces the diaphragm (sensing element). Diaphragm then pushes on the control element, causing it to move away from the gas pressure regulator's seat. The orifice becomes larger in order to provide the flow and pressure required.

3.3 Operation of Pressure Regulator

This section elaborates the operation of the pressure regulator that incorporates three elements within its structure. The combined motion of the entire mechanism is described with the aids of a simplified example shown in Figure 2.6 below. The restricting element determines the amount of gas being transferred from the upstream-pressurized compartment to the downstream-regulated compartment. A spring rests on the diaphragm, while vent holes allow atmospheric pressure to reach the atmospheric side of the pressure reducing stage. The loading element encourages the restricting element to permit gas from the upstream to flow to the downstream. The measuring element moves against the loading element to restrict the gas flow to reduce the downstream pressure. When the downstream pressure is lower or equivalent to the set-point pressure, the spring is fully extended, the diaphragm is in a relaxed position while the valve seat is fully open as shown in Figure 3.2.

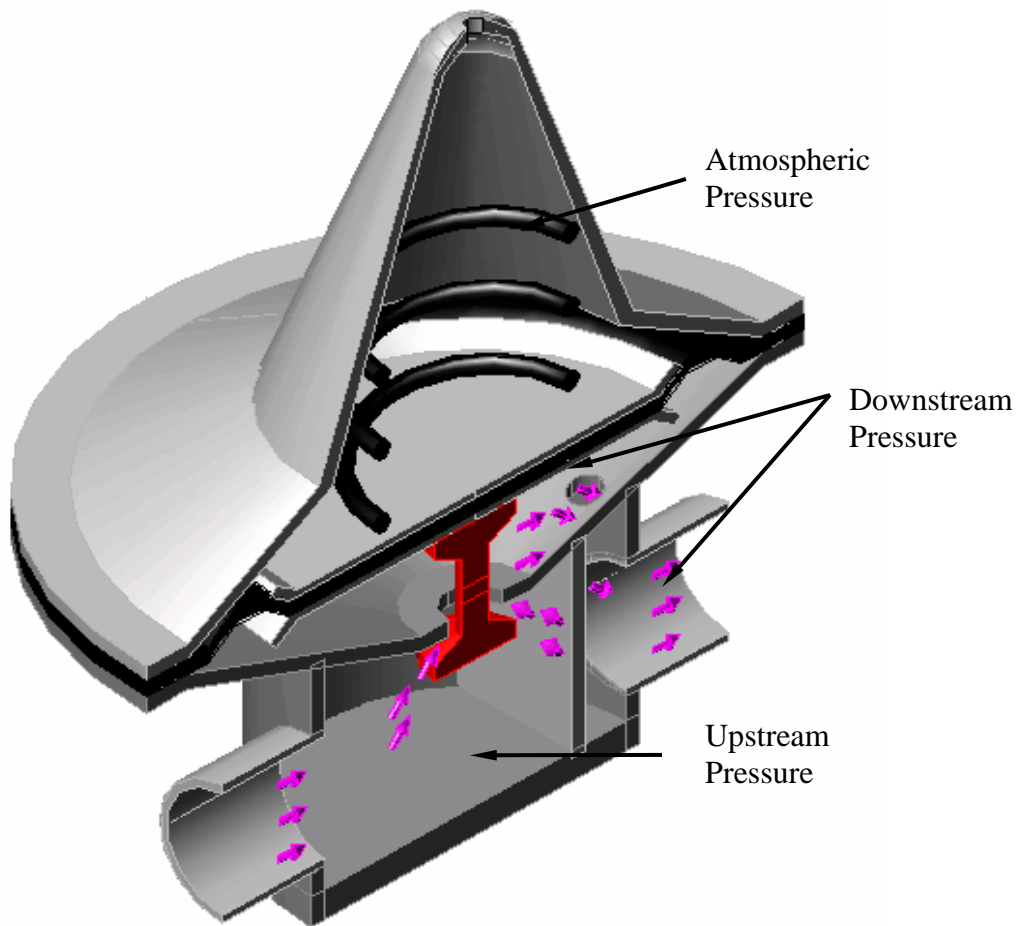


Figure 3.2: Schematic Diaphragm of Open Restricting Element.

When downstream demand reduces, the pressure build-up causes the regulator to react to reduce and maintain the downstream pressure. This downstream pressure build-up acts on the diaphragm causing the diaphragm to push against the spring force. This will cause the restricting element to prevent upstream pressure from being transferred downstream as shown in Figure 3.3. This inevitably reduces the flow to the downstream and maintains the downstream pressure close to set point pressure. Once the downstream pressure is lower than the set point value, the loading element would open up again and permit gas to flow downstream. This set-point pressure is the relation between the forces of the fluid pressure translated to force that is measured and countered by both loading and measuring element.

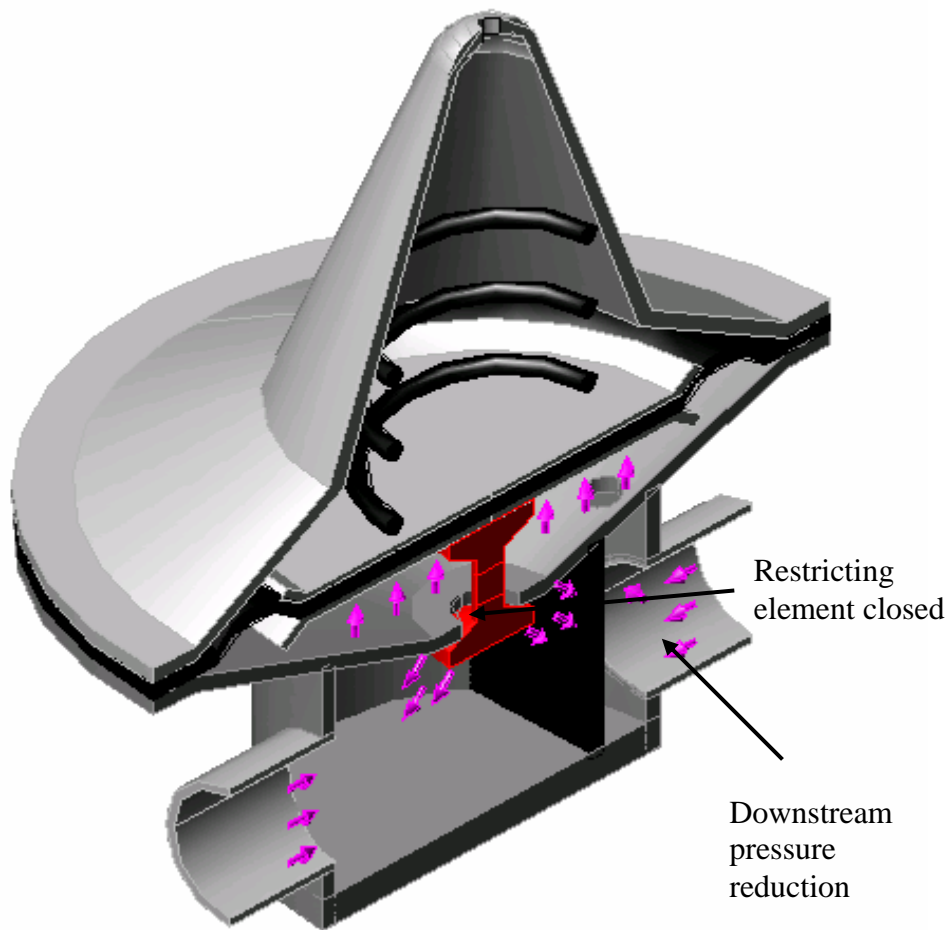


Figure 3.3: Schematic Diagram of Closed Restricting Element

3.4 Principle of Pressure Regulator Operation

Compressed gases are generally not useable until a pressure regulator is incorporated to reduce the gas pressure to a workable level that can be safely utilized in equipment and instruments. The basic design and construction material differ according to the type and pressure of gas as well as the type of application. There are two basic configurations in pressure regulator:

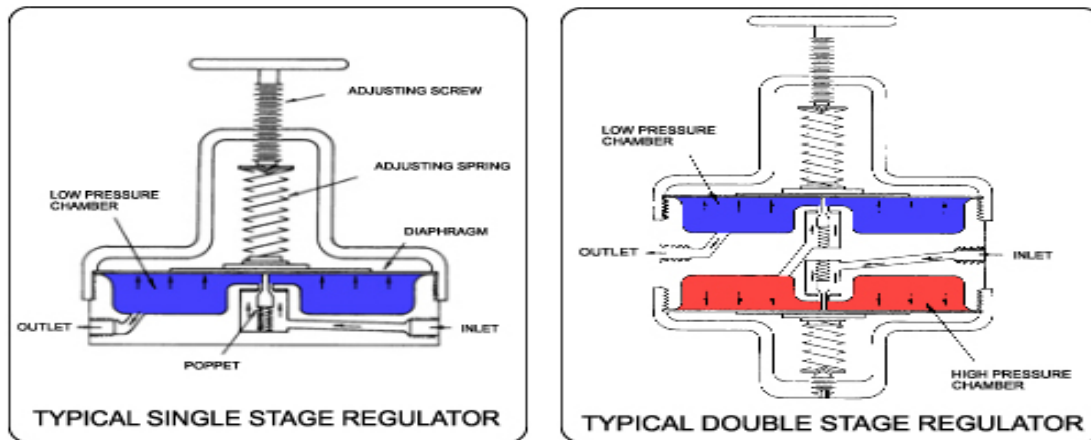


Figure 3.4: Typical Stage Regulator

3.4.1 Single Stage Design

Single stage pressure regulators reduce the cylinder gas pressure to the delivery pressure in a single step. This one step pressure reduction results in a slight change in delivery gas pressure as the cylinder pressure decays. In most cases, the delivery pressure will rise. The single stage regulator is a satisfactory and cost effective selection if slight variations in delivery pressure and/or periodic adjustments are not detrimental to the application. In the case of liquefied gases, the cylinder pressure is constant and single stage regulators are recommended.

3.4.2 Double Stage Design

Double stage pressure regulators reduce the cylinder gas pressure to a working level in two steps. A double stage regulator functions similar to two single-stage regulators in series. The cylinder gas pressure is reduced by the first stage to a preset, intermediate level, which becomes the gas pressure at the second stage inlet. This allows the second stage to fine-tune the final delivery pressure. Thus, double stage regulators provide a constant delivery pressure unaffected by cylinder pressure decay.

3.5 Natural Gas Vehicle (NGV) Pressure Regulator

The pressure regulator is a pneumatic or electro-pneumatic device designed to reduce the cylinder pressure close to atmospheric level and to supply fuel on engine demand. The function of a pressure regulator is to regulate the storage pressure to suit the fuel metering device regardless of the flow rate. This is achieved by the regulation of the line fluid quantity through the restricting valve. Tight closure may be obtained but this should be a secondary consideration in the choice of equipment. Without accurate pressure regulation it is difficult, and costly, to obtain low emissions and good performance benefits from NGV. All CNG vehicles operating as mono-fuel, dual-fuel or bi-fuel uses similar type of pressure regulator. Early developments resulted in the spring and diaphragm pneumatic actuator which, on attachment to the valve, made remote operation possible. Among all types of regulator, the direct acting type is the most widely used with the NGV fuel system.

The self-acting regulator or reducing valve is generally acknowledged to be the forerunner of the modern control valve. The regulator design changes according to the manufacturer but they utilize three basic elements, namely the restricting element, loading, and measuring. The restricting element is a variable orifice, controlled directly or through a lever action by the measuring element. Typically the variable orifice is a combination of a fixed orifice and a moveable seat disc. The fixed disk is made from a soft material like rubber to insure tight sealing when fully closed. The loading element can either be a weight, spring or a pressurized area that acts to counter the force exerted by downstream pressure on the underside of the measuring element. The measuring element is usually a diaphragm made of a gas tight flexible material, which senses downstream pressure and moves up or down to open or close the restricting element.

Sensing from the line fluid and utilizing the pressure energy available, the valve controls the flow to give a regulated condition downstream. The valve controls flow by absorbing pressure from the line fluid, the quantity passing being a function of the pressure drop across the valve. Movement of the valve plug in relation to the seat

provides an orifice of variable area that is utilized to regulate the flow from minimum to maximum. The pressure regulator inlet is equipped with an electrical operated solenoid valve. This solenoid permits the high pressure gas to flow into the regulator only when required by the engine. Due to the pressure drop that occurs in the regulator, the natural gas may cool to temperature below to water freezing point. This may hinder the operation of the regulator as icing of the water condensate in the natural gas may form. The NGV regulators are provided with engine radiator water circulation to ensure the gas leaving the regulator is at constant temperature. The fluctuation of gas temperature may affect the density of the gas which would interrupt the operation of the fuel metering device.

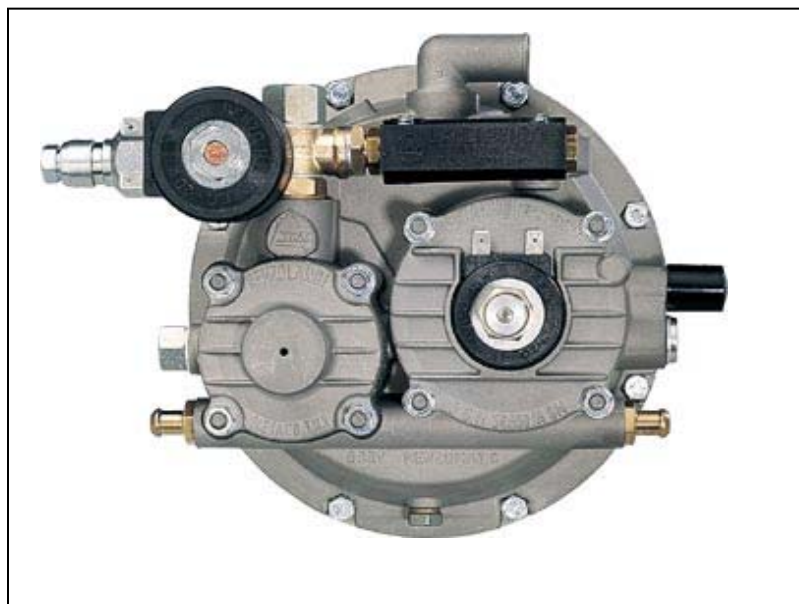
The ISO 15500 covers all the components related to the NGV fuel line. Part 9 of the ISO 15500 cover the NGV pressure regulator requirements. The local Malaysian standard MS 1096 covers the installation of the NGV fuel system on board vehicles. Market research indicates the design criteria for an NGV pressure regulator requires the following considerations as highlighted by Heenan below.

- a) Many mounting options
- b) Small, neat architecture
- c) Low cost
- d) “Instant On” high pressure solenoid (HPS)
- e) Automotive durability
- f) Easy filter change
- g) High flow
- h) Integral fuel pressure sender (FPS)
- i) Light weight
- j) Good transient response
- k) Controlled heat exchange
- l) Low P_{out} error

Among these considerations the flow performance, heat exchange control and outlet pressure error are the prime governing factors that effect the performance of the regulator. The next chapter elaborates on the methodology of this study.

3.5.1 Typical NGV Regulator System

The electronic control device to reduce the natural gas pressure will allow a regular flow of gas every time the engine requires it. It is equipped with three natural gas reduction stages that allow stability at both high and low pressures and a high pressure solenoid valve upstream from the first stage. The absorption of heat, taken from parts of the regulator heated with the liquid of the engine cooling circuit, prevents the natural gas freezing during the fall in pressure phase. The flow of gas necessary for engine idling has a positive pressure from the second stage and is activated by means of a gas pipe separated from the main flow. It includes an electronic starting device with a built-in safety system that trips and shuts off the gas solenoid valves if the engine is switched off or even stalls. Figure 3.5 shows the figure of TN I SIC Regulator produced by Landireenzo.



(Source: http://www.landi.it/eng/prodotti/scheda_prod_met536116000.html)

Figure 3.5: TN I SIC Regulator produced by Landireenzo

3.6 Pressure Regulator Types

Pressure Regulators also known as Pressure Control Valves or Pressure Reducing Valves are used to control pressure in a system and do not require an external power source to activate them. These regulators are installed where it is required to reduce from one level of pressure to another, while providing the required fluid flow to satisfy a downstream demand, irrespective of fluctuations in the inlet pressure or flow demand. The valve is automatic in operation. Self- operating valves can be designed with a single seat, which usually indicates the ability to close tight under “no flow” or “dead end” conditions, or they can be of double seat construction, which improves the maximum flow rate and accuracy of pressure control, but incurs the penalty of the loss of ability to control pressure at zero or very low flow rates. Self-operated pressure reducing valve falls into two main categories, direct acting and pilot operated.

In the case of direct acting valve, the controlled pressure acts directly through a diaphragm, piston or bellow against an imposing force from a compressed helical spring, weight or weighted lever, or from compressed air (accumulator). The construction is simple and robust and based on the axiom that the simpler a control system the better it is (as long as it is functional). Such a valve can provide long life, with maintenance free operation, even under adverse working conditions. Although the pressure control provided by the direct acting valves is not as accurate as with pilot operated valves, they are less costly and have many applications for which the fine control offered by the pilot would be unnecessary. Because of the complexity of design, pilot operated valves require regular maintenance and clean working conditions.

CHAPTER 4

DESIGN AND DEVELOPMENT

4.0 Introduction

The sole dependency on conventional fuel for vehicles and its polluting emission has caused the growth of alternative fuel vehicles. Natural gas is the most widely used alternative fuel as described vividly in Chapter 2. The commercially available fuel system described in Chapter 2 serves as a basis for the new fuel system design. The natural gas motorcycle's successful implementation of the alternative fuel is elaborated in previous chapter. This has been the prime driving force of this current study which is the second generation fuel system for the natural gas motorcycle. This second generation fuel system is compared with the first generation fuel system to identify its strength. Due to the variation of the second generation fuel system, new components are required to be developed. This point is described in as the problem statement which then moves on the research objectives in Section 1.3. This methodology chapter is derived from the scope of work given in Section 1.4. The flow diagram in Figure 4.1 provides the frame work for the entire study and the following sections describes them in detail.

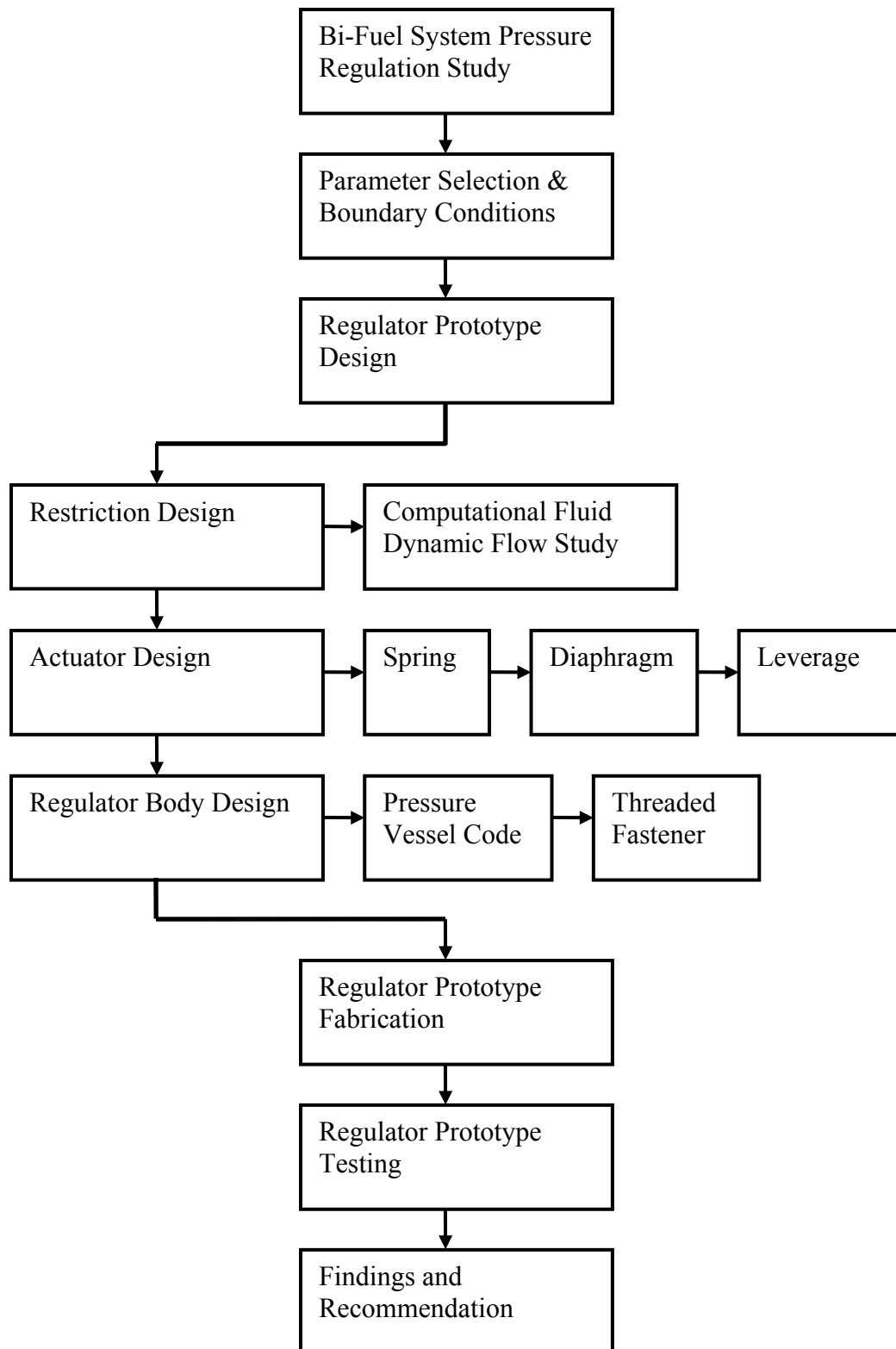


Figure 4.1: Methodology Flow Diagram of Study

4.1 Bi-Fuel System Pressure Regulation Study

A bi-fuel engine test skid as discussed in Section 2.1.4 is designed and fabricated to form strong theoretical and practical understanding on its functionality and operation. A Proton Magma 1.5 litre 12 Valve carburettor engine is fitted with an NGV conversion kit to form the bi-fuel engine test skid. This kit consists of a fuel selector switch, a spark advancer, air fuel mixer, pressure regulator, CNG solenoid valve, petrol solenoid valve and a storage cylinder. The working of this system has been described in depth in Section 2.1.4. All three mounting points are made adjustable in both horizontal and vertical direction to aid the alignment of the engine. The test skid has closure panels to safe guard the operator from moving component hazard. The skid is also fitted with wheels to ease the maneuvering of the skid. The skid metal structure is coated with epoxy (powder coating) to avoid corrosion caused by extreme working conditions in terms of heat and corrosive fluids. The installations of the NGV fuel system was based on the MS 1096 and NFPA 52 to ensure safe operation. Drawing of this test skid is shown in Appendix A, the engine wiring diagram in Appendix B and the bi-fuel wiring diagram in Appendix C. The display and control panel has various control devices such as the throttle control, ignition key, emergency shut-off, pressure and temperature display.

4.1.1 Lesson Learned from the Bi-Fuel Engine Test Skid

1. Safety in terms of wiring is seen extremely crucial in a natural gas fuel system compared to conventional liquid fuel. Liquid fuel is visible where as gaseous fuel can not be seen. For this reason, all wirings are done in suitable manner to avoid the occurrence of spark that may ignite the gaseous fuel.
2. Issue that relates with high pressure fitting must be properly addressed to avoid leak. All fittings must be ensured to meet the operating pressure and have sufficient safety margin in case of over pressure. In the case of over

pressure, the pressurized system must be equipped with pressure relief device.

3. Flammable material handlings are addressed in accordance to the National Fire Protection Agency code NFPA52 and MS 1096 that covers natural gas vehicle.
4. Suitability of wiring system is studied as the natural gas fuel system requires electric current to power its solenoid valve and its spark advancer. Similar conditions must be made available else where to enable the natural gas system to work.
5. Solenoid valve to cut-off the natural gas supply to the regulator is mandatory and must be made available in the current study.
6. Heating for regulator using circulating radiator water is seen in this test skid. This is due to the cooling effect that occurs during the expansion of the compressed natural gas within the regulator. Heating is provided to avoid any formation of ice within the regulator that may hinder its operation. The temperature homogeneity of the gas regulator is crucial as it would affect the air fuel mixer's performance.
7. The varying natural gas supply to the engine based on engine RPM is achieved by having vacuum actuation to the final stage for the pressure regulator. This vacuum signal varies the amount of natural gas (flow rate) leaving the pressure regulator.
8. The requirements of pressure, temperature and flow metering points are seen crucial in order to monitor and study the natural gas fuel system.

9. It is seen that the outlet pressure and temperature would determine the density of the gas supply to the fuel metering device. If the fuel metering device is based on volumetric measurement, then the fuel metering would fluctuate according to conditions.
10. The flow measurement basis if possible should be done on mass flow and not volumetric to avoid any variation in flow monitoring.

4.2 Parameter Selection and Boundary Conditions

Through all the materials covered until this point, it is seen that the regulator needs to meet the fuel flow rate requirement of the Kriss 110cc engine that tops at 24 litres per minute. This fuel flow rate requirement would fluctuate with engine speed. It is also noted that the fuel injector operates at 4.5 bar of pressure thus requiring the outlet pressure of the regulator to be that value. It is seen that the flow temperature vary due to the pressure drop. This temperature profile would be taken as a study parameter and monitored.

Design conditions begin with the material selection. The selection of material governs pressure regulator wall thickness, spring design and the obturator seal. The fabrication of the prototype pressure regulator depends on material selection as well.

4.3 Regulator Prototype Design

The compressed natural gas from the storage tank is directed by the high pressure tubing to the regulator. At the entrance of the regulator, a high pressure solenoid valve and a filter is fitted. The filter installed could obstruct the entry of any foreign matter that may affect the regulator operation. The high pressure solenoid valve is used to block the

supply of CNG when the regulator is not in use; this reduces the unnecessary load on the restricting element when not in operation. The design of the pressure regulator begins at this point after these two components.

The literature in Chapter 3 has made clear that the direct acting self operated regulator would suit our requirements better compared to the pilot operated type. Chapter 3 also describes that this type comprises of the regulator body, trim (restricting element) and actuator that is further divided into loading element and measuring element. Each of these components is discussed well in its respective Sections 3.1.1. The regulator trim would comprise of a globe type valve for flow restriction and the actuation would be of a diaphragm and spring combination.

The globe type valve restricting element comprising of a valve seat paired with an obturator that varies flow area is used to control flow rate. This element receives prime design attention as this flow rate control determines the amount of gas entering the system thus primarily manipulating the pressure value within the system. The actuation, selected to be a combination of a helical spring and diaphragm receives the next design attention. The design interest then moves to the regulator body, its cover and threaded fastener. All related minimum wall thickness are evaluated from the ASME pressure vessel code. This cover is held-up in place by threaded fasteners which are also used extensively within the regulator body to hold the internal components. Material selection for all the above is done meticulously as it contributes greatly to the operation of the device.

4.3.1 Regulator Restriction Design

The second generation natural gas motorcycle fuel system uses an injector as the fuel metering device which requires a constant pressure supply for proper operation. The outlet pressure " P_{out} " for compressed natural gas vehicle pressure regulator varies from 3.8 to 17 bar. The set-point value selection depends on the chosen injector, and trade-off between the following injector characteristics: maximum flow, durability; and dynamic

range. For the system under development, a set-point pressure of 4.5 bar is selected to suit the injector intended to be used. The flow path of the natural gas from the storage tank to the fuel metering device is described in the Figure 4.2. Gas from the storage cylinder is transferred via high pressure tubing to the pressure regulator. The fluid passes through the solenoid valve at the inlet of the regulator before going to the restricting element of the regulator. The fluid passes through the solenoid valve at the inlet of the regulator before going to the restricting element of the regulator.

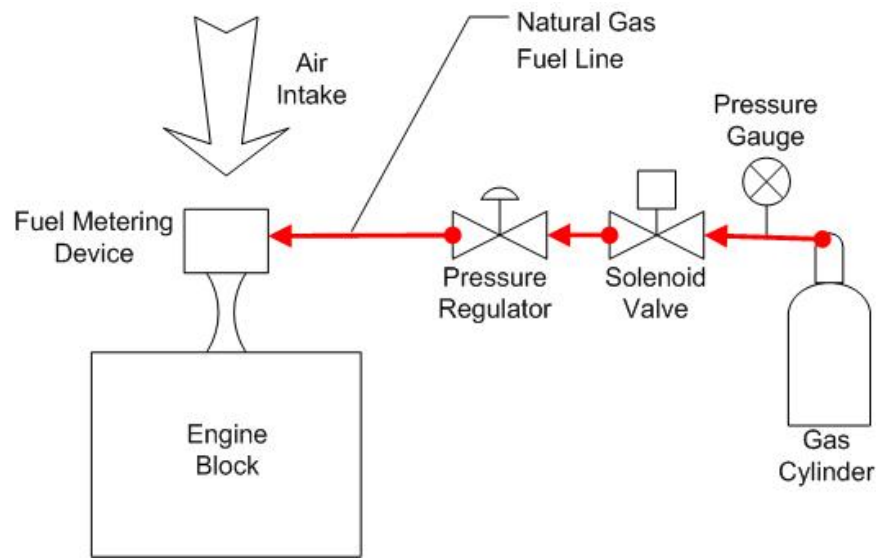


Figure 4.2: Compress Natural Gas Fuel Line

The mass of gas flowing through a close conduit is limited by the occurrence of a phenomenon called “choke flow” which occurs when the flow velocity is equivalent to the speed of sound. Choked flow occurs at any throat if the ratio of the upstream pressure to downstream pressure exceeds a critical value. Equation 4.1 provided by Oosthuizen and Carscallen⁴⁶ relates the critical area with other parameters such as specific heat ratio, mass flow rate, stagnation pressure and density.

$$A^* = \frac{\dot{m}}{\sqrt{\gamma P_o \rho_o}} \left(\frac{2}{\gamma + 1} \right)^{\left(\frac{\gamma + 1}{2(\gamma - 1)} \right)} \quad (4.1)$$

A^* = Critical Area
 \dot{m} = Mass Flow rate

$$\begin{aligned}\gamma &= \text{Specific Heat Ratio} \\ P_o &= \text{Stagnation Pressure} \\ \rho_o &= \text{Stagnation Density}\end{aligned}$$

The stagnation condition occurs as the natural gas storage tank is considered to be a large reservoir compared to the flow of gas into the pressure regulator through the valve seat. The equation shows that the smaller the area the smaller the amount of mass of natural gas that would be able to flow through. This argument would be used to evaluate the entire path taken by the natural gas from the storage tank to the regulator. The outcome of this evaluation takes two parameters into account. This includes the area of the path taken by the natural gas traveling from the tank to the valve seat of the restricting element and the nature of the regulating mechanism that requires the obturator to oppose inlet pressure force during closure.

Next, we deal with the obturator positioning of the restricting element design under consideration as shown in Figure 4.3. The valve seat sizing is followed by the determination of the obturator movement locus which dynamically controls the amount of gas entering the system to sustain the desired set point pressure. The movement of the obturator away from the valve seat dictates the amount of gas entering the system. Insufficient opening may restrict the regulator from supplying sufficient gas into the system. On the other hand large opening may cause great amount of gas to enter and creates over pressure the system in the occurrence of a failure on the loading and measuring element. Because of this, there is a need to predetermine the maximum distance of the obturator movement to provide the required gas to the fuel metering device. The locus of the obturator movement and the required force would be used to design the diaphragm and spring combination. Based on the sizes of the internal components, the regulator body would be designed.

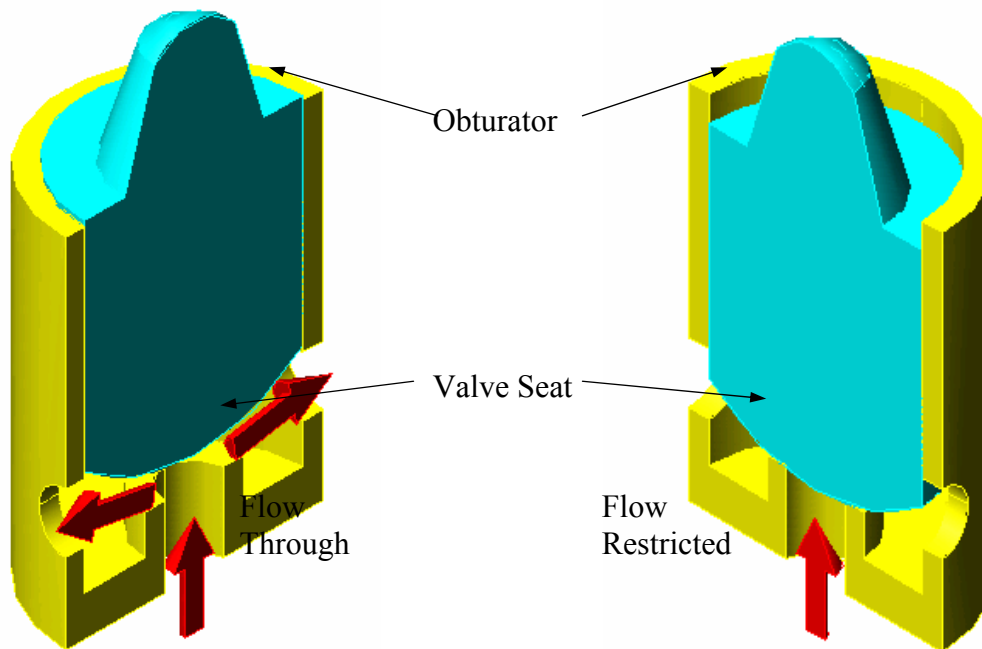


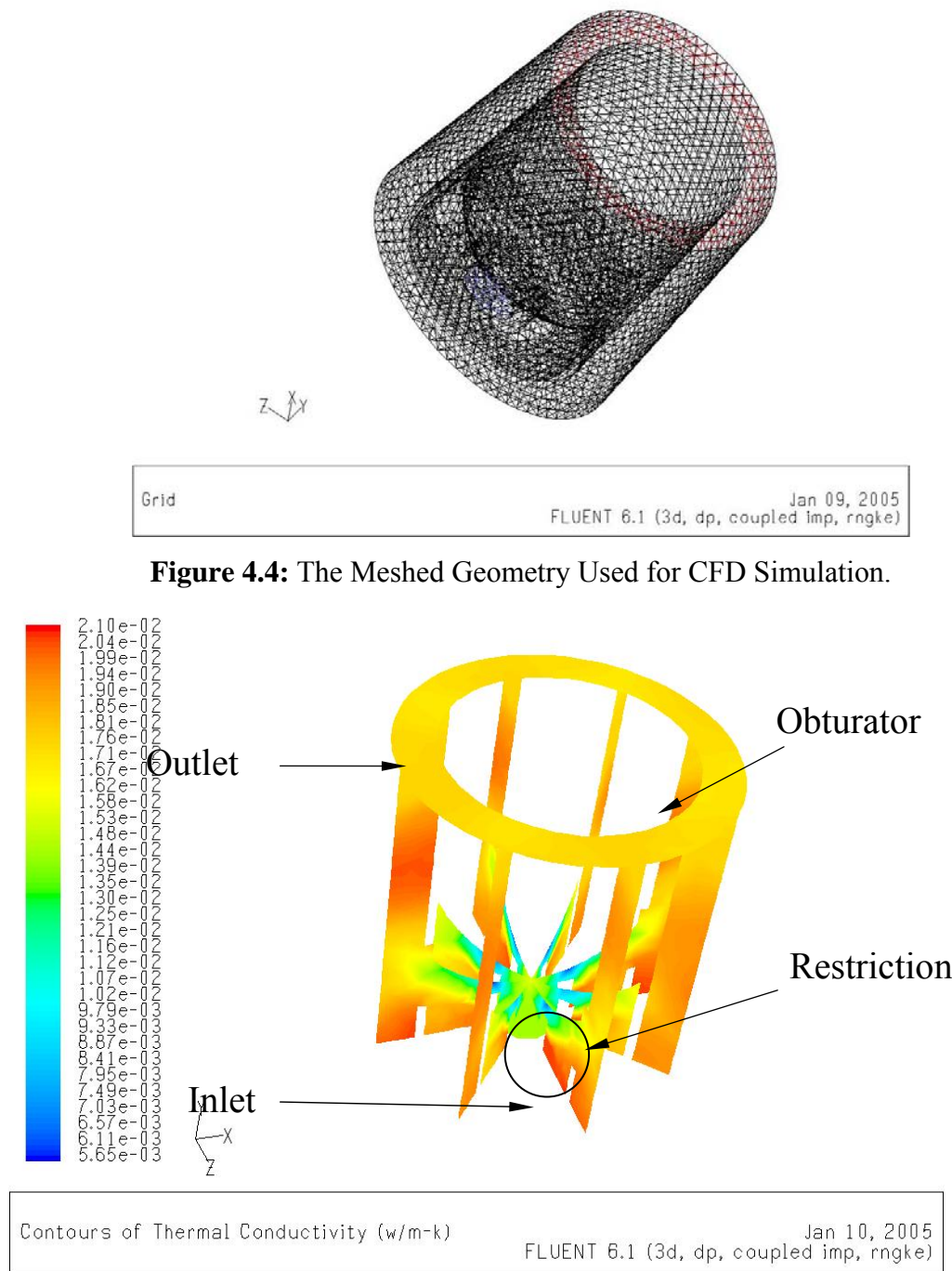
Figure 4.3: Open and Close Position of the Restricting Element

The complex geometry of fluid flow pattern through the opening between the valve seat and the obturator makes manual calculation to predict the amount of mass flow at various obturator positions to be difficult. The computational fluid dynamic software called FLUENTTM was used to simulate the flow of gas through the restricting element at various obturator positioning.

4.3.2 Computational Fluid Dynamic Evaluation

The valve seat and the obturator would be positioned virtually as desired in the geometry generation software called GAMBIT. The geometry within the GAMBIT software will be meshed and the related boundary conditions assigned accordingly. The geometry is then imported in to FLUENTTM and simulated. The coupled, implicit solver combination was used as it pairs the equations and solves them while the segregated solver does this separately. The energy equation and viscous heating was enabled for the simulation. The k-epsilon 2 equation model with RNG and standard wall functions were used. The thermophysical properties of the fluid are defined within the user-defined

function as given by Friend et. al to cater for the compressibility effect which varies from the ideal default condition of the software.



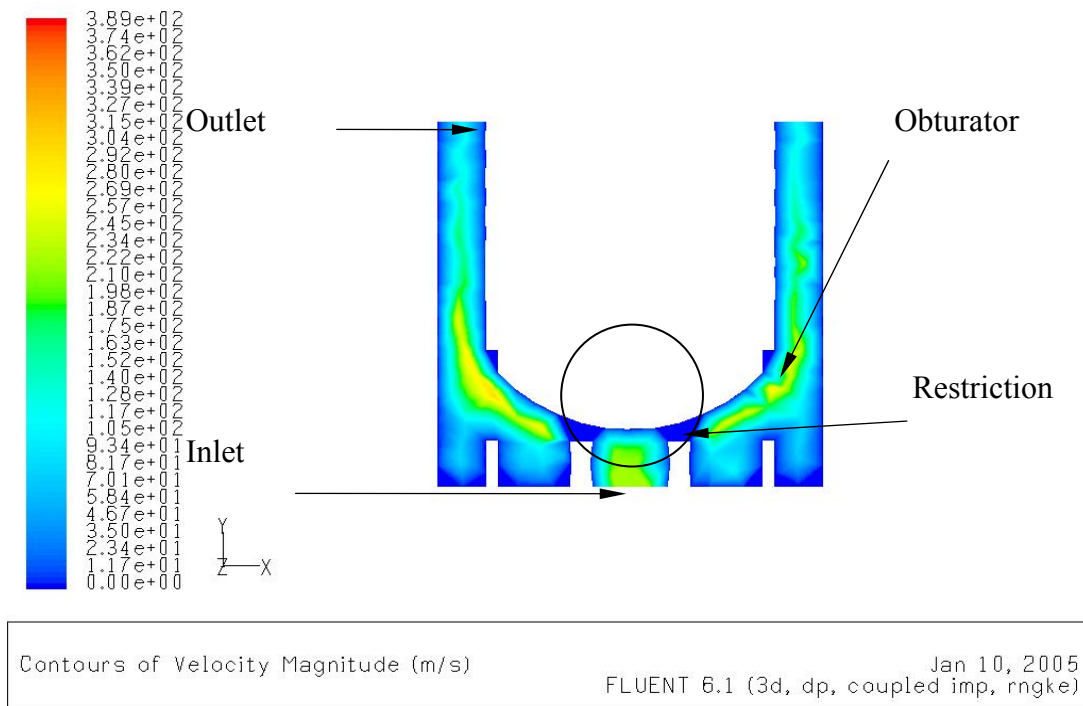
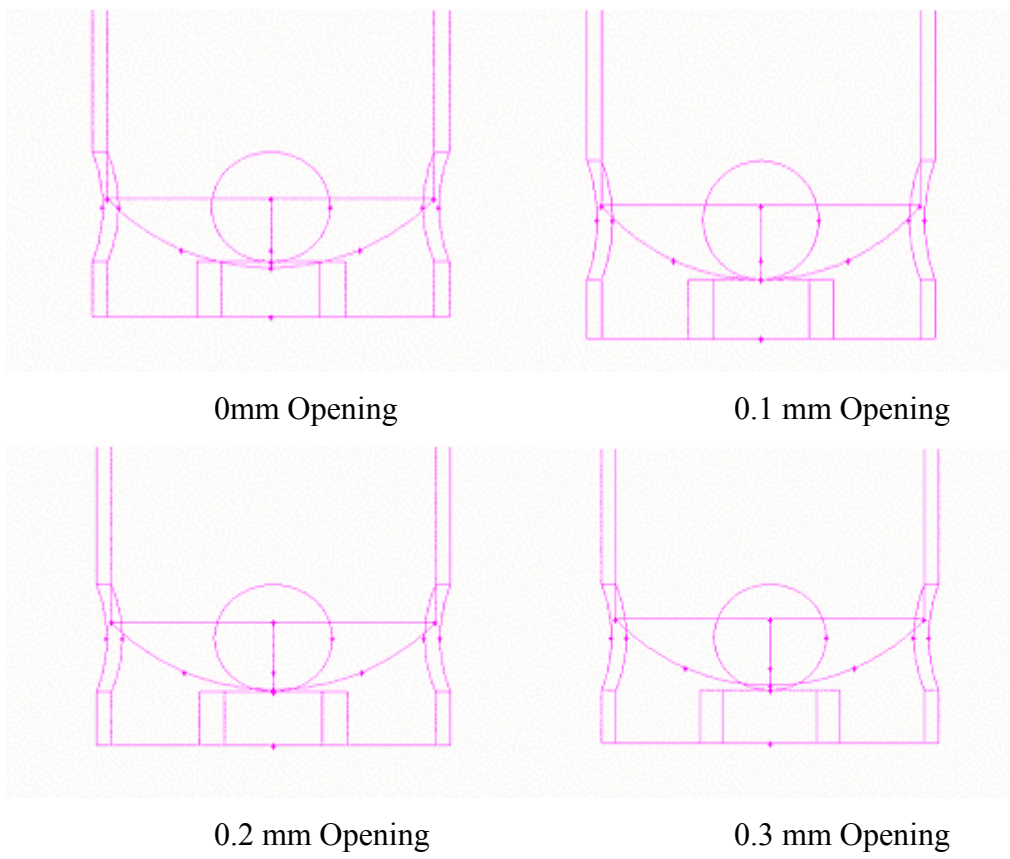
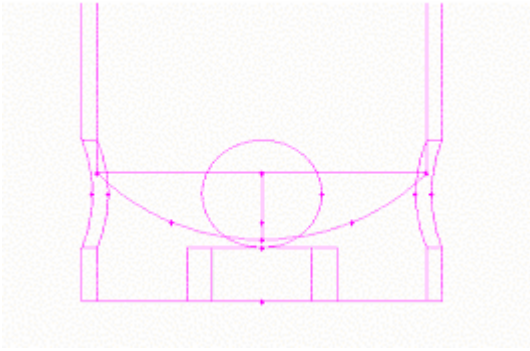


Figure 4.5: 2-Dimensional Fluid Flow Pattern Around The Restricting Element.





0.3 mm Opening

Figure 4.6: Obturator positioning simulated by CFD software.

The assumption on the fluid of being isentropic is rectified via the Computational Fluid Dynamic simulation where viscous heating is taken into consideration in the model. The model will be conducted on a compressible, steady state adiabatic wall basis. The fluid is taken as methane as Malaysian natural gas contains 93% methane. The inlet boundary condition was defined as pressure inlet and the pressure was set to 4.5 bar within the simulation software. This 4.5 bar pressure value is the desired set point pressure of the pressure regulator. The inlet pressure would range from a full cylinder charge pressure of 206 bar down to set point pressure of 4.5 bar. It is known that the mass flow through the restricting element would be critical during low pressure due to the occurrence of choke. For this reason the simulations are done using the lowest expected inlet pressure which is the set-point pressure of 4.5 bars. The greater the upstream pressure the greater the amount of mass that would pass through an opening while the lowest inlet pressure which is the set-point pressure would require the greatest opening to permit the desired mass of gas to get through.

The outcome of this simulation is given in the results and discussion Chapter 4 where the mass flow rate of gas is plotted against the distance of the obturator away from the valve seat. The required movement of the obturator from the valve seat to provide the desired mass flow rate is attained from the graph. This value is used as the maximum distance the obturator would move away from the valve seat during the fabrication and assembly of the regulator. Knowing the required distance of the obturator to permit and

to restrict flow, the loading and measuring elements would be designed as described in the following section.

4.3.3 Regulator Actuation Design

The combination of the loading (spring) and measuring (diaphragm) elements is used to actuate the restricting element. These two elements are linked using a mechanical linkage to direct the restricting element. Force exerted by the fluid on to the obturator shown in Figure 4.5 is opposed by the force generated by the compartment fluid onto the diaphragm. This linkage is designed based on fundamental force calculation which mainly evolves on moment evaluation. This diaphragm would convert the compartment fluid pressure that requires governing to force, based on the fundamental physic relation where pressure equals force over area exposed to the pressure. Circular shapes are the best geometry to equally distribute force on a given surface. This sensing diaphragm would also serve as a gasket seat between the regulator body and its bonnet cover. The diaphragm would be made of three-ply elastomer as it is the most suitable material for the given situation.

The spring force depicted as serves as the loading element which goes against the closure of the obturator to allow the compartment pressure to rise to the desired set point. The measuring element (diaphragm) closes the gas inlet of the compartment when the compartment pressure exceeds the set point value. The linkage provides the obturator with sufficient force to hold the inlet gas flow from entering the compartment to avoid pressure build up. Usage of the gas from the regulator compartment by the outlet stream will cause the compartment pressure to deplete from the set point thus allowing the obturator to open the inlet again. The best loading element for the required condition would be the helical compression spring which is described in depth in the flowing sections.

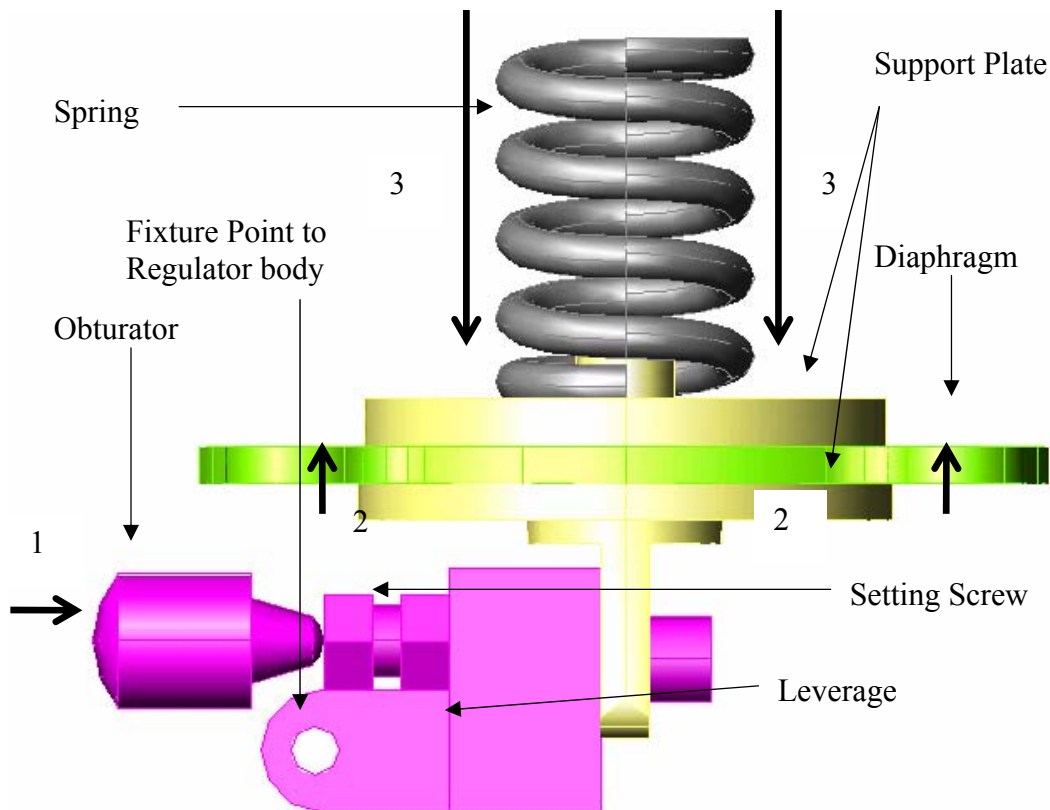


Figure 4.7: Mechanical Linkage Relating All Three Elements

4.4 Compression Springs

Compression springs made from round wire are the easiest to design and produce. They are accurate, reliable, tolerable to high stress, have longer fatigue life, and should be used in preference to any other type. They have an automatic stop when compressed solid that prevents over deflection, thus limiting the stress, whereas extension and torsion springs can easily be overextended. However, even with all these advantages, they can still be troublesome-usually due to buckling or improper design specification.

There are basically four types of ends for a fully formed helical compression spring. Plain ends which is also called open ends, is a simple cutoff with no attempt to

close the end coil. This prevents a spring to stand upright and causes uneven forces distribution that makes the spring to buckle quickly. They are occasionally used when a spring is supported over a rod and inaccurate forces or where buckling is not detrimental to the application. All coils are active; the solid height equals the total coils plus 1 times the wire diameter.

The second type known as plain ends ground is also called open ends ground. This type is made by grinding a small portion of a spring having plain ends. About 25 percent of the end coil may be ground. The amount varies with the pitch or angle of the end coil. This small amount of grinding does not help retard buckling, but it does reduce the solid height of the spring, which is advantageous when a limited distance is necessary. They are hazardous when handled. The total coils plus 1 the solid height equals the total coils times the wire diameter. The third type which is the closed ends not ground are also called squared ends. This type, automatically made on spring coilers, retard tangling, provides a fairly good seating and is particularly useful on light sections of wire under 1/32 in. (0.080mm) and especially so when the spring index D/d is over 10. The total coils equal the active coils plus 2; the solid height equals the total coils plus 1 times the wire diameter.

Closed ends ground also called squared and ground is the fourth type of ends implied on a helical compression spring. This type is made by coiling the springs with closed ends automatically as described for closed ends not ground, the springs are individually inserted into supporting tubes or plates, and both ends are then ground simultaneously in specially designed spring grinding machines. Closed and ground ends are often necessary to comply with specifications, for accurate precision force requirements, for low force tolerances, to reduce buckling, and to be within the specified tolerances when a spring must stand upright within 3° or 4° or less. The total coils equal the active coils plus 2; the solid height equals the total coils times the wire diameter. The loading element spring of the pressure regulator will be designed to have the closed ends ground as it requires accurate precision force requirements and resistance towards buckling.

4.4.1 Compression Springs Principles

The single coil of the compression spring shown in the figure below will have a load tending to compress it. This means that there is a force, tending to pull “A” downwards and “B” upwards. The effect of this force is to try to twist the spring wire at “C”. There will be a little bending action in the lengths AC and BC, therefore the criterion for the spring wire will be the shear strength.

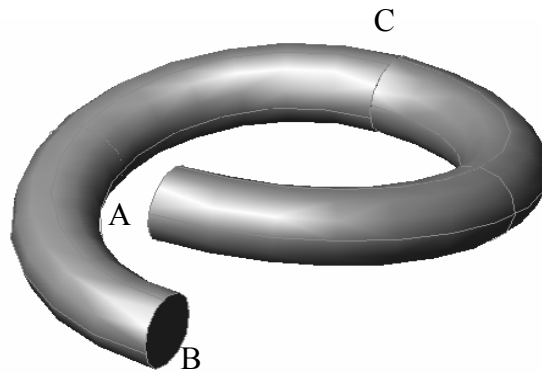


Fig. 4.8: Single Coil of a Helical Compression Spring.

In helical compression and extension springs, the wire is stressed in torsion when the spring is loaded. The torque moment which produces the twist is caused by the load acting along the helical spring and at the mean coil radius, or the distance from the spring axis to the center of the coiled wire. In common straight torsion bar spring or circular cross section, the

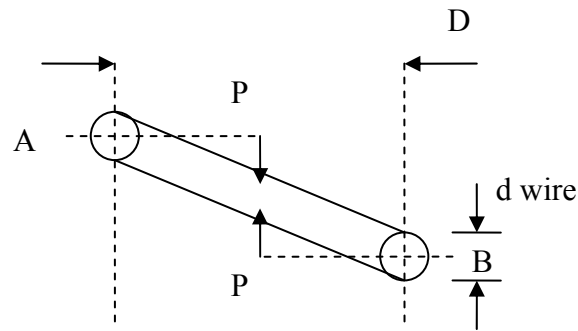


Fig. 4.9: The twisting moment on the spring coils.

In the straight torsion bar spring of circular cross section, the twisting produces a shear stress which is uniform at every point of the bar surface; but in the helical spring coiled from round wire, the stress pattern on the wire surface gets complex. Two reasons that causes this occurrence are the torque moment that results in a steeper twist angle for the short wire fibers at the outside of the coil, which produces a higher shear stress at the inside of the coil. The second reason is that the axial load causes a direct shear stress which adds to the shear stress from the torque moment at the inside of the coil, but subtracts from it at the outside of the coil.

Under static loading conditions, the variations in stress over the cross section of the spring wire can be neglected. The standard stress formula can be used, as it will furnish an average stress over the entire surface of the wire. However, when the spring is subjected to fatigue loading, the standard formula is inadequate because it conveys neither the higher local stress nor the wider stress range prevailing during each cycle at the inside of the coil. Fatigue failures are induced by a combination of high stress level and wide stress range, and it is a common experience that fatigue failures in helical springs occur at the inside of the coil. A failure at some other point can usually be traced to a local flaw in the wire surface or to severe coiling or presetting stresses.

The maximum design stresses allowed for loading with various spring materials for helical springs are established as a percentage of the minimum tensile strength of the

material. It has been found convenient to take into account the stress conditions at the inside of the coil by using a “corrected stress”. This is obtained by computing the stress from the standard formula and then multiplying the result with a stress correction factor K_w . The factor increases with greater curvature of the coiled wire. Greater curvature is equivalent to a smaller spring index, which is the ratio of mean coil diameter to wire diameter. The Wahl factor K_w is most commonly used, and its values may be calculated based on the equation below.

$$K_w = \left[\frac{4 \cdot C - 1}{4 \cdot C - 4} + \frac{0.615}{C} \right] \quad (4.2)$$

$$C = \frac{D}{d} \quad (4.3)$$

As we can see the correction factor given above is a function of the spring index (C). The ratio of the mean coil diameter D divided by the wire diameter d is called the spring index and is one of the most important factors in design and manufacture. Low ratios under 4 cannot always be coiled on automatic coilers because the high pressure of the cutoff tool needed to sever the wire may break the portion of the arbor used as a cutting edge. Low ratios also may cause pre-tempered wire to crack or may reduce its ability to withstand the deflection desired. High indexes over 16 and particularly those over 20 causes greater flexibility in the coils and require tolerance at least 50 percent larger than standard. Higher ratios require modification on the coiling tools and cause difficulty large variations in coil diameter. Indexes 3.5-15 are commercially practical to manufacture, but indexes in the range of 5.5-9 are preferred, particularly for close tolerance springs and those subjected to cyclic loading.

The number of coils does have an effect on the spring performance; in many cases the spring deflection under load is almost as important as the load itself. The corresponding end B of the bottom half coil is thus displaced upwards where as end A is displaced downwards. The total deflection is 2 “ δ ” where “ δ ” movement downwards for point A and δ upwards for B. Add another pair of half coils and the next end will move by 4 “ δ ”, and so on. Deflection depends on the number of coils. In spring work, this deflection is usually stated as the Rate of the spring “R” and in Imperial measure is

defined as the load in lbf/in. (in S.I. units this would be stated, for our size of spring, in Newton/mm.) Spring rate is called by many names including scale, gradient, constant, load per inch, force per unit of deflection, and other terms which add to the confusion. The simplest way is to deflect a compression or extension spring any convenient distance and note the first force and then deflect the spring any convenient second distance and note the second force. The difference in the two forces divided by the second amount of deflection is the rate. Rate should be determined between 20 and 60 % of total deflection when test lengths are not otherwise established. If these factors are unknown, the deflection under a given load W is given by the formula below:

The basic design formulae for round wire compression and extension spring are shown below:

$$P = \frac{G \cdot d^4 \cdot F}{8 \cdot D^3 \cdot N_a} \quad (\text{Force N}) \quad (4.4)$$

$$R = \frac{P}{F} = \frac{G \cdot d^4}{8 \cdot D^3 \cdot N_a} \quad (\text{Linear spring rate N/mm}) \quad (4.5)$$

$$S = \frac{8 \cdot D \cdot P}{\pi \cdot d^3} \quad (\text{Basic Stress MPa}) \quad (4.6)$$

$$S_c = \frac{8 \cdot D \cdot P \cdot K_w}{\pi \cdot d^3} \quad (\text{Corrected Stress MPa}) \quad (4.7)$$

F= deflection, (mm)

N_a = number of active coils

G = Torsional modulus of elasticity. MPa

R= spring rate, lbf/in. of deflection.

P = Force, N

d = diameter of spring wire (mm)

D = Diameter of coil (mm)

Iteratively equation 4.7 is used to determine suitable spring index that gives the working torsional stress below the allowable limit given in the sentence above. A ten coil spring will carry exactly the same safe load as one with only two if the wire and coil diameters are the same. Having these values, we then determine the amount of coils that are required to provide the desired deflection based on the preloading and force distributions involved in actuating the restricting element with the help of the measuring element which is the diaphragm

4.5 Valve Body Wall Thickness

The American Society of Mechanical Engineer (ASME) Boiler and pressure vessel code provides rules for the construction of boilers, pressure vessels and nuclear components. This includes requirements for materials, design, fabrication, examination, inspection and stamping. This code is further divided into 11 sections covering a vast number of applications related to the field. Section VIII Division 1 covers pressure vessel in general which is suitable for the current study. For this reason, the 1977 ASME Boiler and Pressure Vessel Code Section VIII Division 1 is referred to determine the minimal wall thickness that surrounds the pressurized compartment. The vast amount of material covered by this code eases material selection based on the operating condition of the vessel under design. All related calculations including gasket and bolt joints are provided within the code.

The following sections describes the equations used based on the code. Three evaluations would be used due to the geometry of the pressure regulator body. This would be the base of the regulator, the surrounding wall and the cover of the regulator body which are elaborated by the sections bellow. Part (a) describes the side wall of the pressured compartment which falls under Section UG- 27: Thickness of shell under internal pressure. Part (b) explains the flat bottom portion of the pressured compartment which complies with Section UG-34: Unstayed flat heads and cover of the pressure vessel code. Part (c) Determines the minimal thickness evaluation would be the cover which is under the field of Section UG-34 as well.

The regulator developed would be fabricated using stainless steel 304 as it is found suitable with the natural gas pressure regulator operating conditions of -20°C to 120°C . The maximum allowable stress value is a function of temperature for the selected stainless steel 304 material, where the value decreases with the rise in temperature. We attain the maximum allowable stress value (S) as 14.1×10^3 psi from table UHA-23 of the code that would be used in all the related calculations.

4.5.1 Minimal Wall Thickness of Shell Under Internal Pressure

The minimal wall thickness (t) is determined in accordance to Section UG-27-Thickness of shells under internal pressure where the minimum thickness or maximum allowable working pressure of cylindrical shells shall be the greater thickness or lesser pressure as given by (1) or (2). The maximum allowable stress value in tension (S) is taken as 14.1×10^3 psi due to the argument described by the previous section. The design pressure (P) is taken as four times the desired pressure regulator outlet set point; the inner radius (R) of shell is obtained based on the design of the measuring element while the joint efficiency (E) is taken as 1 for perfect defect free joint. Both equation (1) and (2) are evaluated where the greater value of thickness would be used as the minimal wall thickness value during fabrication.

- (1) Circumferential stress (longitudinal joints). When the thickness does not exceed one-half of the inside radius, or P does not exceed $0.385 SE$, the following formulas shall apply:

$$P \leq 0.385SE = 348 \leq 1732.5$$

$$t = \frac{PR}{SE - 0.6P} \quad \text{or} \quad P = \frac{SEt}{R + 0.6t} \quad (4.8)$$

- (2) Longitudinal stress (circumferential joints). When the thickness does not exceed one-half of the inside radius, or P does not exceed $1.25 SE$, the following formulas shall apply:

$$P \leq 1.25SE = 348 \leq 5625$$

$$t = \frac{PR}{2SE + 0.4P} \quad \text{or} \quad P = \frac{2SEt}{R - 0.4t} \quad (4.9)$$

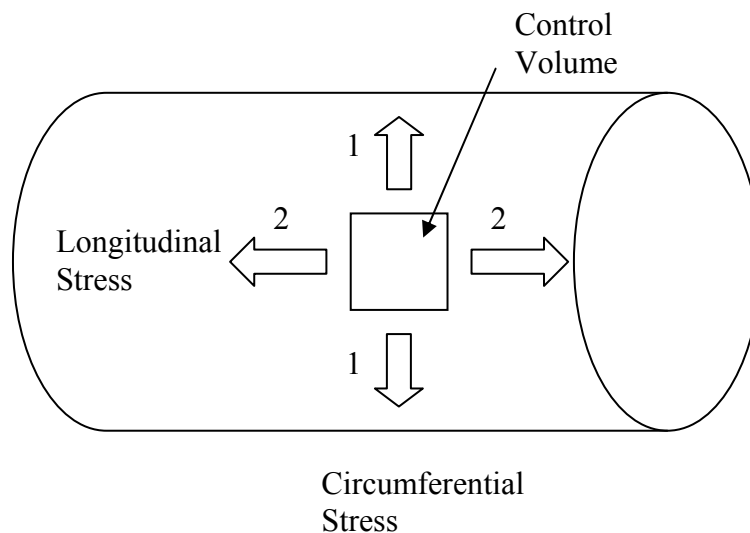


Figure 4.10: Pictorial Description of Longitudinal and Circumferential Stress

4.5.2 Minimal Wall Thickness of Unstayed Flat Heads

The minimum thickness of the flat headed bottom of the regulator base is calculated in accordance with Section UG -34 Unstayed Flat Heads and Covers which provides equation 4.11. The depth of the pressure compartment (d) is acquired based on the design of the loading element and the mechanical linkages involved within the regulator. The value of C for the use of equation 4.11 is 0.2 given in Section UG-34 as described in figure 4.11. The equations provide the minimal flat head wall thickness and the required radius between the flat head and the side wall.

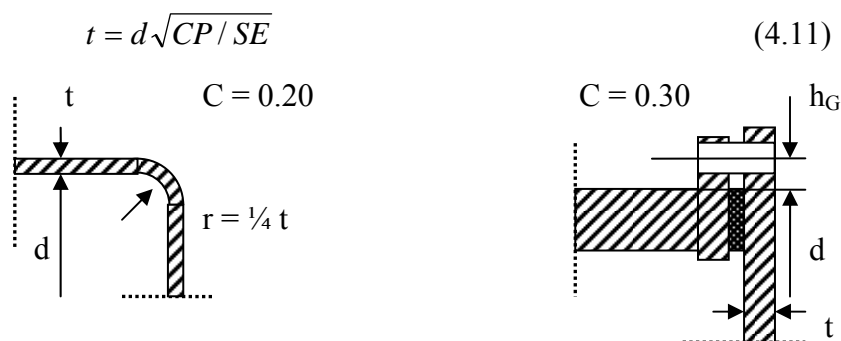


Figure 4.11: Types of Unstayed Flat Heads and Covers

4.5.3 Minimal Wall Thickness of Unstayed Covers

The minimal thickness of the cover to be used with the pressure regulator base is covered by the same section of the pressure vessel code where equation 4.11 is used. The dimension less factor C is taken as 0.30 for the design understudy as described by figure 1. The diameter value (d) as described in figure 1 is determined from the design of the internal components. The bolt circle diameter (C) is based on the cylindrical shell thickness and the use of threaded fasteners. The radial distance from gasket load reaction to the bolt circle is given in equation 4.12

$$h_G = \frac{C - G}{2} = \frac{2.795 - 2.56}{2} = 0.1175in = 3mm \quad (4.12)$$

The Flange Design Bolt Load (W) is evaluated for operating condition and gasket seating condition as shown below. The greater value between W_{m1} (operating condition) and W_S (gasket seating) will be used in equation 4.13. The bolts loads used in the design of the flange during operational conditions shall be values obtained from formulas (5) for operational conditions.

$$\begin{aligned} W &= W_{m1} \\ W_{m1} &= H + H_p = 0.785G^2P + (2b \times 3.14GmP) \\ W_{m1} &= 0.785 \times (2.46)^2 \times 348 + (2 \times 0.0492 \times 3.14 \times 2.46 \times 2.25 \times 348) \\ W_{m1} &= 2249.47 \end{aligned} \quad (4.13)$$

$m =$ is given as 2.25 for Elastomers with 3-ply asbestos fabric insertion, with or without wire reinforcement.
 $G =$ when $b_0 \leq 0.25in$ $G =$ mean diameter of gasket contact face, in. (mm) = 62.5 mm
 $b =$ b_0 when $b_0 \leq 0.25in$ in our case, $b_0 = 2.5mm/2 = 1.25mm$

Where additional safety against abuse is desired, or where it is necessary that the flange be suitable to withstand the full available bolt load, the gasket value for the flange design bolt load is taken as the full available bolt load as provided by the M6 Bolt of 8.04 kN (1807.46lb_f) Giving $W_S = 1807.46$. It is clear that the W value calculated based on

W_{ml} for the operational condition is greater than W_s thus it would be used in equation 4.14.

$$t = d \sqrt{CP / SE + 1.9Wh_G / SE d^3}$$

$$t = 2.56 \sqrt{\frac{0.3 \times 348}{14100 \times 1} + \frac{1.9 \times 2249.47 \times 0.118}{14100 \times 1 \times 2.56^3}} \quad (4.14)$$

4.6 Regulator Loading Element Design

Compression springs made from round wire are the easiest to design and produce. They are accurate, reliable and tolerable to high stress, have longer fatigue life, and should be used in preference to any other type. They have an automatic stop when compressed solid that prevents over deflection, thus limiting the stress, whereas extension and torsion springs can easily be overextended. However, even with all these advantages, they can still be troublesome-usually due to buckling or improper design specification.

There are basically four types of ends for a fully formed helical compression spring. A plain end, which is also called open ends, is a simple cut-off with no attempt to close the end coil. This prevents a spring to stand upright and causes uneven forces distribution that makes the spring to buckle quickly. They are occasionally used when a spring is supported over a rod and inaccurate forces or where buckling is not detrimental to the application. All coils are active; the solid height equals the total coils plus 1 times the wire diameter.

The second type known as plain ends ground is also called open ends ground. This type is made by grinding a small portion of a spring having plain ends. About 25 percent of the end coil may be ground. The amount varies with the pitch or angle of the end coil. This small amount of grinding does not help retard buckling, but it does reduce the solid height of the spring, which is advantageous when a limited distance is necessary. They are hazardous when handled. The total coils plus 1 the solid height

equals the total coils times the wire diameter. The third type which is the closed ends not ground are also called squared ends. This type, automatically made on spring coilers, retard tangling, provides a fairly good seating and is particularly useful on light sections of wire under 1/32 in. (0.080mm) and especially so when the spring index D/d is over 10. The total coils equal the active coils plus 2; the solid height equals the total coils plus 1 times the wire diameter.

Closed ends ground also called squared and ground is the fourth type of ends implied on a helical compression spring. This type is made by coiling the springs with closed ends automatically as described for closed ends not ground, the springs are individually inserted into supporting tubes or plates, and both ends are then ground simultaneously in specially designed spring grinding machines. Closed and ground ends are often necessary to comply with specifications, for accurate precision force requirements, for low force tolerances, to reduce buckling, and to be within the specified tolerances when a spring must stand upright within 3° or 4° or less. The total coils equal the active coils plus 2; the solid height equals the total coils times the wire diameter. The loading element spring of the pressure regulator will be designed to have the closed ends ground as it requires accurate precision force requirements and resistance towards buckling.

The maximum design stresses allowed for loading with various spring materials for helical springs are established as a percentage of the minimum tensile strength of the material. It has been found convenient to take into account the stress conditions at the inside of the coil by using a “corrected stress”. This is obtained by computing the stress and then multiplying the result with a stress correction factor K_w . The factor increases with greater curvature of the coiled wire. Greater curvature is equivalent to a smaller spring index, which is the ratio of mean coil diameter to wire diameter. The Wahl factor K_w is most commonly used, and its values may be calculated based on the equation below.

$$K_w = \left[\frac{4 \cdot C - 1}{4 \cdot C - 4} + \frac{0.615}{C} \right] \quad (4.15)$$

$$C = \frac{D}{d} \quad (4.16)$$

The correction factor given above is a function of the “spring index” (C). The ratio of the mean coil diameter D divided by the wire diameter d is called the spring index and is one of the most important factors in design and manufacture. Low ratios under 4 cannot always be coiled on automatic coilers because the high pressure of the cut-off tool needed to sever the wire may break the portion of the arbor used as a cutting edge. Low ratios also may cause pre-tempered wire to crack or may reduce its ability to withstand the deflection desired. High indexes over 16 and particularly those over 20 causes greater flexibility in the coils and require tolerance of at least 50 percent larger than standard. Higher ratios require modification on the coiling tools and cause difficulty large variations in coil diameter. Indexes 3.5-15 are commercially practical to manufacture, but indexes in the range of 5.5-9 are preferred, particularly for close tolerance springs and those subjected to cyclic loading.

Deflection depends on the number of coils. In spring work, this deflection is usually stated as the Rate of the spring “R” and in Imperial measure is defined as the load in lbf/in. (in S.I. units this would be stated, for our size of spring, in Newton/mm.) Spring rate is called by many names including scale, gradient, constant, load per inch, force per unit of deflection, and other terms that add to the confusion. The simplest way is to deflect a compression or extension spring any convenient distance and note the first force and then deflect the spring any convenient second distance and note the second force. The difference in the two forces divided by the second amount of deflection is the rate. Rate should be determined between 20 and 60 % of total deflection when test lengths are not otherwise established⁵¹. If these factors are unknown, the deflection under a given load W is given by the formula below:

The basic design formulae for round wire compression and extension spring are shown below. Where F represents deflection (mm), N_a represents the number of active

coils, G represents Torsional modulus of elasticity (MPa), R_s represents spring rate of deflection (lbf/in), P_F represents Force (N), d represents diameter of spring wire (mm), D represents the diameter of the spring coil (mm).

$$P_F = \frac{G \cdot d^4 \cdot F}{8 \cdot D^3 \cdot N_a} \quad (\text{Force N}) \quad (4.17)$$

$$R_s = \frac{P_F}{F} = \frac{G \cdot d^4}{8 \cdot D^3 \cdot N_a} \quad (\text{Linear spring rate N/mm}) \quad (4.18)$$

$$S = \frac{8 \cdot D \cdot P_F}{\pi \cdot d^3} \quad (\text{Basic Stress MPa}) \quad (4.19)$$

$$S_c = \frac{8 \cdot D \cdot P_F \cdot K_W}{\pi \cdot d^3} \quad (\text{Corrected Stress MPa}) \quad (4.20)$$

Iteratively Equation 4.18 is used to determine suitable spring index that gives the working torsional stress below the allowable limit. A ten coil spring will carry exactly the same safe load as one with only two if the wire and coil diameters are the same. Having these values, we then determine the amount of coils that are required to provide the desired deflection based on the preloading and force distributions involved in actuating the restricting element with the help of the measuring element which is the diaphragm.

4.7 Regulator Body Design

The American Society of Mechanical Engineer (ASME) Boiler and Pressure Vessel code provides rules for the construction of boilers, pressure vessels and nuclear components. This includes requirements for materials, design, fabrication, examination, inspection and stamping. This code is further divided into 11 sections covering a vast number of applications related to the field. Section VIII Division 1 covers pressure vessel in general which is suitable for the current study. For this reason, the 1977 ASME Boiler and Pressure Vessel Code Section VIII Division 1 is referred to determine the minimal wall thickness that surrounds the pressurized compartment. The vast amount of material covered by this code eases material selection based on the operating condition of the

vessel under design. All related calculations including gasket and bolt joints are provided within the code. All calculations on minimal wall thickness of the pressure regulator body and bonet cover using the Stainless Steel 304 are shown in Appendix G

4.7.1 Threaded Fasteners

Several countries have combined their research resources and working together in ISO technical committees to design the ISO metric nut strength grade system. Properly used, the system guarantees as fool-proof safe bolt and nut assemblies as sound engineering and prudent economics can provide. Once installed, the failure mode if the assembly is overstressed will normally be bolt fracture and not thread stripping. One of the distinct advantages of the ISO metric nut strength system is that each property class of nut was specifically designed, dimensionally and metallurgical, to properly mate with a property class of bolt. Consequently, when the correct class of nut is selected, even under the most adverse combination of conditions, the bolt will initially break. This occurrence eases the detection of failures prior to loading.

There are just two metric screw thread forms, the M profile which is the standard for commercial fastener and the MJ which is the standard for aerospace quality fasteners. The differences between these two profiles are in the root radiusing where the M profile has radiusing of $0.125p$ and the MJ forms recommend $0.15p$. Both the metric screw thread comes with root radiusing which provides better fatigue resistance of the fastener⁵⁴. This is due to the fact that fatigue failure occurs at locations of high stress concentration, such as notches or abrupt changes in cross-sectional configuration. The highest stress concentration in threads occurs at the roots and the magnitude of the stress concentration factor relates directly to whether the root is rounded and to what degree. The Standard commercial fastener M profile is selected for the current study as it is easily attainable in the market.

4.8 Regulator Material Selection

The selection of material to design is crucial as it ensure safe working of the entire pressure regulator at the operating condition. The material of the pressure regulator body is required to externally suit the engine compartment heat and corrosive environment. The inner part of the pressure regulator body should be able to with stand low temperature due to the pressure drop within the regulator body. Selection of component materials for high temperature or corrosive service is generally limited to stainless steels or high nickel alloys. For the spring material, metals such as carbon steels and the non-ferrous alloys have a maximum service temperature of 400 F. In addition; they are not normally resistant to corrosion and other forms of high temperature attack. The high nickel alloys such as Inconel and the beryllium-copper are about 3 to 4 times the cost of Type 18-8 stainless steel. 18-8 hard drawn stainless steel is a very useful material, especially for situations where the temperature may be high or there is risk of corrosion, it can be worked up to 300°C, whereas carbon steel wire is unable to perform above 125°C. It has an elastic limit in shear very slightly higher than regular carbon steel.

The austenitic group, generally nonmagnetic, is the most important for process industry applications. By virtue of their austenite-forming alloy additions, notably nickel and manganese, these stainless steels have the face-centered austenite structure from far below 0°C (32°F) up to near melting temperatures. They are not hardenable by heat treatment, but can be strain-hardened by cold-work. The conventional 18-8 austenitic stainless steels are exemplified by Type 304 (S30400). These alloys have rare combination of corrosion resistance, high-temperature strength, and oxidation resistance, ease of fabrication and weldability, good ductility and good impact resistance down to at least -183°C (-216°F). Their mechanical properties in general, are excellent. Other grades, such as Types 17-4 PH (S17400) and 17-7 PH (S17700), as well as a molybdenum-bearing variant such as PH 15-7 Mo (S15700) can be precipitation-hardened while retaining corrosion resistance more or less equivalent to that of S30400 or S31600.

Consistent performance of a spring is ensured if the spring material retains its original properties. Many metals are subject to 'work-hardening' where a change of hardness occurs when stressed. Experience shows that all working springs are subject to cycles of stress. Brass, for example, is a metal that is relatively soft, but repeated stressing or 'working' causes its hardness to increase, with the metal becoming springier as a consequence. Thus whilst soft brass is quite useless as a spring material, fully hardened brass possesses reasonably good spring properties. Even with the best materials and apparently correct design, failures occasionally occur due to defective materials, improper selection of materials, incorrect sizes, or any other event. By large, early failures may be caused by high stress, shock loading, stress corrosion, high or low temperatures, hydrogen embrittlement, sharp bends, improper winding or one of many other conditions.

Heat treatment used upon spring material to improve the material properties is preferably avoided as it commonly causes spring failure. Without considerable experience in the techniques of heat treatment, therefore, spring materials should always be used 'as is'. Among the types of stainless steel, the Type (18-8) cannot be heat treated as these alloys do not respond to the hardening and tempering method. At low temperatures, the stainless steels of the 300 series are useful, but those of the 400 series are not. A creep comparison carried out between the music wire widely used for highly stressed springs and Type 304 stainless steel which has ability to withstand the effects of moderately elevated temperature previously carried out proved the credibility of the Type 304 stainless steel. At room temperature the creep of music wire spring and Type 304 stainless steel springs is about the same, but at 150°C, the creep of music wire is considerably greater than that of Type 304. At 250°C the stainless springs show fair creep resistance preliminary tests on music wire at this temperature have shown it to be unsuitable for service.

The arguments above prove that the best common component material that would oblige the design requirement is the stainless steel Type 304 (18-8). This material would be used throughout the pressure regulator due to its advantages over other materials for

the fabrication of all metal components. The most suitable material for the diaphragm is the 3-ply elastomer, as it is tabulated in the ASME pressure vessel code. It is strong to transfer the force exerted by the compartment fluid to the loading element to actuate the restricting element. The tip of the obturator is required to have Teflon as the most suitable material as it suits the condition best. This would be incorporated in the fabrication section of the restricting element.

4.9 Regulator Prototype Fabrication

The successful completion of the design method would result in a complete geometry which is presented in Chapter 6. This geometry requires to be fabricated using the material of interest to form a prototype pressure regulator model. This section covers methods implied during the fabrication, assembly, and configuration of the pressure regulator prototype. The materials used for fabrication of the components are dependent on the material selection. The resulting geometry of the restricting element from the Computational Fluid Dynamic simulation is fabricated based on the material selected.

All components are manufactured in the most cost effective manner to ensure the cost is minimal as this involves only one prototype unit. Other methods could be evaluated during the production of this product at a greater volume. The tip of the obturator requires Teflon as it is required to provide pressure tight seal to ensure the inlet gas is restricted from entering the pressure regulator compartment. The lathe machine is used to shape the obturator and its tip. The same equipment is also used to shape the inlet valve seat, while other holes are drilled according to the desired thread.

The loading element which is the helical compression spring is fabricated using an automatic spring coiler. The wire was selected to be stainless steel 304 while the wire diameter and the spring diameter were selected based on the design calculation of the spring. The measuring element which works together with the loading element is

fabricated using 3-ply elastomer that suits the condition best. The fabrication method implied here is the press method where a mould is made according to the required geometry and is used to cut the material to form the desired shape.

The biggest component of all which is the pressure regulator body is fabricated based on the most suitable manner in terms of time consumption and cost. The Computer Numerical Configuration Machining is seen to be the most suitable method to produce a single piece of the pressure regulator body. The cap of the pressure regulator is machined using a lathe machine as the shape suits the equipment. The threaded fasteners are used as required to secure parts and components in place as designed.

The assembly is given equal amount of attention as it jointly contributes to the integrity of the pressure regulator prototype. All components are fastened with suitable fasteners firmly to ensure proper working. Accurate tightening is crucial as it would ensure there is no leak of gas from the regulator. The spring should be loaded accordingly during the assembly; any variations would cause the set point pressure to vary as the loading element which is the spring would exert access force open the restricting element.

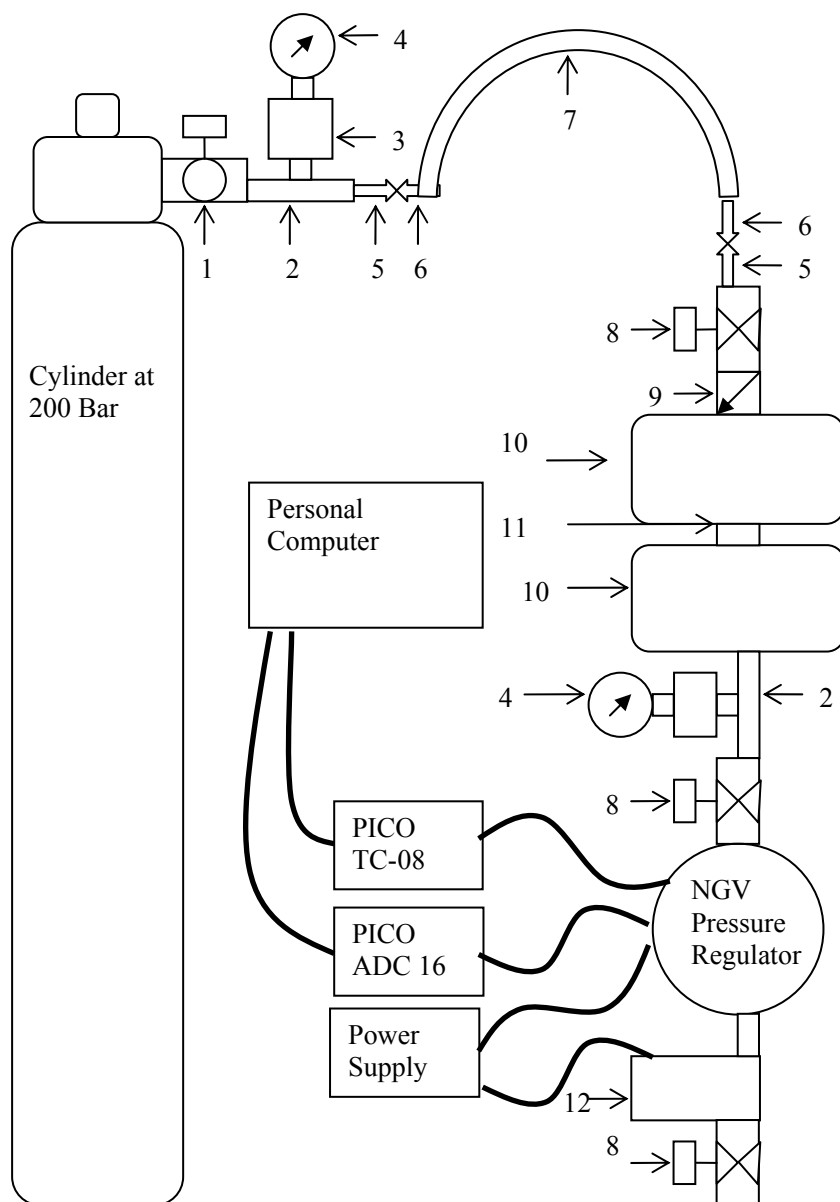
4.10 Regulator Prototype Testing

In order to conduct the test on the pressure regulator, a special pressure regulator test bench has been successfully developed. The bench is required to hold high pressure compressed natural gas (CNG). The handling of high pressure flammable gas requires meticulous design consideration. Related Standard by the National Fire Protection Agency NFPA 52-1984 and local Malaysian Standard MS 1096 were viewed. Referring to Chapter 3, the high pressure fluid line begins with the 55 litre bulk storage cylinder has a built-in needle valve to control the gas flow leaving the cylinder. A quarter turn ball valve provides quick open and close to the gas flow leaving the bulk storage cylinder. The tee-joint splits the flow to the manifold and the other goes to fill the onboard system.

This manifold block is fitted with pressure gauge to monitor the pressure within the hose connection. The manifold block also provides bleed capability for depressurization prior to dismantling of line.

The Teflon hose used to link the storage cylinder and the sample cylinder onboard the test bench is fitted with a quick-connect connection that eases the fitting which just snaps on. The combined sample cylinders have two ends, one for charging and the other is to dispense the gas to the pressure regulator. The charging end is fitted with a check valve to ensure one way flow and a needle valve to control the rate of gas transfer. The other end is fitted with a pressure gauge to measure the pressure within the sample cylinder and a needle valve that would control the flow of gas out of the sample cylinder and to the pressure regulator.

The outlet of the cylinders is connected to the NGV pressure regulator via high pressure tubing. The natural gas flow from the storage tank to the regulator is controlled by a high pressure solenoid valve. The test bench is equipped with a power supply to activate the high pressure solenoid valve to allow natural gas to enter the pressure regulator. The outlet of the pressure regulator is fitted with a flow meter and a needle valve. This controls the outlet flow rate allowing performance test to be conducted in a controlled manner. Two pressure sensors were used in this system, where one is designed to measure the upstream pressure which is the storage pressure that enters the regulator and the other is positioned at the pressure regulator compartment after the gas pressure has been regulated. An upstream pressure sensor having an operating range of 0 to 250 bar and a downstream pressure sensor having an operating range of 0 to 10 bar are installed before and after regulator. The ACD-16 by PICO is used to convert the output of the sensor to pressure values through the user interface software. The thermocouple is solely operated with the Pico TC-08 which is connected to the personal computer. Both the signals from the pressure sensors and the flow meter are processed by the Pico ADC-16. Pico log software provided with both the TC-08 and ADC-16 is used to provide real time data logging and can be stored onboard the personal computer.



No.	Description	No.	Description
1	Ball Valve	2	Tee Joint
3	2 Valve Manifold	4	Pressure Gauge
5	Quick Connect (female)	6	Quick Connect (male)
7	Teflon Hose	8	Needle Valve
9	Check Valve	10	1 litre Cylinder
11	Connector	12	Flow Meter

Figure 4.10: Schematic Drawing of the Pressure Regulator Test Bench

4.11 Regulator Prototype and Test Bench Testing

Testing begins with the leak test of the entire fluid flow that begins from the storage tank to the outlet of the flow meter to ensure there is no leak. The “Snoop” produced by Swagelok is used due to its common acceptance by many in the industry and the natural gas vehicle fuel line inspection practices in Malaysia. This step is then followed by the sensor and data acquisition system calibration. Calibration of the data acquisition system is required as it would ensure accurate results during the performance testing. All pressure sensor thermocouple and flow meter are purchased newly.

This is followed by the final performance test method that would evaluate the performance of the regulator to meet the set point outlet pressure regardless of the flow demand posed upon it. The high pressure test gas is supplied to the pressure regulator through the high pressure fluid system. The outlet of the pressure regulator is artificially controlled by a needle valve. The needle valve is used to vary the out going fluid flow just as it would be done in the actual system by the injector due to engine speed.

The outlet flow rate is varied from no flow up to the maximum flow consumable by the Modenas Kriss 110cc motorcycle which is 24 Liters/minute. While the flow rate is being varied, the pressure and temperature is logged using the data acquisition system. The prime motive of this test is to prove that the pressure regulator is capable of producing constant outlet pressure regardless of the outlet flow rate demand. The results this test is shown and elaborated in the results and discussion chapter.

4.11.1 Pressure Regulator Test Bench Operation

Basically two types of gas mediums are used to test the pressure regulator, compressed nitrogen or Compressed Natural Gas. The bulk storage cylinder has a built-

on needle valve to control the gas flow leaving the cylinder. This outlet is fitted with the dispense unit which enable the quick connect hose connection to transfer gas, pressure monitoring, bleed and control of flow. This unit is dedicatedly designed to enable the charging of the storage cylinders onboard the test bench. The dispense unit consist of fittings that would suite the outlet of the cylinder. A quarter turn ball valve provides quick open and close to the gas flow leaving the bulk storage cylinder. The flow then enters the 2 valve manifold block. This block is fitted with pressure gauge to monitor the pressure within the hose connection. The manifold block also provides bleed capability for depressurization prior to dismantle the hose after charging.

The test bench is equipped with a pair of high pressure storage cylinders having connected to provide a combined capacity of two litres. Both ends of the storage cylinders are fitted with needle valve to control the gas flow entering and leaving the cylinder. The inlet is fitted with a check valve between the needle valve and the cylinder to ensure there is no back flow if the valve is accidentally opened. The outlet is fitted with a pressure gauge prior to the needle valve to provide the storage pressure of the cylinders. The outlet is connected to the NGV pressure regulator via high pressure tubing. The high pressure solenoid built in with the pressure regulator provides additional safety to the system. A flow meter is attached to the outlet of the regulator to measure the flow rate of gas leaving the system. A needle valve is paired with the flow meter to vary and control the flow rate.

With the set up explained above, we would be able to obtain the pressure and temperature at every stage of the regulator and the overall regulator outlet flow. The experimental rig is fitted as shown in the schematic diagram above. A similar AutoCAD picture is provided below.

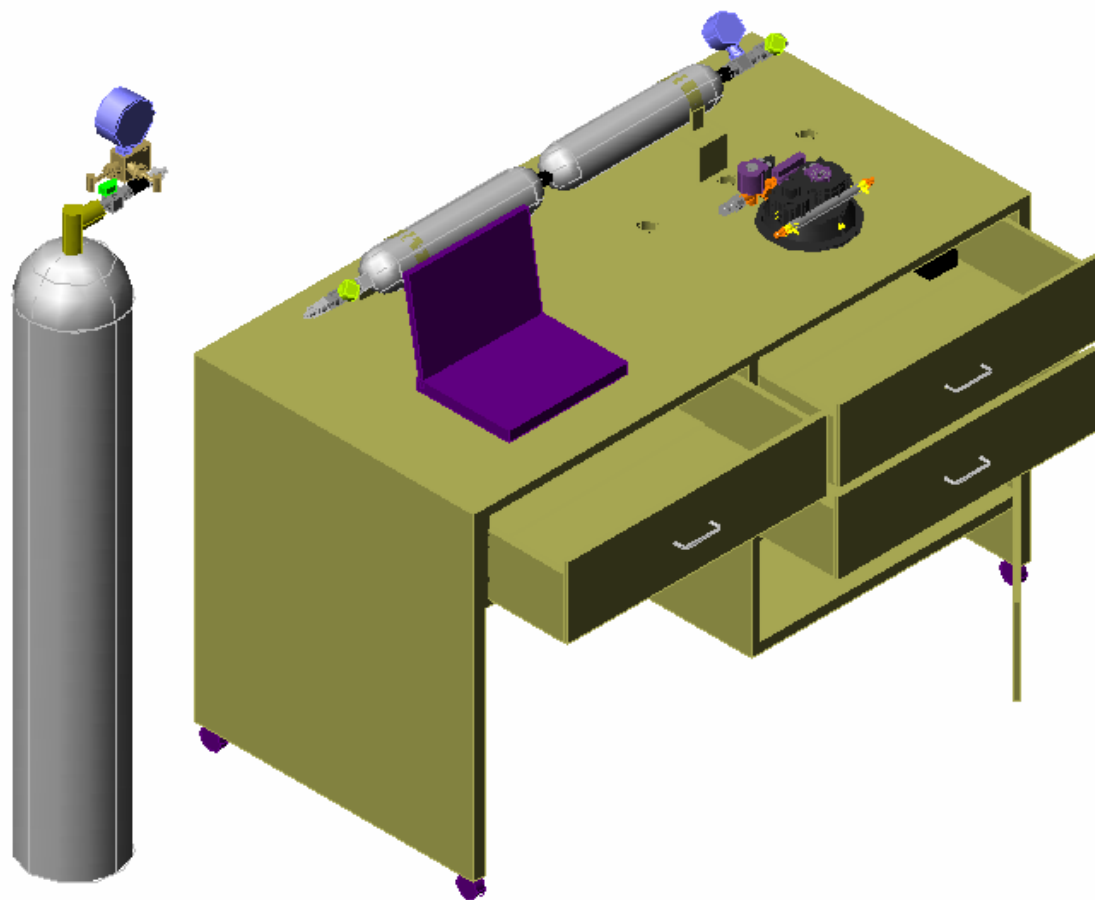


Figure 4.21: Pressure Regulator Test Bench

CHAPTER 5

REFINEMENT OF PRESSURE REGULATOR DESIGN

5.0 Introduction

In order to acquire an optimum design of pressure regulator, an improvement of design regarding to the previous prototype pressure regulator design has been completed by using finite element analysis. A structural analysis on pressure regulator of Natural Gas Vehicle-Motorcycle (NGVM) implemented through finite element analysis (FEA). The finite element method uses a substitute structure, whose parts are in a sense, pieces of the actual structure. Our substitute structure is a finite element. Serious study of solid and contact element have to be conducted prior to continue with the modeling process.

Detailed drawing of the pressure regulator model is visualized in three dimensions, symmetric and asymmetric via AUTOCAD V2004 and SOLIDWORK V2005 computer programmed. The model then exported to MSC/NASTRAN to perform analysis of flow rate deformation and stress of regulator base. In addition, structure vibration also is analyzing in order to verify the structure body of NGVM pressure regulator

In the analyzing process, the process have to be repeated if it does not well performing these way errors contributed from convergence to boundary conditions, meshing and material properties. The simulation work is considered completed if simulation result is successfully obtained. Comparison of the various results obtained has

to be carried out to predict the characteristics of fluid flow in term of pressure reduction caused by various setting of valve and forces exist on the regulator wall.

The exact deformation and stress tensor provided by the selected material of construction is analyses when pressure 3000psi applied to regulator base to authenticate the ability of the structure to resist the force excreted by the flowing gas. Satisfactory results using the latest NGVM pressure regulator model obtained indicates the final step of the process. Figure 5.1 below showed the process flow of this research project.

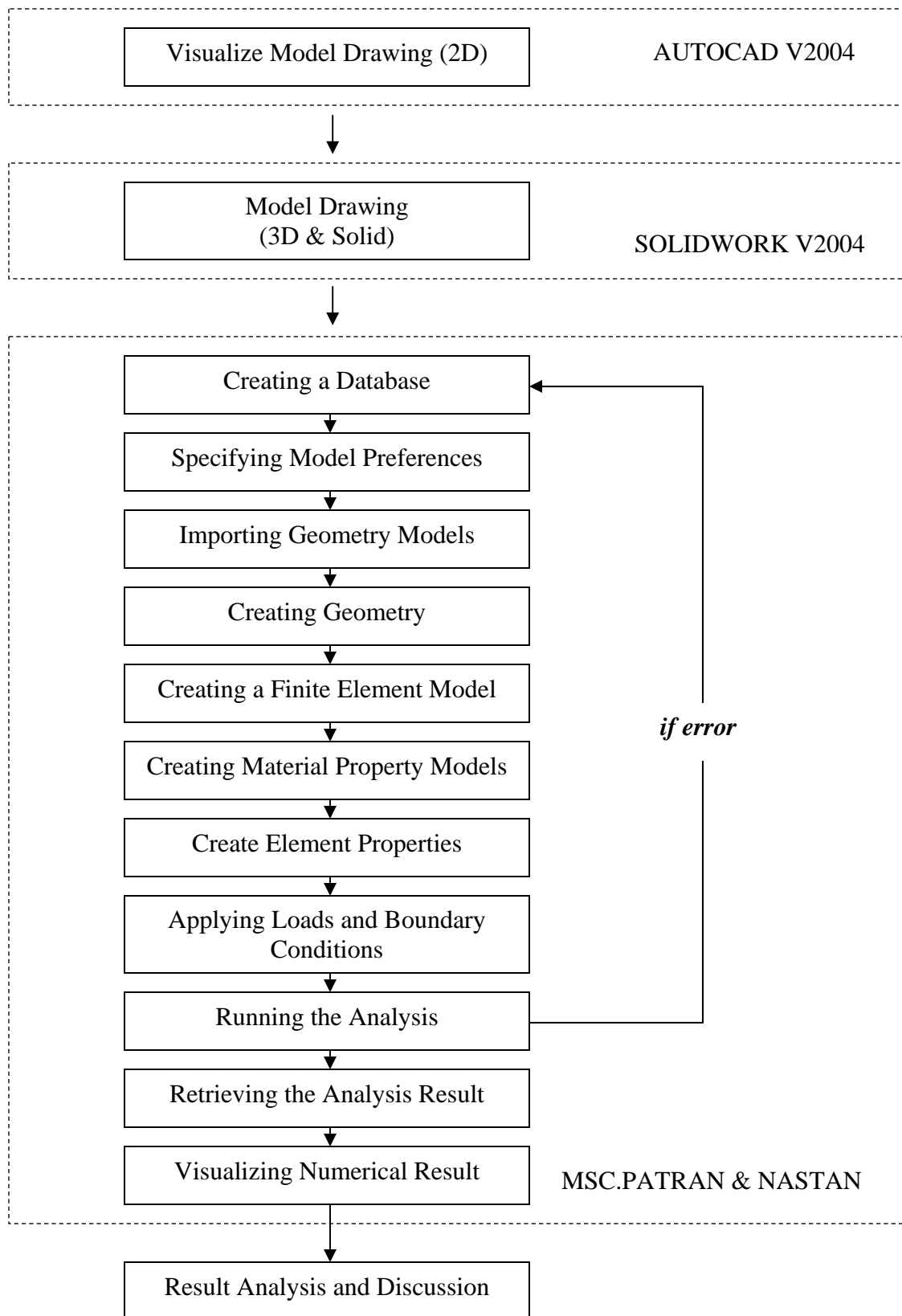


Figure 5.1: Methodology Process Flow

5.1 AutoCAD (v2004) Model Drawing

Preliminary, regulator body is drawn separately into two parts using AUTOCAD which known as Part A and Part B. Part A represents the bowl of the regulator and Part B represents the cap of the bowl. The model is based on the prototype model developed by Rahmat M., Zulkefli Y., and Shameed A in the project Development of Regulator Base. Both parts of the body is drawn in two dimensional (2D) form which shows the upper profile of Part A and bottom profile of Part B. Drawing process is carried out using AutoCAD v2004.

5.2 SOLIDWORKS (v2005) Model Drawing

Two dimensional drawing of the regulator model, then represented in solid profile by using computer program of SOLIDWORK v2005 ha been constructed. From this process, the model can be viewed in three dimensions (3D). The model of regulator is drawn separately in Part A and Part B for easier analysis process. Drawing process based on the two dimensional (2D) drawing. At this stage, structural modification and thickness are carried out on the original model of regulator in order to obtain the ideal design of NGVM regulator with the optimized thickness.

For the finite element analysis, the entire solid drawing model has to be saved in IGES File (*.igs) by changing the format of saving file in the SOLIDWORK (*.prt;*.sldprt). It is important to ensure the MSC.PATRAN (v2005r1) programming can read the file for the simulation analysis on the structure.

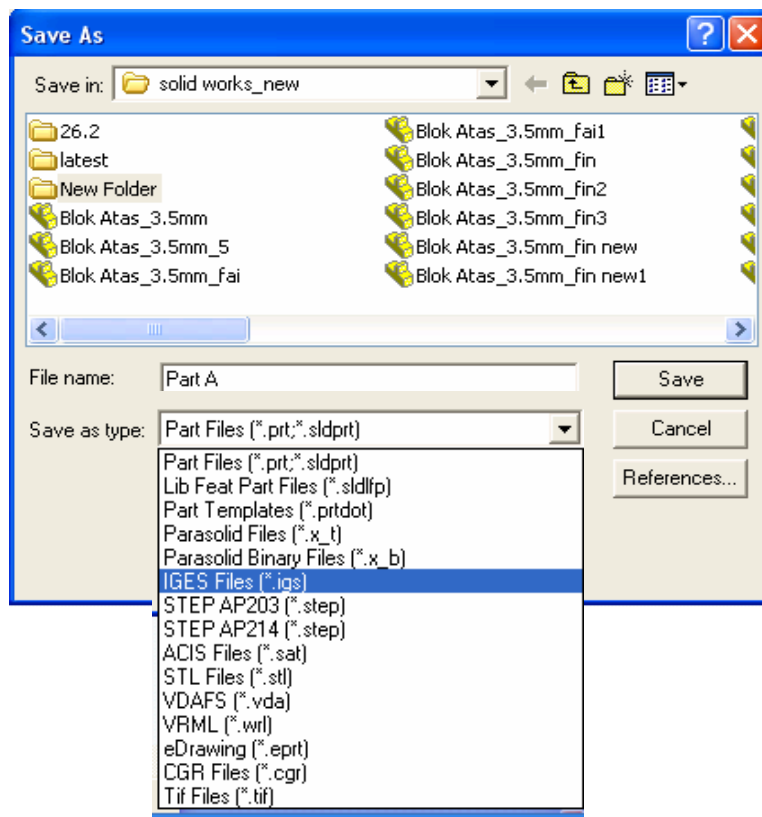
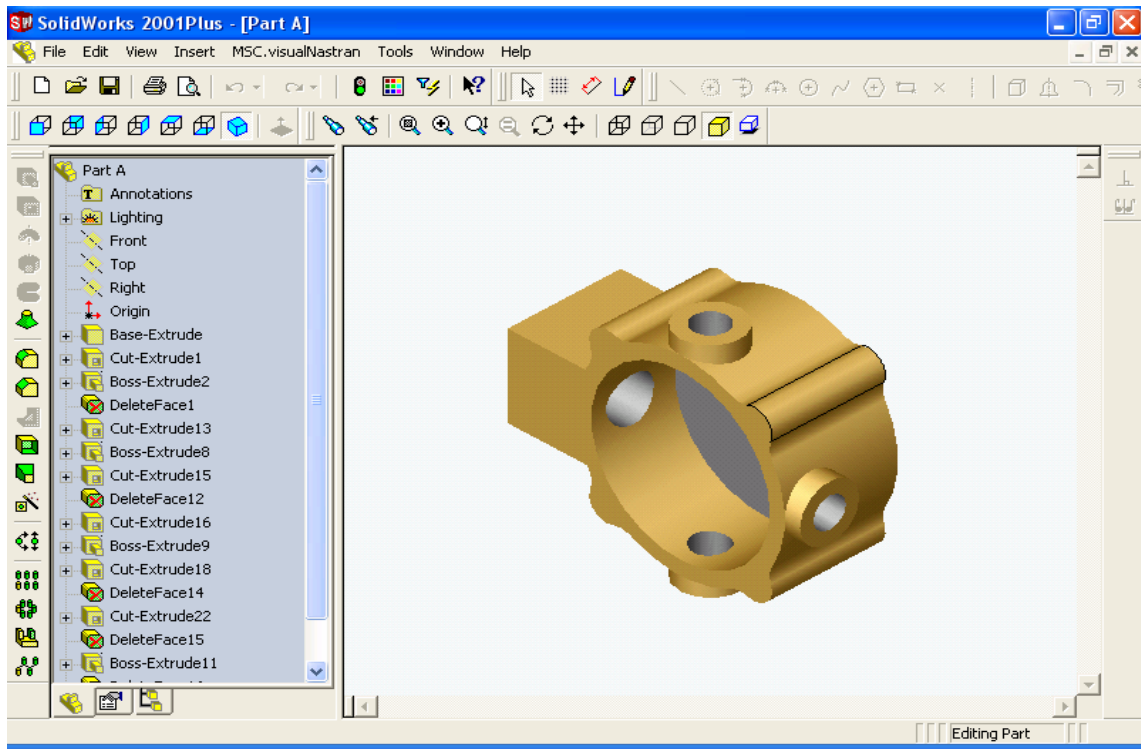


Figure 5.2: SOLIDWORK IGES File Save Format

5.3 MSC.PATRAN (v2005r1)

MSC.PATRAN v2005r1 is the platform used to develop and establish all the requirement of the model required to perform finite element analysis. It is considered crucial to carry out pre-processing prior to solve mathematically of the model using NASTRAN solver. Both of the two programming system are bundled in a package. The analysis of the result will be presented graphically by using the MSC.Patran platform.

Finite element analysis codes use sophisticated structure analysis techniques to predict the response of the model. A computer model submitted to an FEA code for evaluation must be broken into small units called finite elements. The code then applies fundamental engineering principles to calculate the response of the model. The analysis in term of deformation and stress tensor are carried out to the structure of regulator body to ensure the model is safe to operate at applied pressure. The following Figure 5.3 shows several tasks has to be taken to perform such analysis.

5.3.1 Database Creation

The first step in this program analysis is creating a new database as shown in Figure 5.3. To create a new data base, 'File' button has to be selected, followed by clicking 'New' in the 'Main menu'. New Database form will display. Specified Project name in the form of New Database, and followed by clicking OK. .Now, the entire icon in the program can be activated.

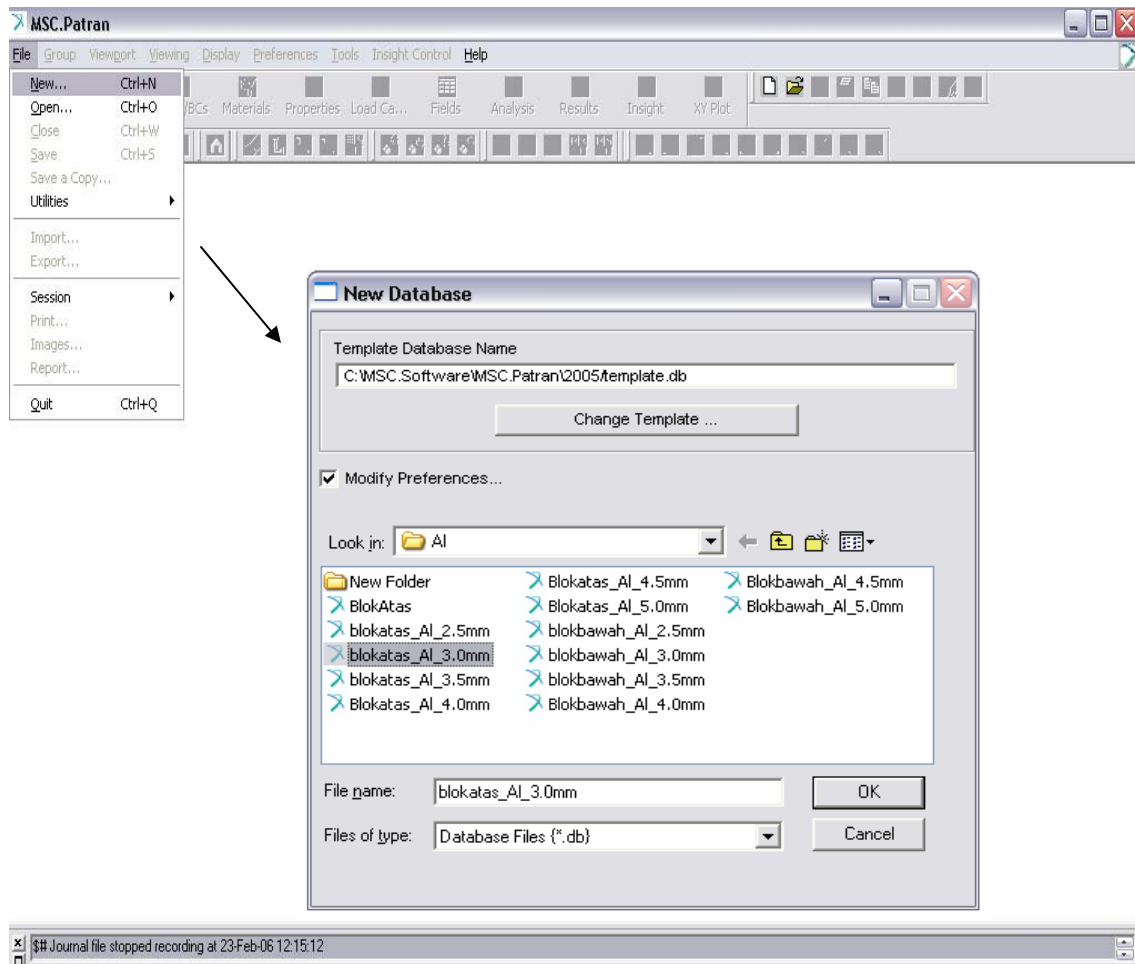


Figure 5.3: Database Creation Window

5.3.2 Model Preferences Specification

It is important to select the Analysis Code, Analysis Type and Global Model Tolerance before begin building analysis model. New Model Preferences form automatically displays right after completing the New Database form as shown in Figure 3.4 below. Global Model Tolerance impact how to construct the model. While, Analysis Code and Analysis Type affect code specific forms as well as the options available for elements types, element properties and material definition. Firstly, **Default** was chosen for the 'Global Model Tolerance', followed by selecting **MSC.NASTRAN** as the 'Analysis Code' and **Structural** as the 'Analysis Type'. The form is complete by clicking 'OK' button.

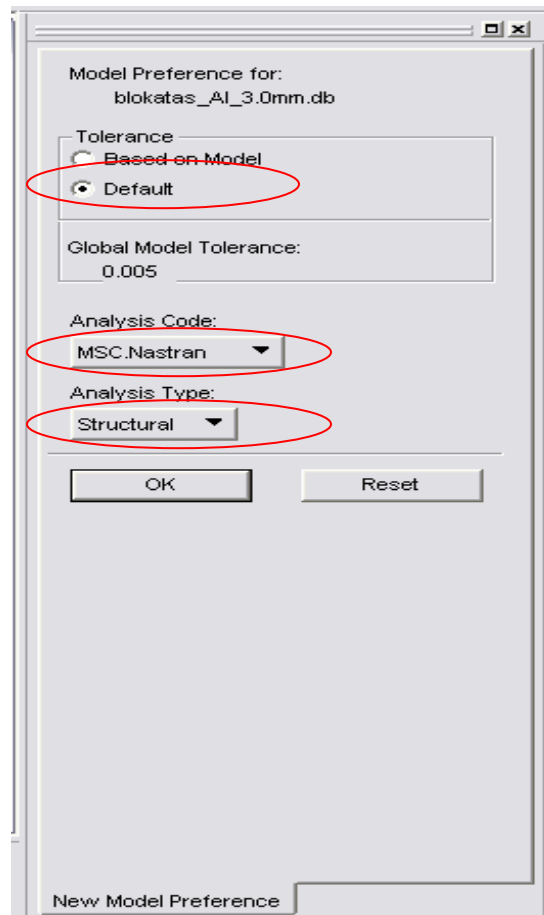


Figure 5.4: New Model Preferences Form

5.3.3 Importing Geometry Model

MSC.PATRAN has two types of choices to develop a model, either by using drawing facilities or by importing the model from other sources. In many cases, it is much more efficient to use an existing CAD geometry model created outside of MSC.PATRAN rather than constructing a new model. Importing CAD model may avoid repetitive modeling efforts and ensure better accuracy between a CAD design model and its analysis model. Other third-party modeling packages can be supported via the use of ANSI industry standard IGES (Initial Graphic Exchange Standard) protocol.

To import a CAD model, select File and click Import in the MSC.PATRAN main menu. The import form will display as shown in Figure 5.5 below. In the Object drop-down menu, select **Model**. Then follow by selecting **IGES File (*.igs)** in the Source drop-down menu. Then, the entire file name where the model was drawn and saves before is selected. The process is finished by clicking the 'Apply' button.

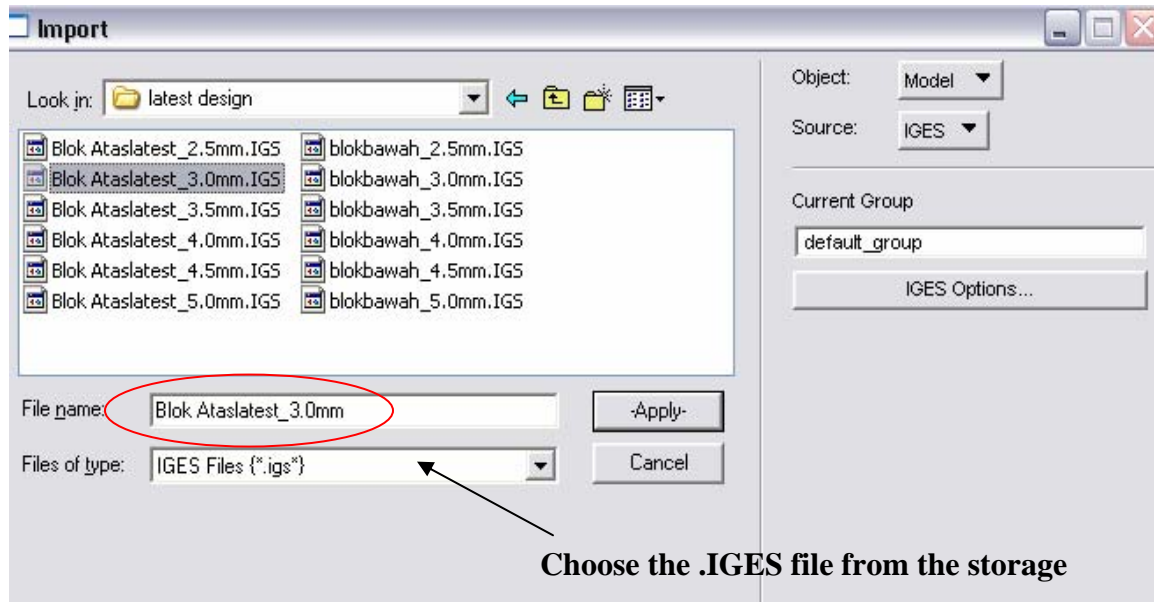


Figure 5.5: MSC.NASTRAN Import IGES File Format

5.3.3.1 Geometry Creation

Geometry creation for the model imported is started by clicking the toggle of Geometry on the MSC.PATRAN main form. The Geometry Application form will appear as shown in Figure 5.6 below. 'Create' is selected in the Action drop-down menu followed by selecting 'Solid' in Object drop-down menu. For the Method, boundary representation (**B-rep**) is selected, that comprises the entire boundary of solid. Solid ID List will become 2. For 'Surface List' textbox, drag the entire model imported on the screen layer. Finish the process by clicking the 'Apply' button.

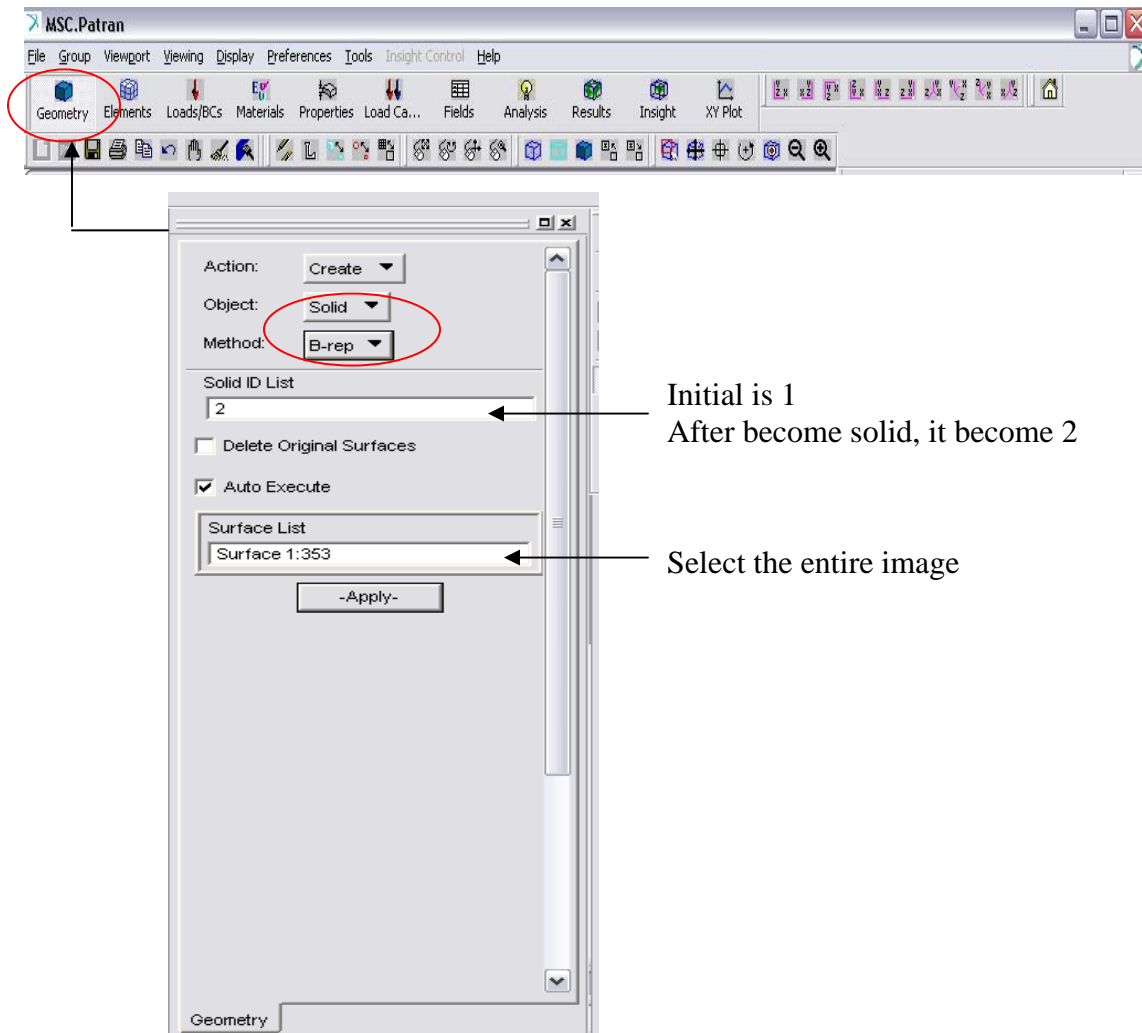


Figure 5.6: Geometry Application Form

5.4 Finite Element Model Creation

Creation of finite element mesh is started by clicking the Element toggle on the MSC.PATRAN main form. The finite Element application form provides numerous Action/Object/Type combinations that create, modify, and qualify the finite elements model to facilitate valid analysis result. The MSC.PATRAN support variety of element shapes and node configurations, and it mesh creation tools include several automated meshing techniques.

Figure 5.7 shows the Finite Element Application Form. In this application form *Create*, *Mesh* and *Solid* has been selected for the Action, Object and Type drop-down menu. Mesh is chosen as the Object because the finite element method required that divide the analysis model into interconnected pieces called element, to which separate analysis equations are assigned. A set of these interconnected elements is referred to as a mesh.

In the same main form, *Tet*, *Tet Mesh* and *Tet 10* need to be selected for the Element Shape, Mesher and Topology drop-down menu. The entire body is selected for the Input list. This process is finished by clicking ‘Apply’ button.

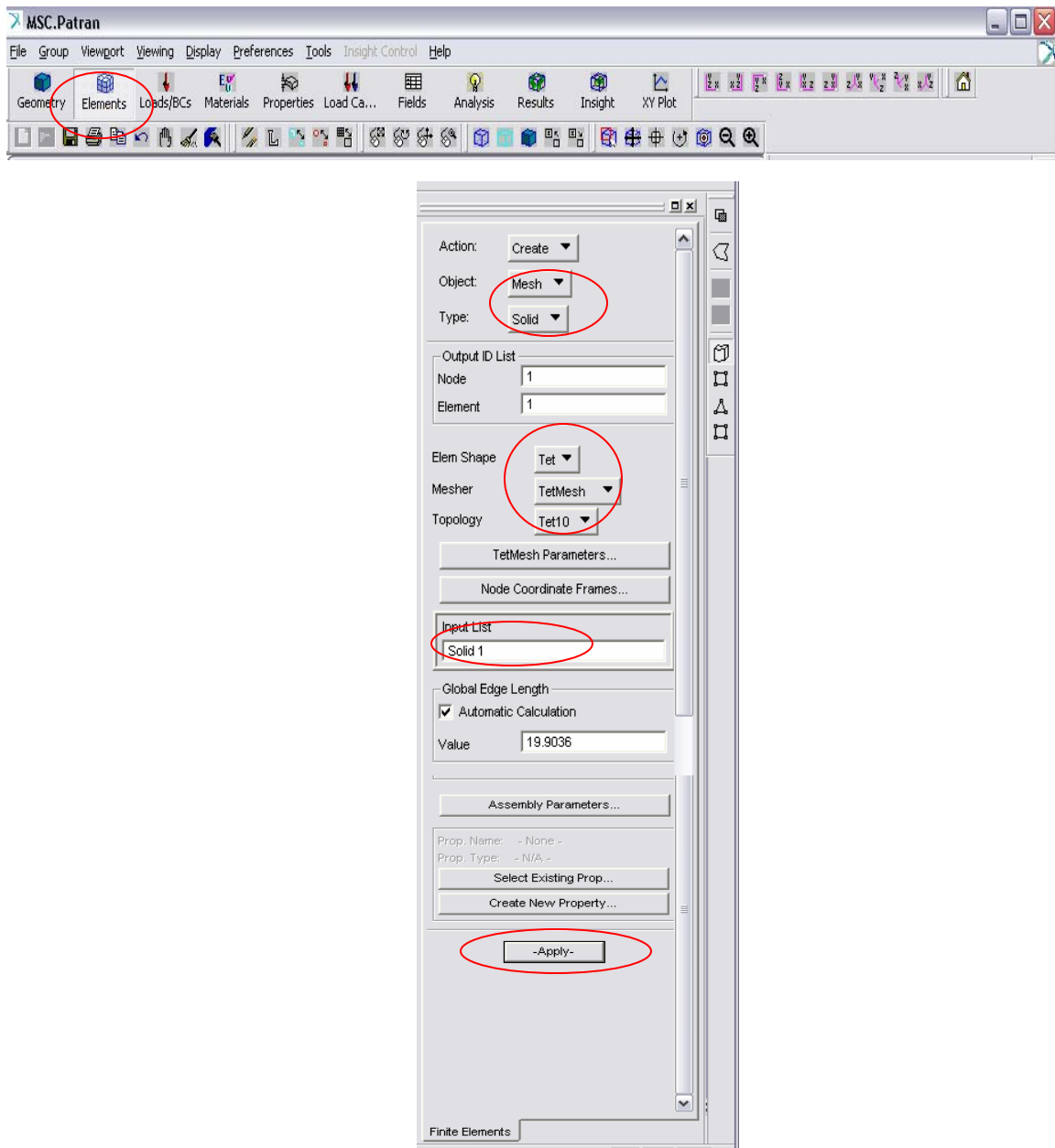


Figure 5.7: Finite Element Model Creation

5.4.1 Loads and Boundary Conditions Application

In MSC.PATRAN, load and boundary conditions (LBCs) are treated as a single type of data to be assigned to portions of geometry or finite element model. In a structural analysis problem, we are generally trying to determine the response of the model to physical loading, or specific structural behaviors such as frequency response or buckling. Some of LBCs may work with included force, pressure, velocity, initial load, displacement, temperature and contact. In this structure regulator base analysis, the LBCs just require analysis in term of pressure and displacement analysis.

The LBCs application is where to define the load and boundary condition sets for model analysis. To excess this application form, click Load/BCs toggle on the MSC.PATRAN main menu. LBCs application form provided function to create, modify and show a range of load and boundary data. To apply displacement force to the analysis model, **Create**, **Displacement** and **Nodal** is selected from Action, Object and Type drop down menu as shown in Figure 5.9.

By clicking New Set Name textbox, the name for the displacement analysis will be specified. The Input Data unfold box has been selected on the application form to bring up the Input Data Sub form. By using this form, displacement data boundary condition has been specified by setting the Load/BC Set Scale Factor as **1**. Then, the Translation <T1 T2T3> and Rotation <T1 T2 T3> specified as **<0 0 0>** in the list box and finishing by clicking 'OK' button.

By selecting the Select Application Region unfold box, the Select Application Region sub form will appear as shown in Figure 5.10. Set Geometry as the choice of Geometry Filter in this sub form. For the, **Select Geometry Entities** list box, surface to applied displacement force will be selected. It is followed by clicking 'Add' button. Figure 5.9 shows geometry model after meshing.

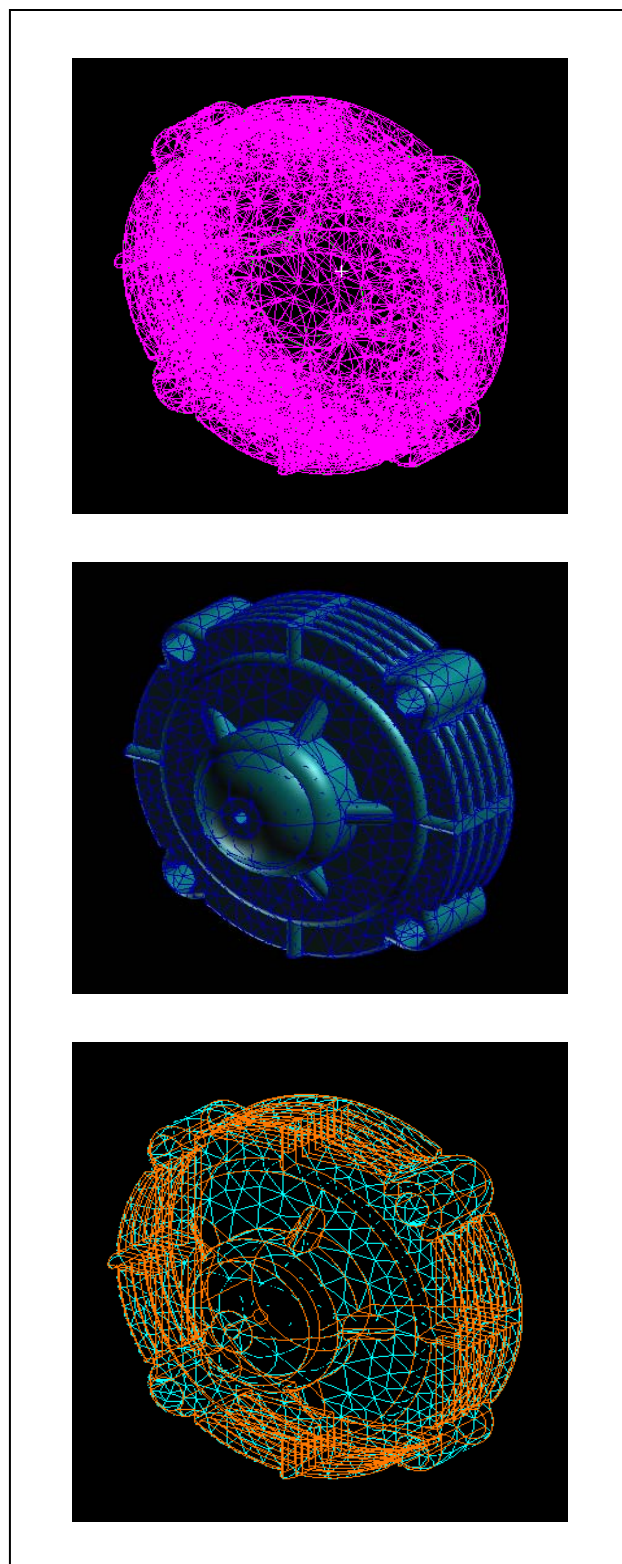


Figure 5.8: Geometry Model After Meshing

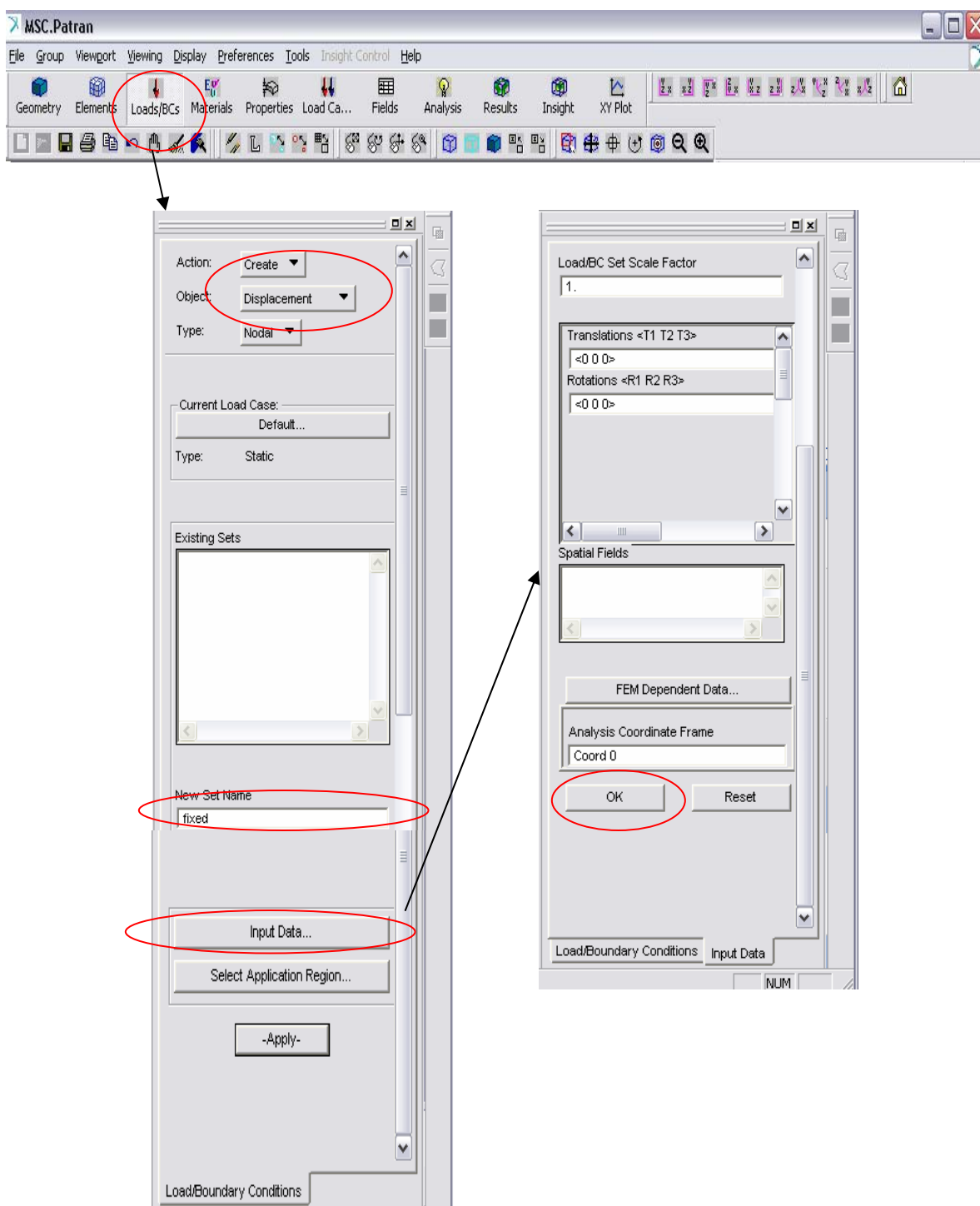


Figure 5.9: Load/BCs Application Form for Displacement Force

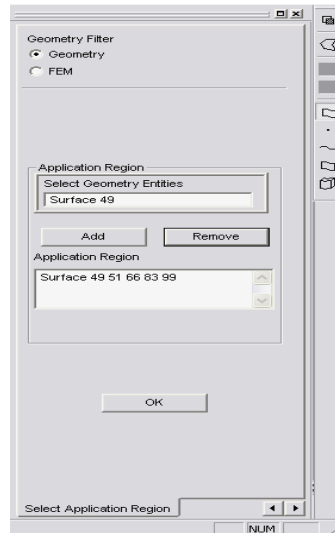


Figure 5.10: LBC Select Application Region Subform for Displacement Force

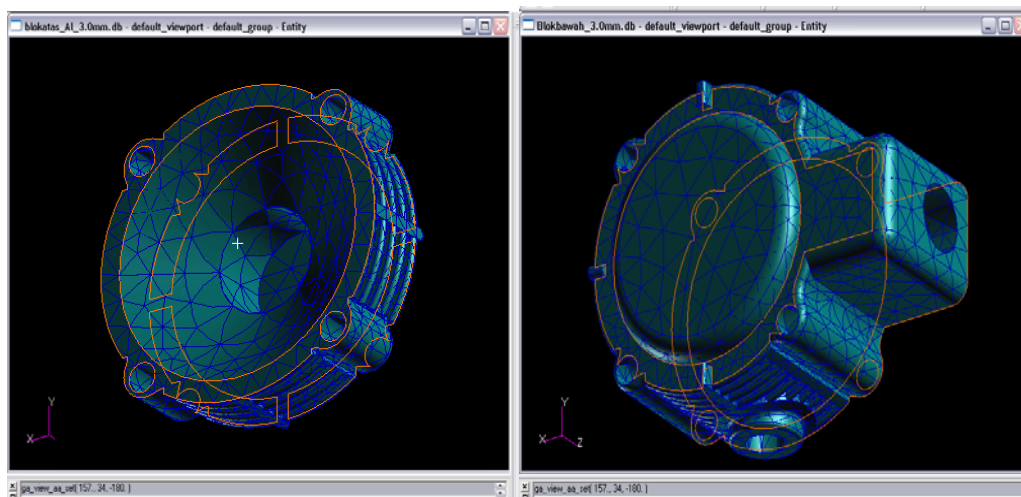


Figure 5.11: Region of Displacement Force Application (Red Line)

After completing applied displacement force to the structure case, the second step of this process is applying the pressure force to the structural. Using the same application form, the Action, Object, and Type drop-down menu is change to **Create**, **Pressure** and **Element Uniform**. Then, New Set Name for this analysis is specified. As procedure before, by clicking on the Input Data, sub form of Input Data will be filled up by the required pressure value, which is 3600psi (20.7 E+07 Pascal). With the same concept, at the Application Region the entire region for the applied pressure force is

selected as shown in Figure 5.12 below. The process is completed by clicking ‘OK’ button and ‘Apply’ button in main application form. Figure 5.13 shows the geometry after displacement and pressure force applied.

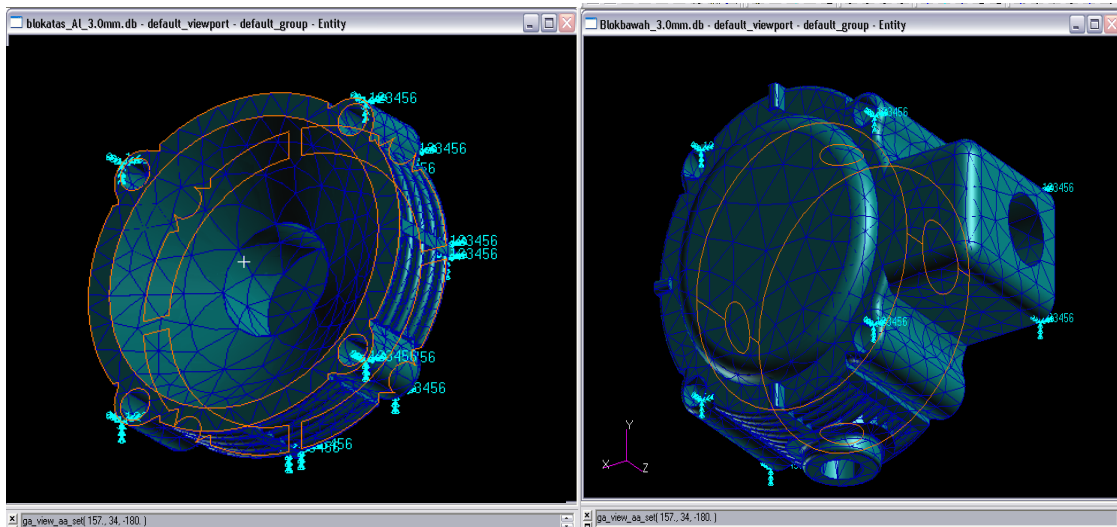


Figure 5.12: Region of Pressure Force Application (Red Line)

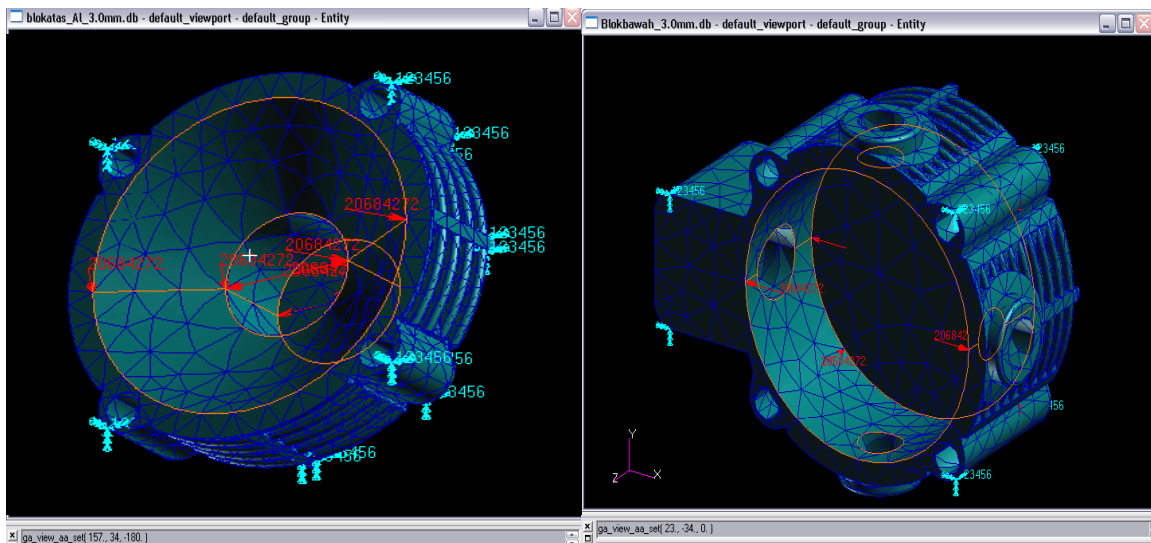


Figure 5.13: Geometry Model after Displacement and Pressure Force Applied

5.4.2 Material Property Models Creation

A material model is a group of material properties that describe what model is made (such as pure element or composite) and the attributes of that material (stiffness, density and so on). The material application is the platform to define materials for model analysis. It can be done by clicking the material button on the MSC.PATRAN main form. The Material Application form will appear in the view port as shown in Figure 5.14.

'Create', *'Isotropic'* and *'Manual Input'* has been selected as Action, Object and Method in drop-down menu. Isotropic is chosen in this analysis because material properties for the model, needed to be developed are the same in all direction. While, Manual Input provided the input option form that used to input material property data. Then, the Material Name textbox is filled with the specific material name that is needed to be used for the analysis process. Each material must have a unique name which will be assigned a sequential Material ID number automatically. By clicking Input Properties button in Material application form, separate Input Options sub form will appear in the view port as shown in Figure 5.14.

For Constitutive Model drop-down menu in this sub form, Linear Elastic is selected and followed by filling the material property values in the form. This project is running the analysis for structure, so the value of Thermal Expansion Coefficient, Structural Damping Coefficient and Reference Temperature are not necessary. This process is completed by clicking 'OK' button in Input Options form and 'Apply' button in Material application form.

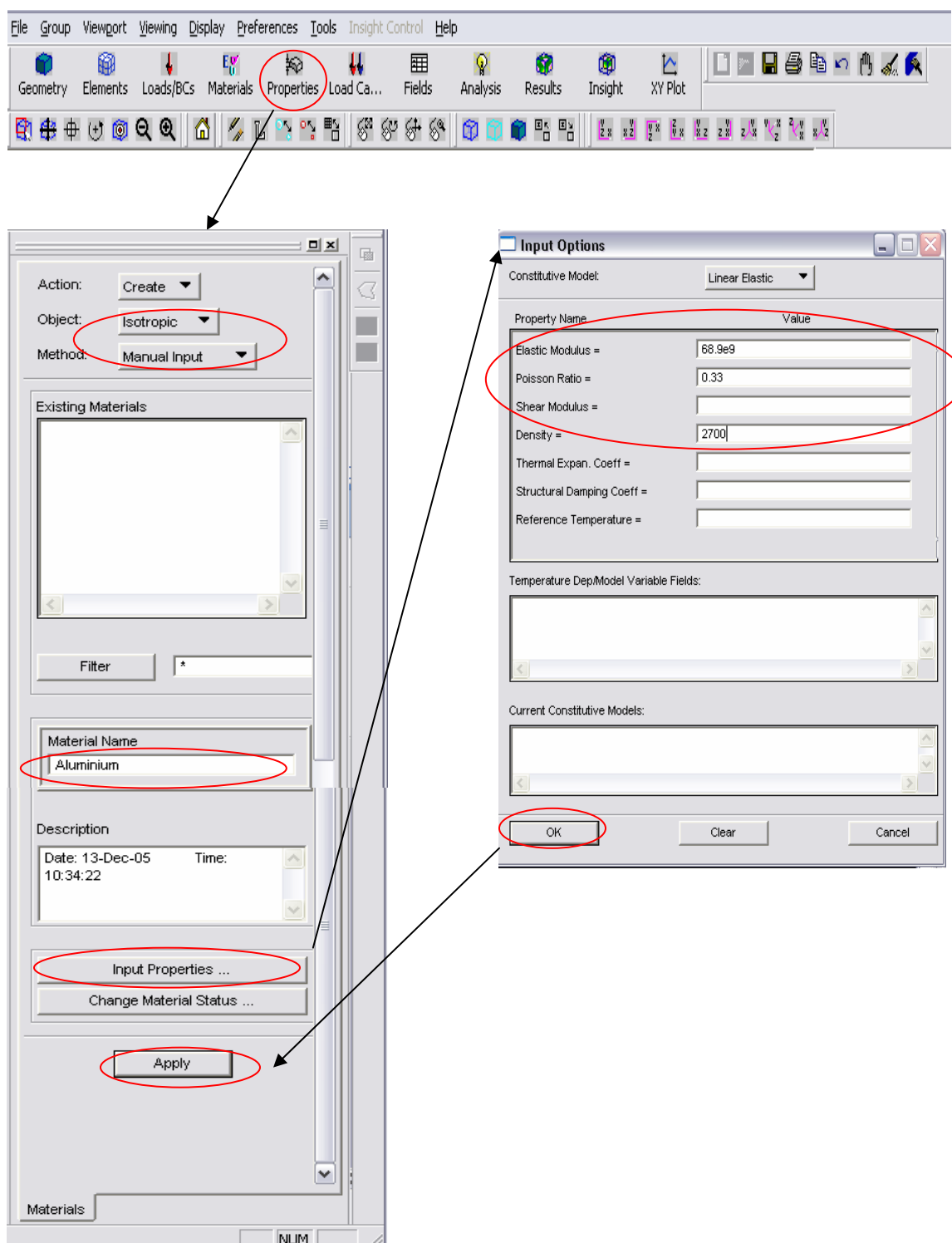


Figure 5.14: Material Property Models Application Form

5.4.3 Element Properties Creation

Through the Element Properties application, element type (such as beam and shell) and element related properties for region of the model is defined. These defecations to geometric or FEM entities is later assigned. Element type selection is based on dimensions of the model and assumptions on model behavior.

Properties toggle has been selected in the MSC.PATRAN main menu to excess the Element Property application form. The Element Property application form will appears in the view port as shown in Figure 5.15 below. In the main screen of this application form, **Create**, **3D** and **Solid** for Action, Object and Type drop-down menu needs to be selected. Properties set name for this analysis in the Property Set Name textbox requires to be specified. It needs another unique name to specify this property. In the Option part, **Homogenous** and **Standard Formulation** has been selected on its drop-down menu. These Option pop-up menus are specific analysis code and have to be referred to documentation for the analysis code.

Sub form of Input Properties will appear as shown in Figure 5.15 by clicking the Input Properties button in Element Properties application. This sub form prompt to provide additional required and optional information. Material name that has been selected before in creating material property models is selected for the Material Name list box, on Input Properties form. It is followed by clicking 'OK' button. Back to the Element Properties form, the entire geometry identity model needs to be dragged for the 'Select Member' list box. This form is completed by clicking the 'Apply'.

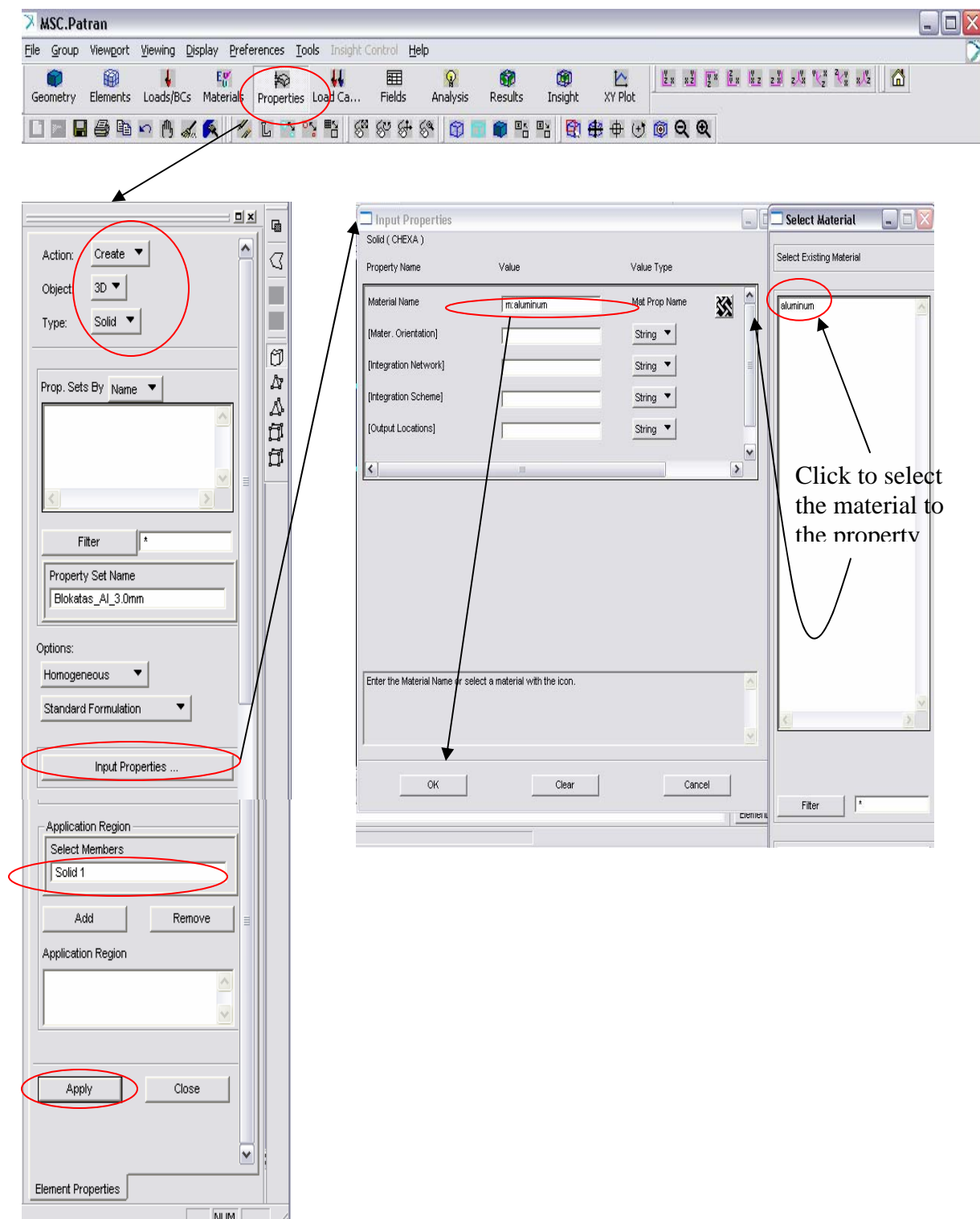


Figure 5.15: Element Properties Application Form

5.4 Running the Analysis

To run the analysis application, Analysis button is selected on the MSC.PATRAN main menu. The analysis form will appear as shown in Figure 5.16 below. **Analysis**, **Entire Model** and **Full Run** need to be selected for the Action, Object and Method drop-down menu. Then, the Code and Type of analysis have to be checked to ensure the code and type analysis used is **MSC.NASTRAN** and **Structural**. Job name for this analysis in Job Name textbox must be defined. This name will be attached to all files associated with this particular analysis run.

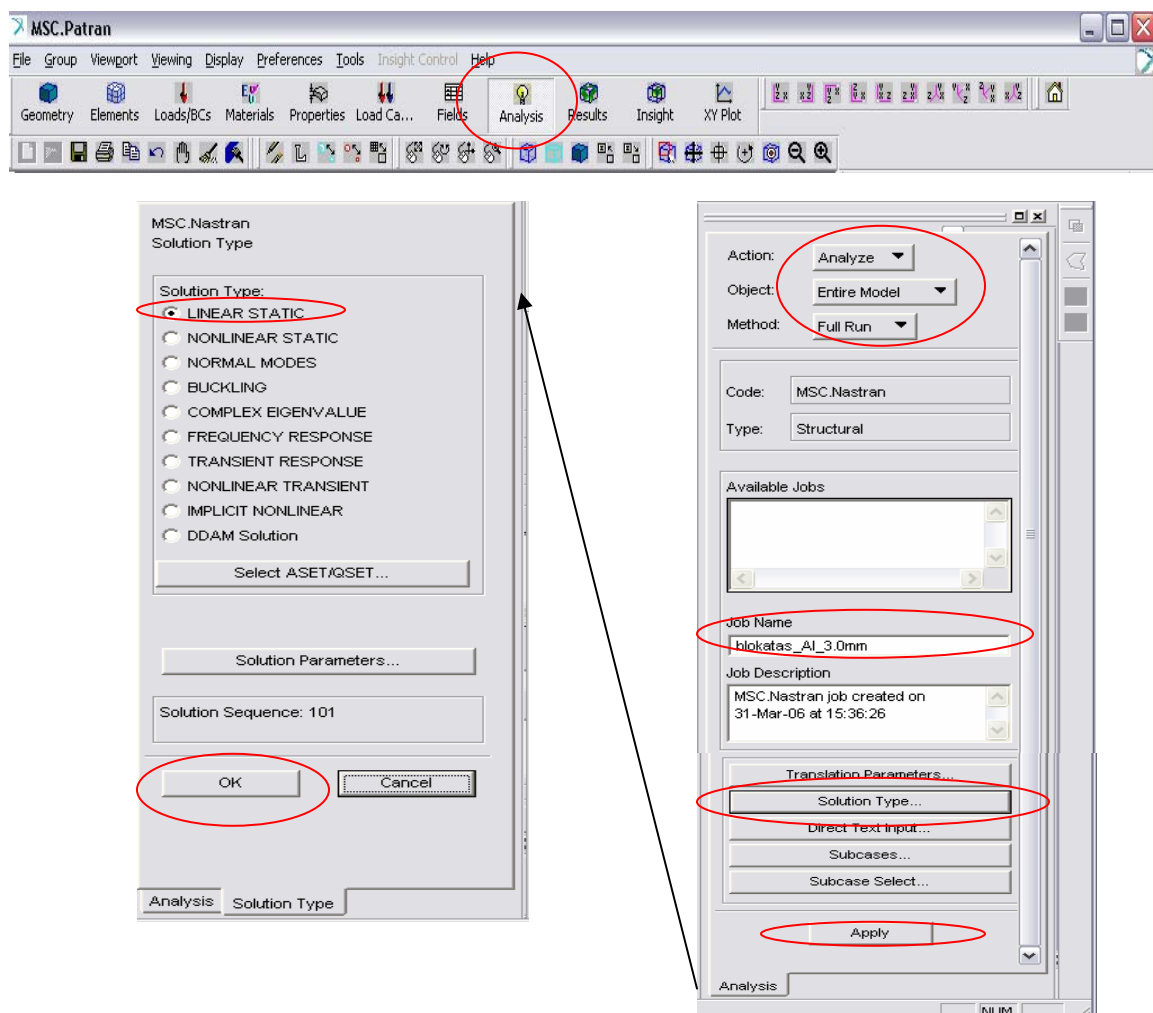
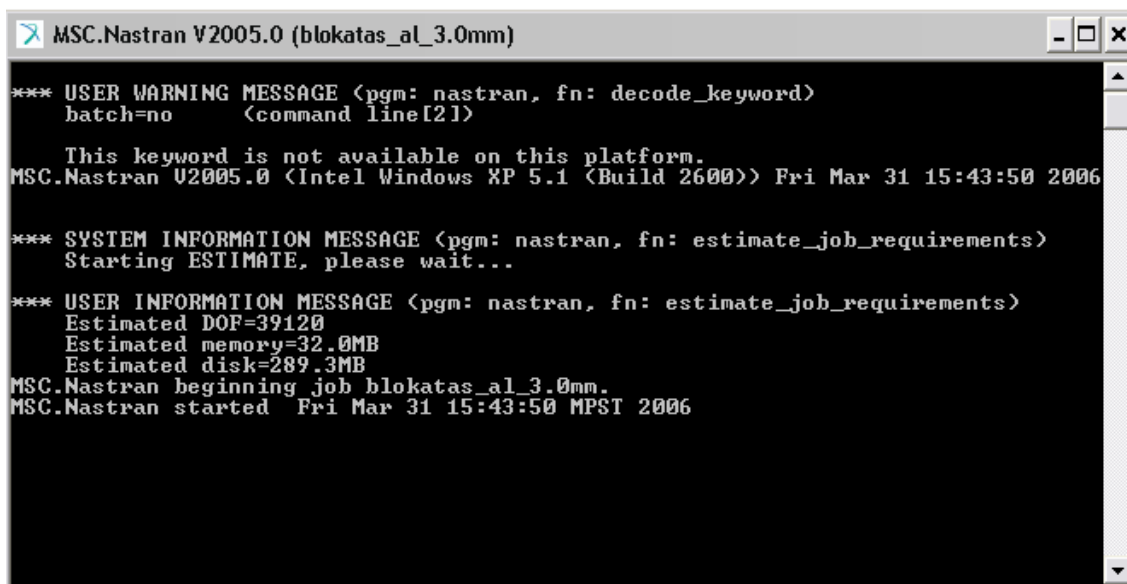


Figure 5.16: Analysis Application Form

Linear Static is chosen as the Solution Type for the analysis and followed by clicking 'Ok' button. Then, 'Apply' button need to be clicked to finish this process in Analysis application form. In running the analysis, we can monitor the analysis by receiving updates as how the analysis is progressing in the MSC.PATRAN history area. A common prompt window will pop out to show the simulation is running, shown in Figure 5.17. After the "bit" sound is heard, this shows that the simulation is done. Once the analysis is complete, we will be noticed in the history blue flagged.



```

*** USER WARNING MESSAGE (pgm: nastran, fn: decode_keyword)
    batch=no      (command line[21])

    This keyword is not available on this platform.
MSC.Nastran V2005.0 (Intel Windows XP 5.1 (Build 2600)) Fri Mar 31 15:43:50 2006

*** SYSTEM INFORMATION MESSAGE (pgm: nastran, fn: estimate_job_requirements)
    Starting ESTIMATE, please wait...

*** USER INFORMATION MESSAGE (pgm: nastran, fn: estimate_job_requirements)
    Estimated DOF=39120
    Estimated memory=32.0MB
    Estimated disk=289.3MB
MSC.Nastran beginning job blokatas_al_3.0mm.
MSC.Nastran started  Fri Mar 31 15:43:50 MPST 2006
  
```

Figure 5.17: Common Prompt Window

5.6 Retrieving the Analysis Result

After running the analysis, result of analysis is read back into MSC.PATRAN by attaching the result file. In the same analysis application form, the Action, Object and Method from the drop-down menu is changed to **Access Results**, **Attach XDB** and **Result Entities**. Form of Select File will appear by clicking Select Results File button as shown in Figure 5.18. In this form the entire file name of the analysis running before is selected,

and followed by clicking 'OK' button. The process is finished by clicking 'Apply' button on the Analysis application form.

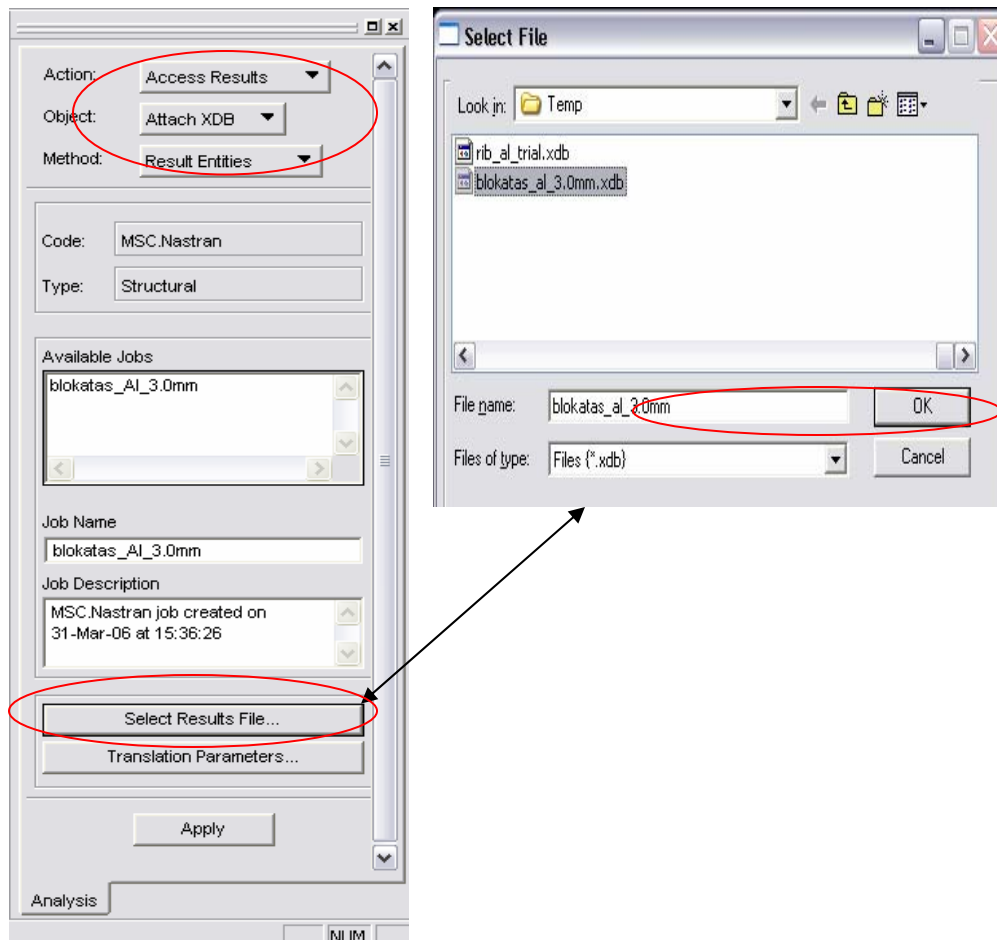


Figure 5.18: Access Result Application Form

5.6.1 Numerical Result Visualization

To visualize the analysis result, the result button needs to be selected on the MSC.PATRAN main menu. Analysis application form will appear as shown in Figure 5.19 below. Quick plot is created by selecting *Create* and *Quick Plot* as Action and Object drop-down menu. Then, *Stress Tensor* is selected as the *Fringe Result* and

Displacement, Translational as Deformation Result. This process is completed by clicking the ‘Apply’ button.

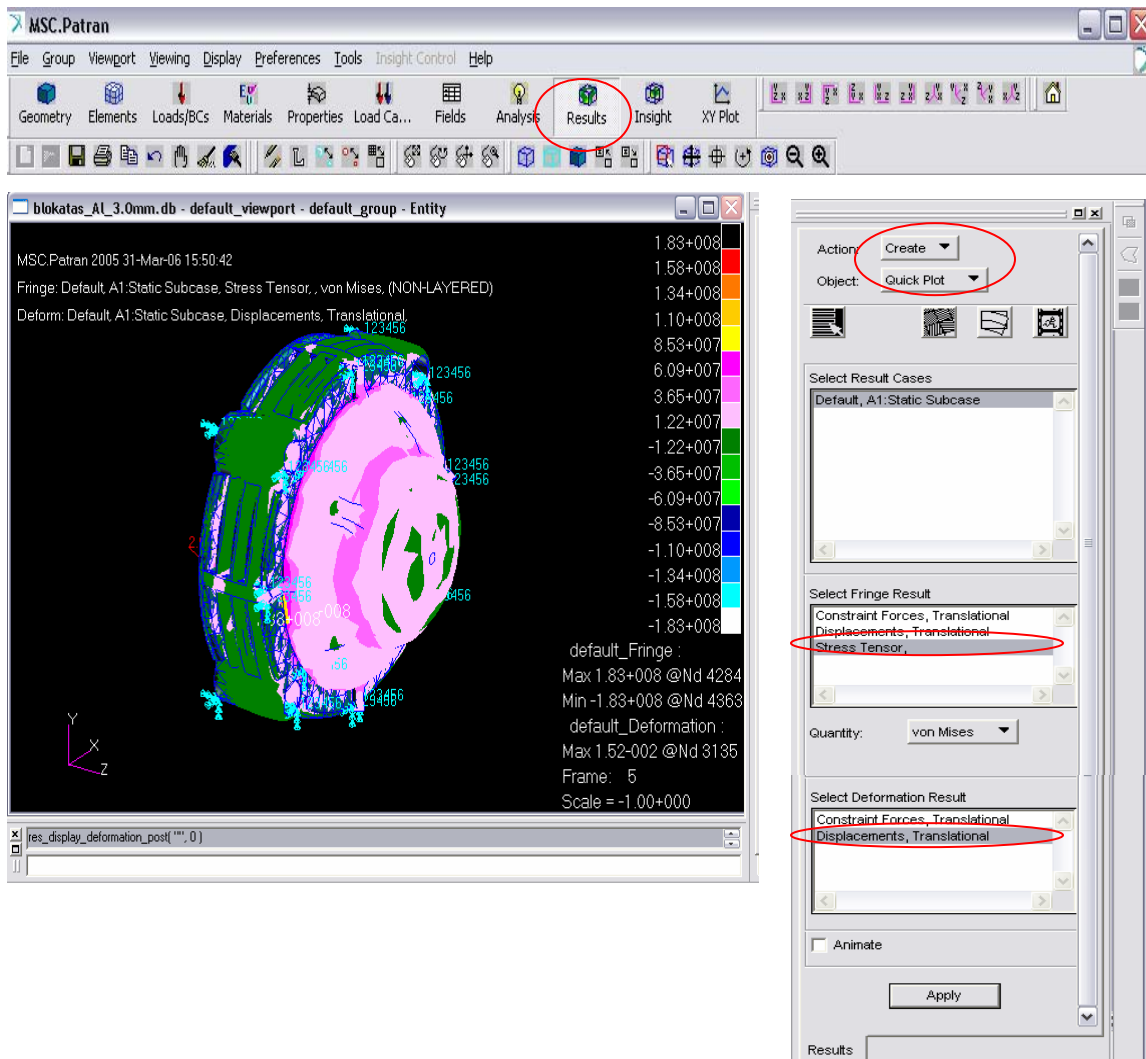


Figure 5.19: Result Visualization

The ability to visualize the results using computer graphics, animation and other results tools provides a real, visual sense of a model's behavior. Interactive results display represents the link between finite elements analysis and the engineering judgment. Visualization of simulation result, such as color –coded result displays, deformed shapes, animations of how the model behave , and numerical result values, give

the insight needed in verifying our model design. It is important for the modification and improvement of the critical or undeformed region of the design.

5.7 Analysis and Discussion

The result of simulation has to be analyzed to obtain the ideal structure of NGVM pressure regulator body structure. The structure analysis is carried out to authenticate the ability of the structure to resist force excreted by the flowing gas through the FEA tool element. Analysis of results obtained, including the comparison of selected material to fabricate the regulator base is further deliberated in the following Chapter 6.

CHAPTER 6

RESULTS AND DISCUSSION

6.0 Introduction

This chapter is designated to discuss the results attained through the methodology undertaken in the previous chapter to meet the objective of this study. The methodology section began with the design and development of pressure regulator combined with the knowledge gained in Chapter 2 and Chapter 3 on regulator provides the regulation mechanism. This is the core of the study where work begins with the restricting element design aided by the computational fluid dynamic and ends in the minimal wall thickness evaluation. Shortly thereafter, it continues with the refinement of pressure regulator design by using Finite Element analysis (FEA) method in order to improve the previous single step pressure regulator design. The outcomes of the evaluations that have been optimized are discussed in this chapter. The prototype results would be the first section of the chapter. This section would begin with the restricting element design followed by the material selection and all other design works. The regulator actuation, loading element, and regulator body results depend strongly on the material selection. This would be followed by the fabrication of the prototype which has resulted from the methods described. The pressure regulator prototype model is then assessed using the pressure regulator test bench. Subsequently, results of an improvement of the pressure regulator prototype design are also being discussed in this chapter followed by the two dimensional modeling, solidified modeling, MSC PATRAN/NASTRAN analysis, simulation analysis for single step regulator, the comparison on

MSC/PATRAN results and lastly the comparison on the material selection. Finally this chapter would present the test results of the pressure regulator using the dedicated pressure regulator testing facilities.

6.1 Regulator Restriction Results

The evaluation on the path taken by the gas from the cylinder to the restricting element showed that the smallest cross sectional area occurs at the high pressure tubing. This high pressure tubing link connects the storage tank and the pressure regulator. This 3 mm inner diameter would cause “choke” to occur. The design of the valve seat to be smaller than this value would cause further choke thus further limiting the maximum amount of gas capable of flowing through. This would limit the maximum capacity of the regulator. On the other hand the design of the valve seat to be greater than 3 mm would not increase the maximum flow rate as the choke would have already occurred to the mass flow downstream. Having a bigger valve seat would impose a greater force for the obturator to oppose during closure. As we know force is pressure multiplied by the area its acting upon, thus the force upon the obturator may be manipulated by decreasing the valve seat area to be minimal. The incoming pressure acting on the obturator is unable to be manipulated as it is a factor of the amount of gas within the storage cylinder. This elaborated argument depicts that the valve seat should be designed to have 3 mm in diameter as it would be the optimal value giving maximum capacity for the regulator with minimal load on the obturator.

As we recall, the choke flow evaluation was used to evaluate suitable valve seat sizing while the Computational Fluid Dynamic Software FLUENTTM was used to evaluate the obturator movement away from the valve seat to provide the amount of gas required by the system. The pictorial description in Figure 6.1 shows the flow of the fluid from the inlet to the outlet around the obturator. The 3-Dimensional simulation results have been sliced to form various planes such as the inlet plane, the

outlet plane and the 4 cross-sectional planes. The values of various parameters such as velocity, temperature and density are viewed as post processing results of the simulation.

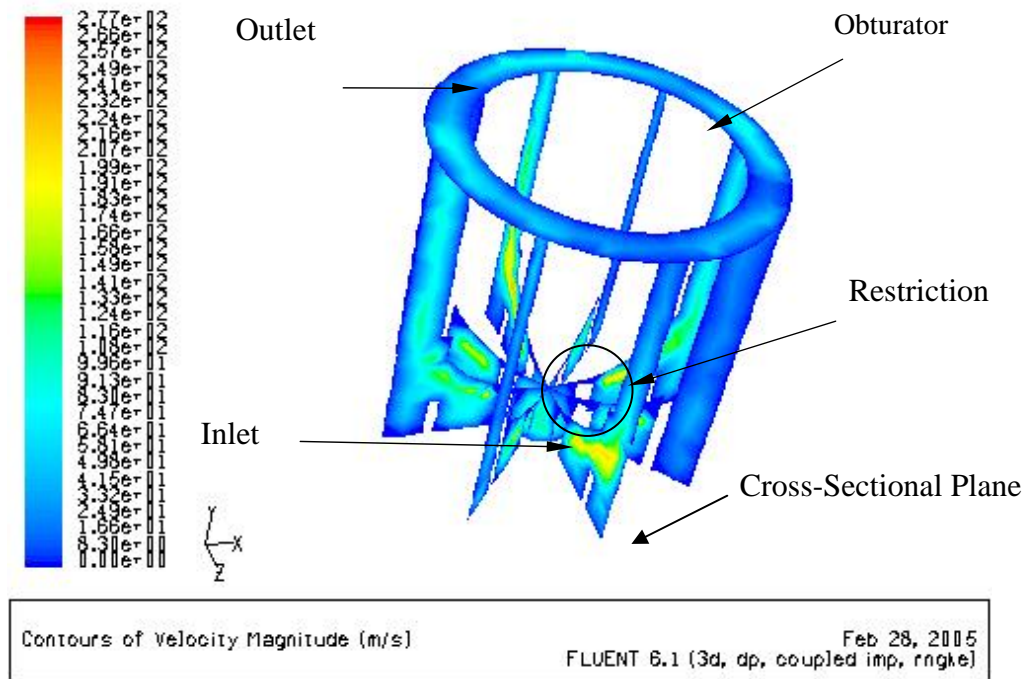


Figure 6.1: 3-Dimensional Fluid Flow Pattern Around the Restricting Element.

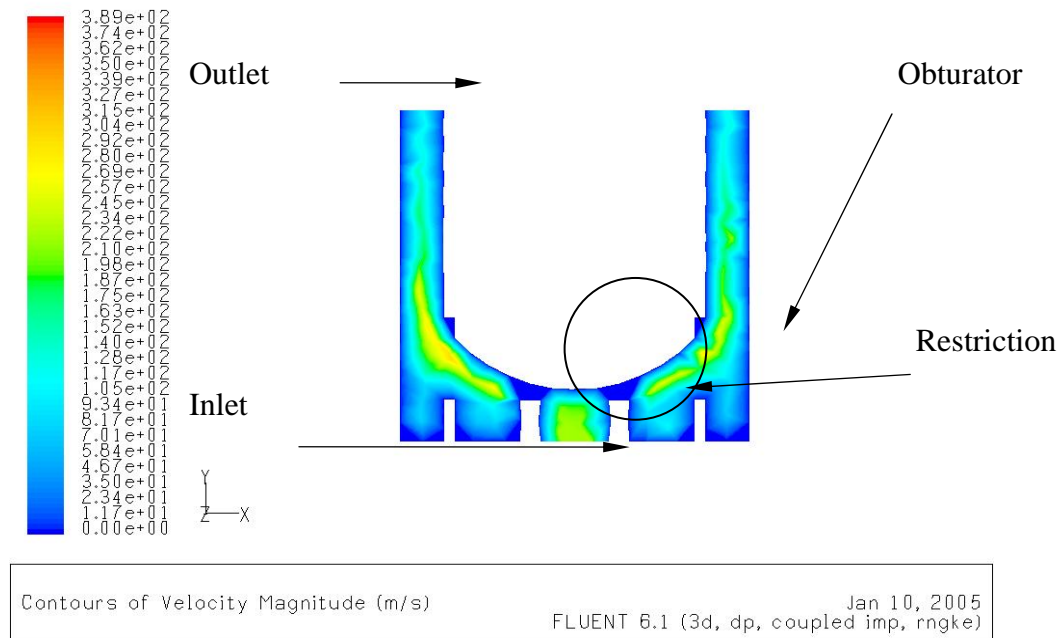
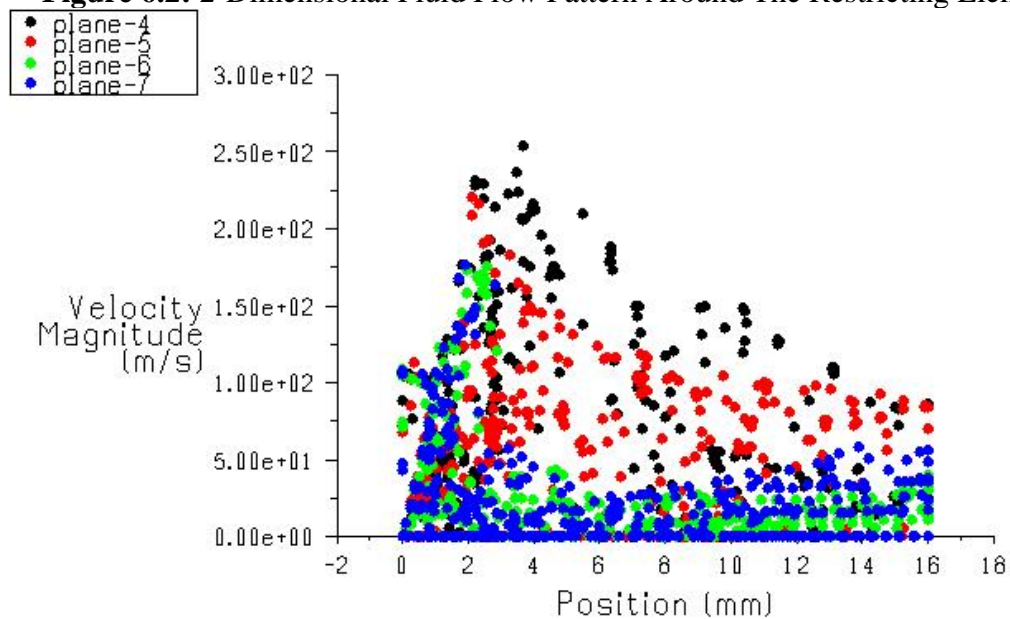
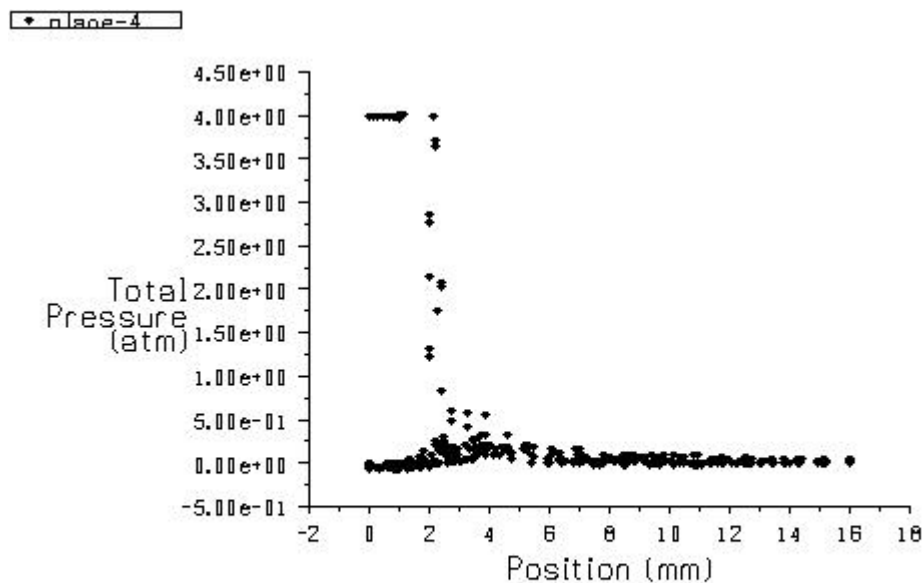


Figure 6.2: 2-Dimensional Fluid Flow Pattern Around The Restricting Element.

Velocity Magnitude

Feb 28, 2005
FLUENT 6.1 (3d, dp, coupled imp, rngke)**Figure 6.3:** Velocity Magnitude of Each Cross-Sectional Plane.

Total Pressure

Feb 28, 2005
FLUENT 6.1 (3d, dp, coupled imp, rngke)**Figure 6.4:** Total Pressure Profile of One Cross-Sectional Plane.

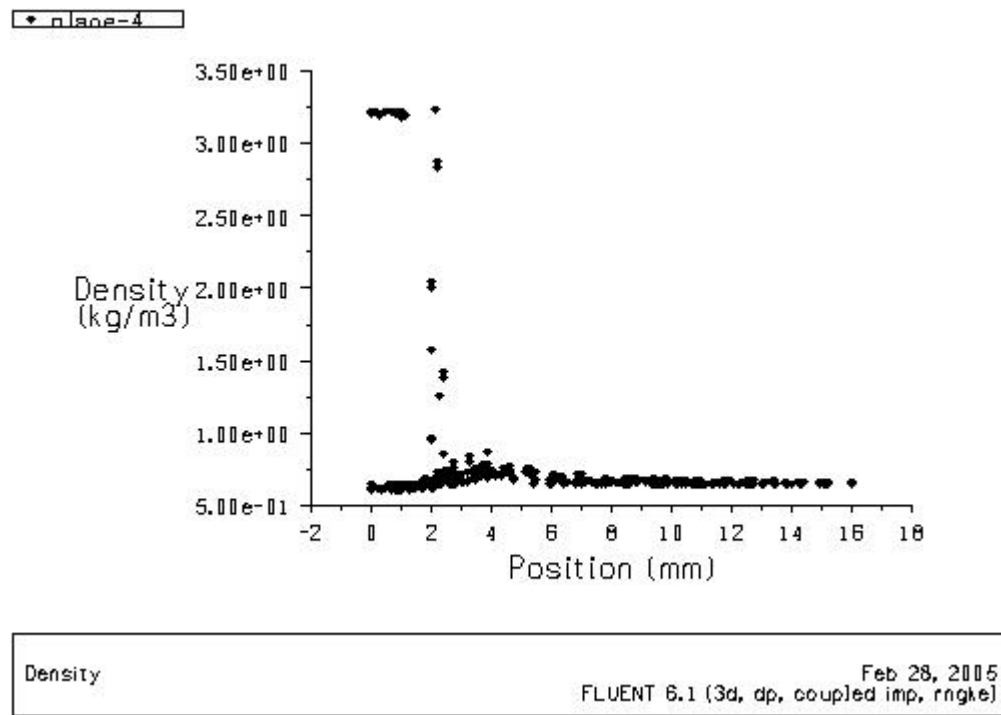


Figure 6.5: Total Density Profile of One Cross-Sectional Plane.

Mass flow rate is a function of gas density which depends on temperature, pressure and other factors. The result of the simulation as shown in Figures 6.3 to 6.5 are examples of the data extraction. These values are the same as the thermophysical property table (Friend et al.). This proves that the simulation has been conducted successfully. Based on the computational fluid dynamic evaluation of the obturator positioning, it is seen that the following flow rate was attained at various opening. Simulations were conducted at inlet pressure of 4.5 Bar. The desired mass of 0.267 grams per second of natural gas is attained with openings of 0.3mm. This would be the maximum travel for the obturator away from the valve seat.

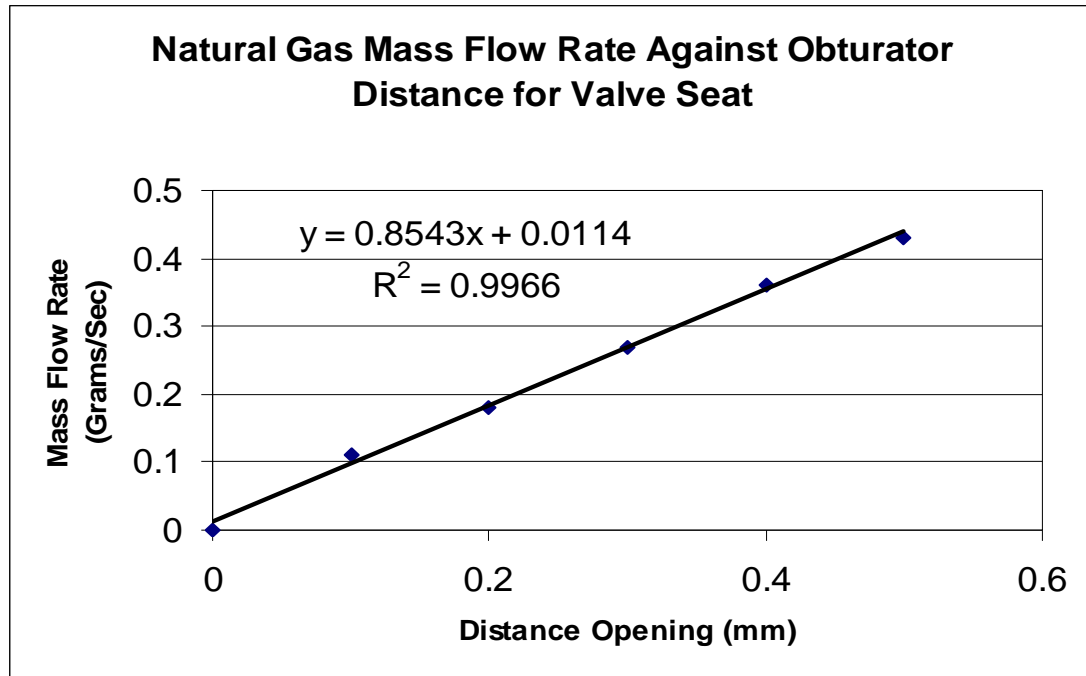


Figure 6.6: CFD Simulation Results Comparing Mass Flow Rate and Obturator Distance of Opening.

6.2 Regulator Actuation Results

Based upon the SAE HS 795⁵⁰ spring indexes in the range of 5.5-9 are preferred, particularly for close tolerance springs and those subjected to cyclic loading. The wire diameter for the spring coil was selected arbitrarily selected as 3mm. Taking the spring index to be 6 which is within the suggested range, we get a coil that would have an inner diameter of 15 mm. The spring diameter (D) however is equivalent to the inner diameter plus the wire diameter which gives 18 mm. The Torsional Modulus of Elasticity for the stainless steel 304 wire is given as 68,900 MPa. Combining these values into Equation 4.20, we attain the maximum corrected allowable stress. This value is compared with the allowable working torsional stress (corrected) for stainless steel type 304 for wire diameter of 3mm (0.118 inch) which is 55, 000 psi as provided by Harold C.R. Carlson⁵¹. It is seen that the value is far below the suggested level thus proving the safe operation of the spring.

The set-point pressure of 4.5 bar would pose a force of 1272.34 Newton when it acts against the diaphragm area of 2.8274×10^{-03} . This is the force that is used to completely obstruct the incoming gas into the regulator compartment. This is done through appropriate leverage that implies elementary moment calculation. The preload force of the spring should hold the restricting element open during pressure below 4.5 bar to allow pressure built-up within the compartment.

Through iterative evaluation on moment calculation paired with valve opening and spring preloading, we attain the appropriate active number of coil for the spring to be 10 giving a solid height of 30 mm. The solid height for closed ends ground as used in the current evaluation is calculated by multiplying the number of active coils with the spring wire diameter. The moment calculations were used to calculate the amount of load the spring should give against the measuring element to permit pressure built-up to the set-point level. A pre compression of 7.5 mm was appropriate to provide sufficient loading force for the desired purpose.

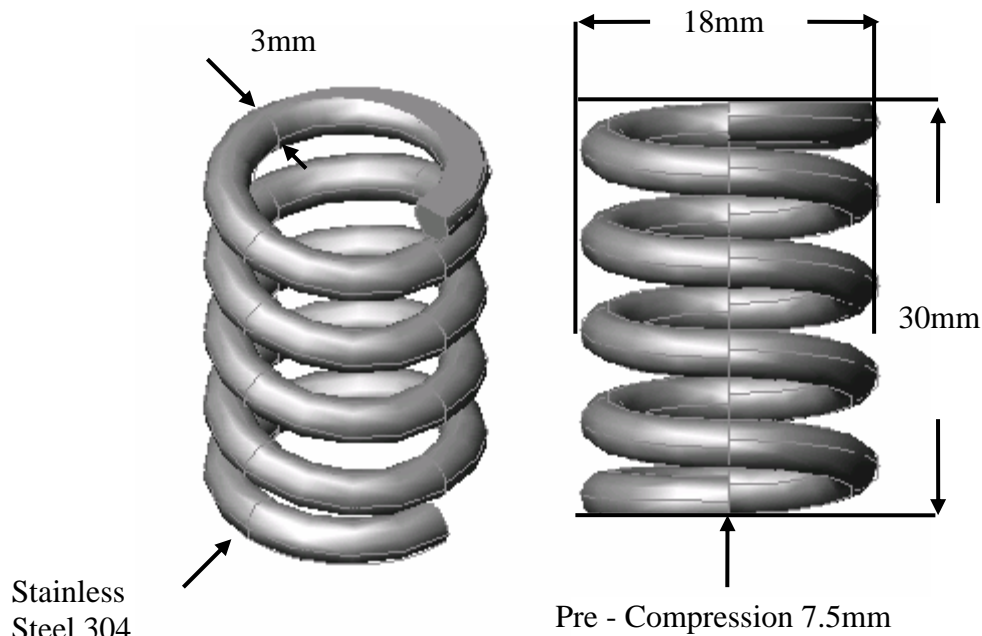


Figure 6.7: Final Loading Element Design

6.3 Regulator Body Results

The regulator side body is designed to be 7.5mm, the bottom is designed at 5.8mm and the bonnet cover is designed to have a thickness of 11.5mm. Based on SAE J1199, Bolt of class 4.6 having M6 x 1 is selected as it has a minimum tensile strength of 8.04 kN which exceeds the force of 7.667 kN acting on the cover. The guideline in bolt and nut selection outlines that the nut selected shall be of a higher class compared to the bolt. Therefore based on ASTM A356M nut from class 5, M6 x1 Hex style 1 was selected.

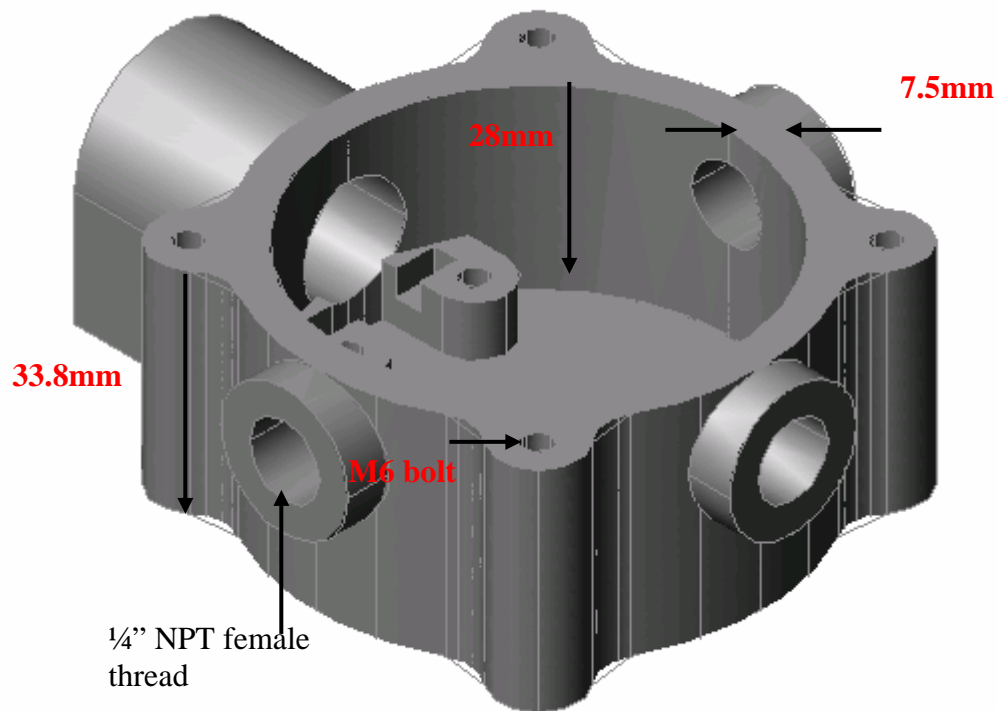


Figure 6.8: Pressure Regulator Body Dimensions

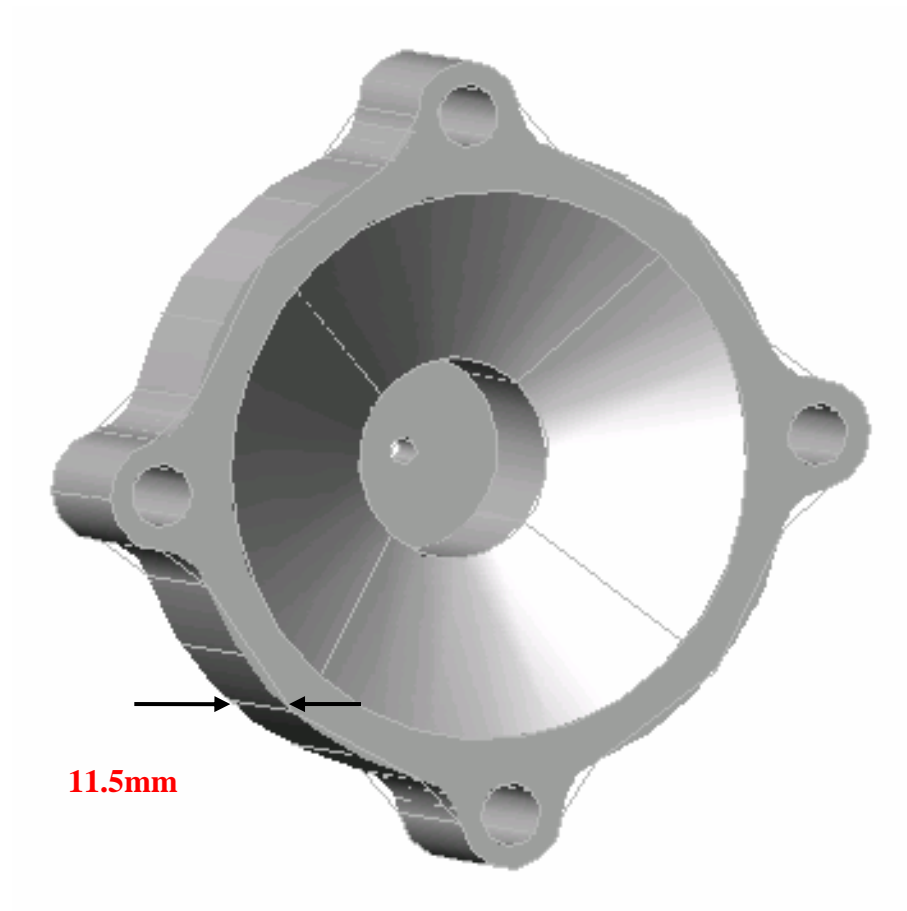


Figure 6.9: Bonnet Cap Dimensions

6.4 Regulator Prototype End Product

The fabrication of each component and the appropriate assembly would result in the finish product as shown in Figure 6.8 and 6.9. As we can see the pressure regulator compartment has four accesses. One the inlet, the second the outlet, the third for the pressure and temperature sensing while the last tapping is fitted with a safety relieve valve which has a relief pressure of 6 bar which is above the set-point pressure of 4.5 bar.

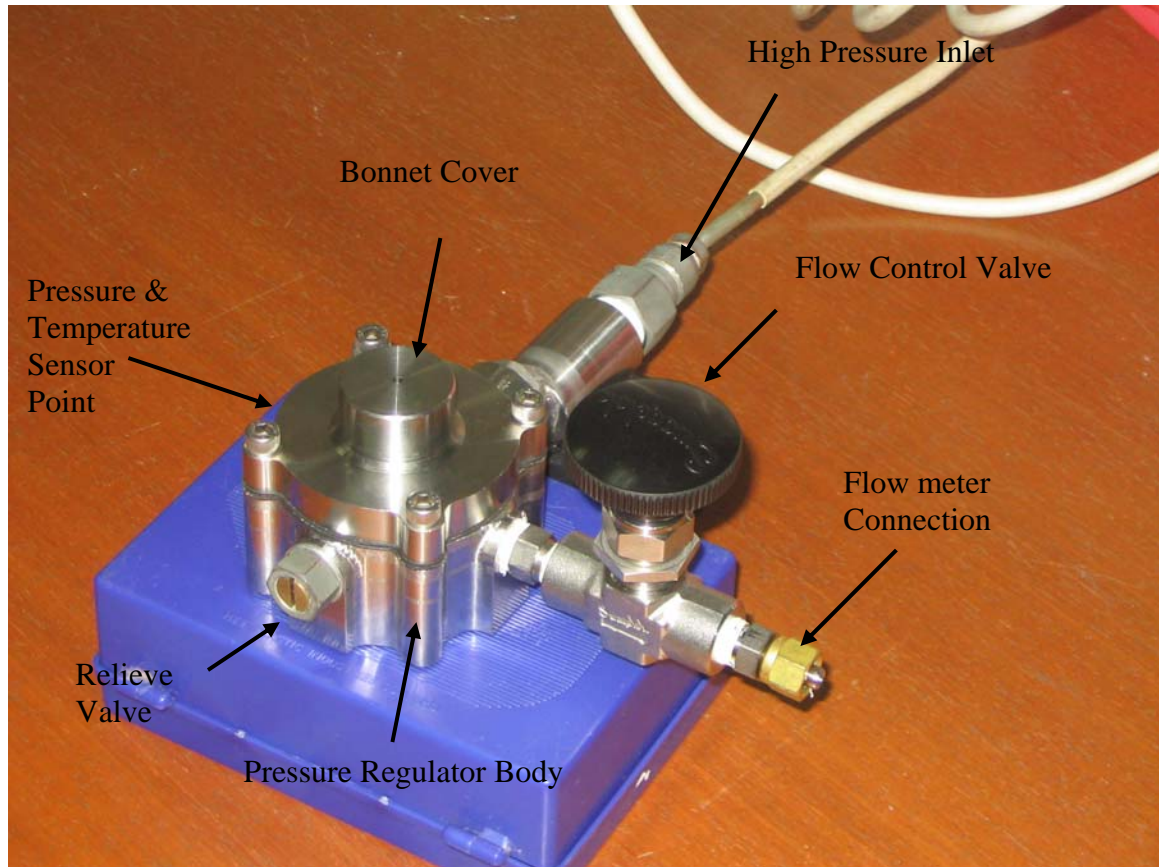


Figure 6.10: Fabricated Pressure Regulator Prototype

6.5 Pressure Regulator Performance Results

The dedicated test bench is used to prove the ability of the prototype pressure regulator to provide constant outlet pressure regardless of inlet pressure and outlet flow rate. The graph below depicts the outlet pressure at varying outlet flow rate. The inlet pressure regulator of the regulator during this test is at 3000 psi as the Compress Natural Gas cylinder was newly charged. From the graph in Figure 6.10, we can see that the flow rate has been increased by 5 litres every 2 minutes. The regulator successfully provides constant pressure of 4.5 Bar at all flow rate. The time limit of 2 minutes for each flow rate allows the stabilization of the system. The results clearly

prove the ability of the pressure regulator to provide constant outlet pressure regardless of output flow demand.

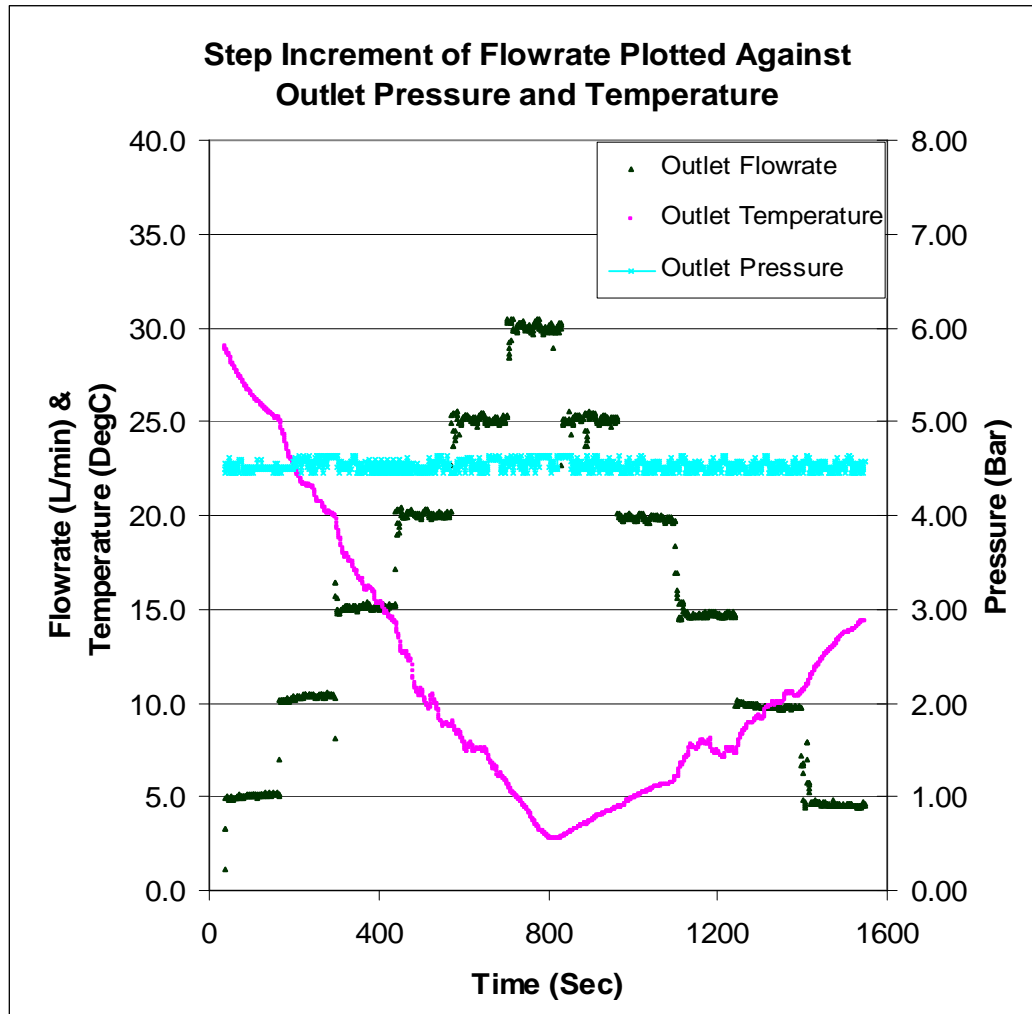


Figure 6.11: Performance Plot of the Pressure Regulator Prototype
Evaluated Using the Pressure Regulator Test Bench

6.6 Refinement of Previous Product

The research on improvement NGVM Pressure Regulator has been completed via finite element analysis in order to optimize the NGVM pressure regulator prototype. A robust regulator is an essential component of a safe and reliable NGV fuel system. It is important to verify that the regulator is capable to effectively manage NGV fuel system regarding to temperature, vibration, flow changes, supply pressure changes as well as imperfect gas composition.

Result obtained from this research work has been such that optimized. The NGVM regulator could manage the maximum force when pressure is supplied to the system. Analysis will seriously focus upon the maximum tensor stress caused by the applied pressure. Besides, selection of the satisfactory construction materials of the body regulator is one of the major considerations.

6.7 Two Dimensional Modeling

Two dimensional model of regulator base is drawn to provide conceptual idea for three dimensional drawing. The model is drawn by using AutoCAD version 2004 computer programming as shown in Figure 6.12. The model will be transformed to solids views for the thickness and structure modification. This model is drawn based on research by Rahmat M, Zulkefli Y, and Shameed A on the project of Development of Regulator base.

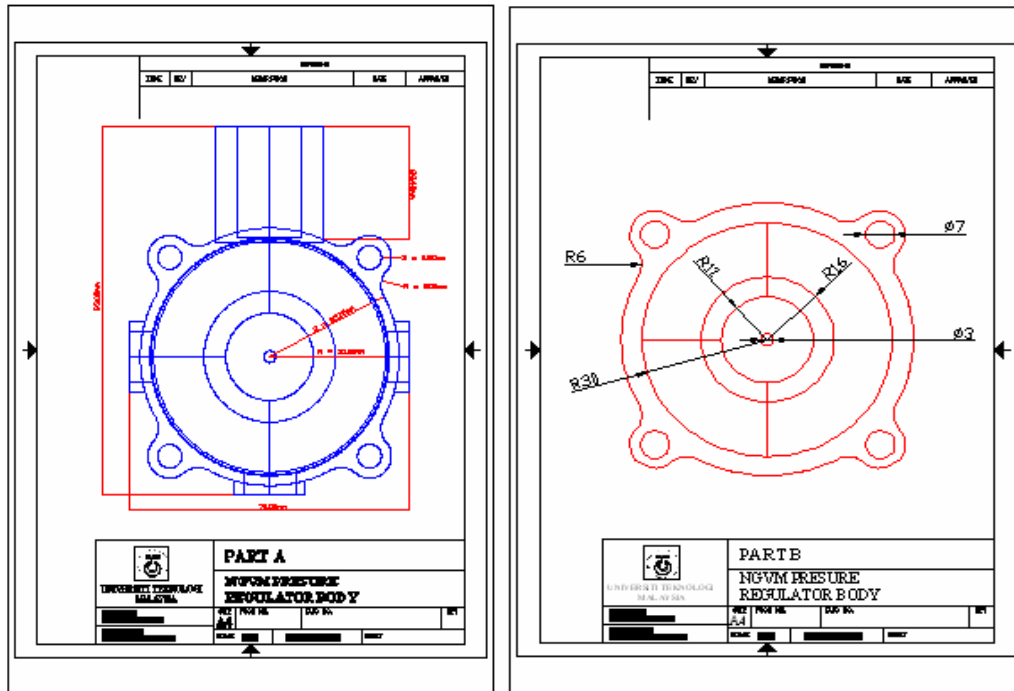


Figure 6.12: Two Dimensional Drawing of Part A and Part B

NGVM Pressure Regulator body divided into two parts, namely Part A and Part B. Each part is drawn separately in shape and dimensional. Part A of regulator body represents the regulator bowl base, and drawn with a projection that shows the regulator bowl base from the upper view. Overall observation of this view shown that the regulator bowl base has 93mm length and 70mm wide with one hollow cylinder for fuel inlet.

Part B of regulator body represents the regulator cap base and drawn from the bottom view. The base regulator cap has 70mm external diameter. Both of Part A and Part B of regulator base have four unit holes with 5.5mm diameter screw in each of its diagonal. It is designed to strongly coupled the bowl and cap of regulator body. The general design of this regulator has been made suitable to be installed on the NGVM system.

6.8 Solidified Modeling

Solid model for regulator base is developing by using SOLIDWORK program based on the conceptual ideal of two dimensional drawing. The solid model is drawn using the prototype system to analyze deformations and stresses.

By structural modification on the critical region of this regulator the optimized thickness could be obtained. Preliminary, the thickness of the regulator base is reduced by 0.5mm until the optimize thickness of the prototype is gained. The thickness reduction of this prototype is done to get the optimize thickness of original regulator base before structural modification is carried out.

Structural modification on the critical region of regulator base is carried out in order to obtain the ideal structure design of NGVM pressure regulator. Evolution of the structure modification design is developed using SOLIDWORK program as shown in Figure 6.13. Thus, result of a new design of NGVM pressure regulator. Figure 6.14 shows Part A and Part B of pressure regulator separately.

Modification has been done to the original base of the regulator by incorporating fins to the body of the regulator, to increase total surface area of the regulator. The fin plays an important role to absorb heat from the surrounding in order to decrease temperature drop during the fall in pressure phase. It is also preventing freezing of natural gas. It is shown that Part A of the regulator has been modified by adding rib and thickness at the top part of the structure. While, Part B of regulator is modified by adding the thickness at the bottom part of the structure.

The optimized thickness of the newly designed NGVM pressure regulator is obtained after the structural modification. All the solid model that has been drawn have to be saved by using IGES format before being exported to MSC. PATRAN

program for the structural analysis. The analysis will subsequently be based on separation of both parts.

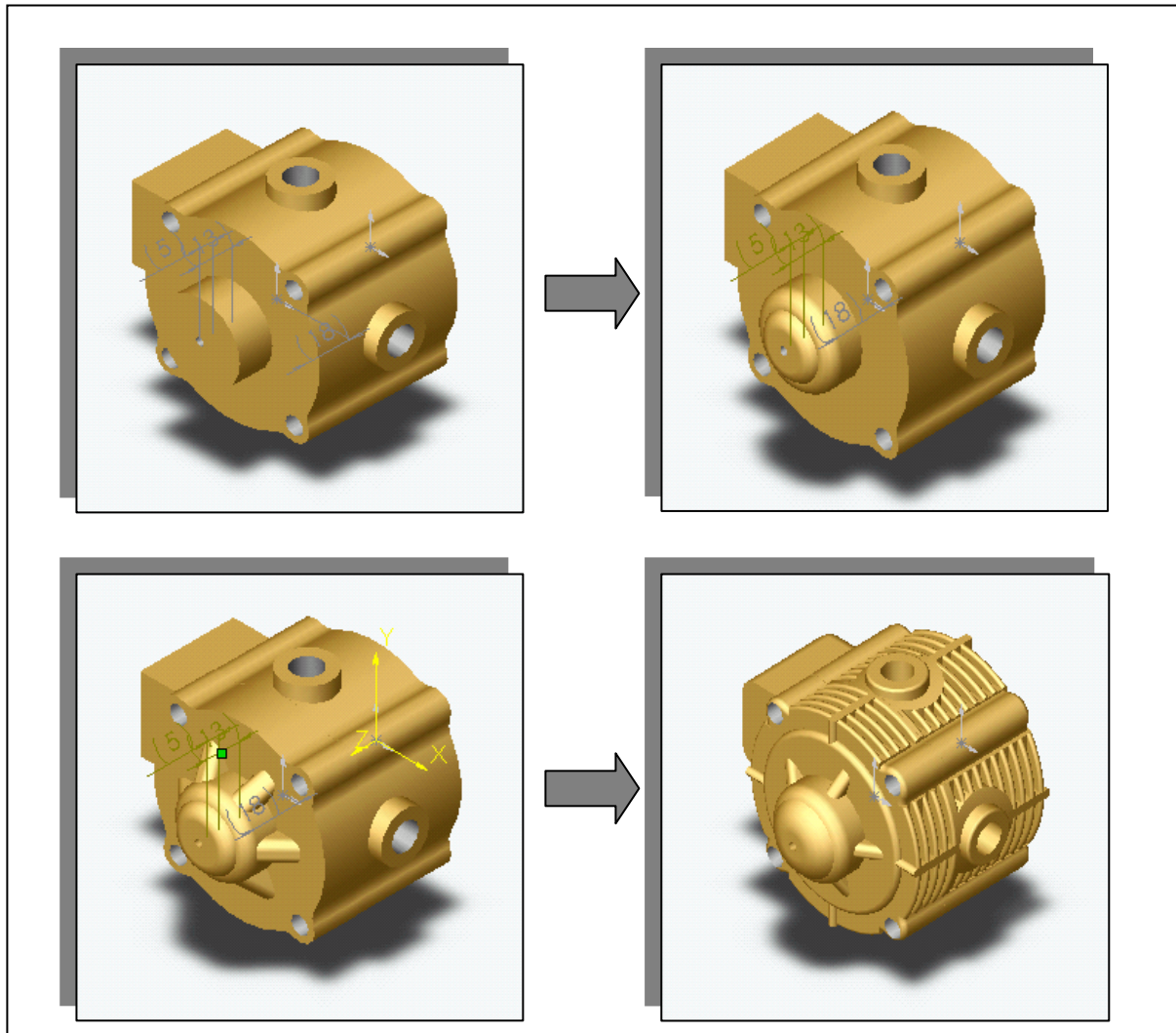


Figure 6.13: Evolution of Structural Design Modification via SOLIDWORK

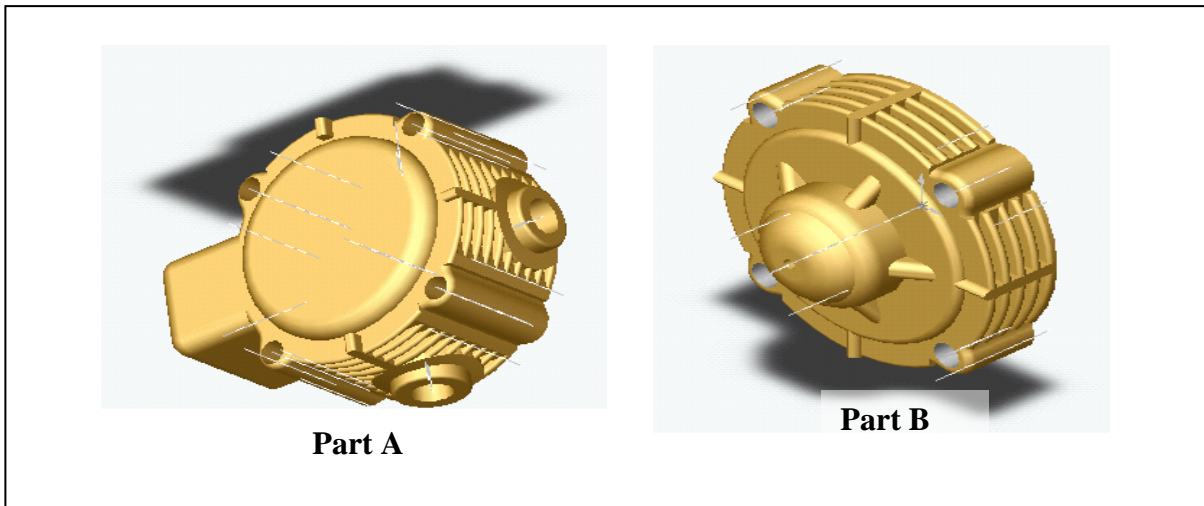


Figure 6.14: Part A and Part B of New Design via SOLIDWORK

6.9 MSC. PATRAN/NASTRAN Analysis

The finite element analysis upon the deformations and stresses of the regulator base is carried out by using MSC. PATRAN/NASTRAN. The applied pressure at the inner surface of the pressure regulator base will force the elements to move from its origin. The analysis will show the displacement nodes. Modification is necessary at the critical region of the prototype design to ensure the safety and durability of the prototype when it is pressurized at 3000psi ($2.07\text{E}+07$ Pascal) from a CNG storage tank. Analysis will also take a serious consideration upon the maximum tensor stress caused by the applied pressure.

Result obtained through the FEA analysis could be used to optimize the design of single step NGVM pressure regulator thickness, in order to handle the applied pressure produced by changes in gas flow rate and deformation.

6.9.1 Simulation Data for Single Stage Regulator

Simulation data for deformations and stresses analysis for single stage of NGVM pressure regulator are shown in Table 6.1 until Table 6.6 below.

i. Regulator Bowl Base (Part A)

Material: Stainless Steel 304 (SS_304)

Table 6.1: Simulation Data for Part A Using SS304

Thickness (mm)	Original Model		New Model	
	Stress ($\times 10^8$ Pa)	Deformation ($\times 10^{-2}$ mm)	Stress ($\times 10^8$ Pa)	Deformation ($\times 10^{-2}$ mm)
5.0	1.77	1.09	1.74	1.59
4.5	2.55	1.31	1.92	1.67
4.0	2.61	1.62	2.17	1.74
3.5	2.79	2.03	2.41	1.83
3.0	4.10	2.62	3.37	1.89

Material: Aluminum Cast Alloy

Table 6.2: Simulation Data for Part A Using Aluminum Cast Alloy

Thickness (mm)	Original Model		New Model	
	Stress ($\times 10^8$ Pa)	Deformation ($\times 10^{-2}$ mm)	Stress ($\times 10^8$ Pa)	Deformation ($\times 10^{-2}$ mm)
4.0	3.54	7.38	1.82	4.25
5.0	2.32	5.68	1.42	3.98
5.5	1.92	4.58	1.27	3.82
6.0	1.66	3.71	1.12	3.70
7.0	1.44	3.13	1.04	3.38

Material: Brass

Table 6.3: Simulation Data for Part A Using Brass

Thickness (mm)	Original Model		New Model	
	Stress ($\times 10^8$ Pa)	Deformation ($\times 10^{-2}$ mm)	Stress ($\times 10^8$ Pa)	Deformation ($\times 10^{-2}$ mm)
5.0	1.77	2.04	1.74	2.46
4.5	2.09	2.44	1.98	3.12
4.0	2.67	3.02	2.16	3.27
3.5	2.78	3.79	2.38	3.40
3.0	4.10	4.88	3.30	3.53

ii. Regulator Bowl Base (Part B)

Material: Stainless Steel 304 (SS 304)

Table 6.4: Simulation Data for Part B Using SS304

Thickness (mm)	Original Model		New Model	
	Stress ($\times 10^8$ Pa)	Deformation ($\times 10^{-2}$ mm)	Stress ($\times 10^8$ Pa)	Deformation ($\times 10^{-2}$ mm)
5.0	1.23	0.667	1.11	0.372
4.5	1.25	0.949	1.23	0.401
4.0	1.47	1.36	1.39	0.433
3.5	2.57	2.00	1.61	0.470
3.0	3.60	2.60	1.76	0.504

Material: Aluminum Cast Alloy

Table 6.5: Simulation Data for Part B Using Aluminum Cast Alloy

Thickness (mm)	Original Model		New Model	
	Stress ($\times 10^8$ Pa)	Deformation ($\times 10^{-2}$ mm)	Stress ($\times 10^8$ Pa)	Deformation ($\times 10^{-2}$ mm)
5.0	1.74	3.59	9.57	1.8
5.5	1.38	2.53	9.17	1.12
6.0	1.05	1.77	9.57	1.17

Material: Brass

Table 6.6: Simulation Data for Part B Using Brass

Thickness (mm)	Original Model		New Model	
	Stress ($\times 10^8$ Pa)	Deformation ($\times 10^{-2}$ mm)	Stress ($\times 10^8$ Pa)	Deformation ($\times 10^{-2}$ mm)
5.0	1.23	1.24	1.27	0.695
4.5	1.24	1.26	1.31	0.749
4.0	1.47	2.57	1.31	0.811
3.5	2.57	3.73	1.43	0.876
3.0	3.44	4.83	1.75	0.942

For structural applications, the yield strength is usually more important property than the tensile strength. Once it is passed, the structure has deformed beyond acceptable limits. Yield strength is the pressure which a substance is capable of supporting without fracturing. In industry, yield stresses are usually not even approached because the applied stresses are kept well below the yield strength by a safety factor on the order of 1.5 to 2.0.

Yield strengths for each material used are summarized in the following table.

Table 6.7: Yield Strength for Each Material

Material	Yield strength	
	Psi	(x 10 ⁸ Pa)
Stainless steel 304	76500	5.27
Brass	57000	3.93
Aluminum Cast Alloy	20000	1.65

Factor of safety (FS), also known as Safety Factor, is a multiplier applied to the calculated maximum load (force, torque, bending moment or a combination) to which a component or assembly will be subjected. Safety factor accounts for imperfections in materials, flaws in assembly, material degradation, and uncertainty in load estimates. An alternative way to use the safety factor is to derate the strength of the material to get design strength.

$$\text{Design Stress} = \frac{\text{Yield Strength}}{\text{Safety Factor}}$$

On this analysis, the safety factor that will be considered is 1.5. Thus, the design stresses calculated for each material are shown in Table 6.8 below:

Table 6.8: Material Design Stress

Material	Design Stress (x 10 ⁸ Pa)
Stainless steel 304	3.51
Brass	2.62
Aluminum Cast Alloy	1.10

The optimize thickness of each material summarized as the following table:

Table 6.9: Optimize Thickness of Each Material Selection

Material Construction	SS304		Brass		Aluminum Cast Alloy	
	Part A	Part B	Part A	Part B	Part A	Part B
Stress Tensor(x 10 ⁸ Pa)	3.37	1.76	2.38	1.43	1.04	0.854
Deformation (x 10 ⁻² mm)	1.89	0.504	3.40	0.876	3.38	1.08
Material Design Stress (x 10 ⁸ Pa)	3.51		2.62		1.10	
Optimize Thickness (mm)	3.0		3.5		6.0	

6.9.2 Comparison on MSC/PATRAN Simulation Result

From Table 6.7, it is clearly shown that Stainless Steel 304 (SS304) gives the minimum value of optimized thickness compared to Brass and Cast Aluminum Alloy. The optimized thickness of SS304 is 3.0mm. Figure 6.4 shows the result in graphical form of Part A analysis, where its material constructions is Stainless Steel 304 (SS304). After the structure modification, by adding fins and additional thickness to the bottom part of the original model, the maximum stress of the Part A structure reduced to 0.337GPa. The maximum stress of new model under the design stresses, 0.351GPa. Maximum stress of node element occurs on node number 13544.

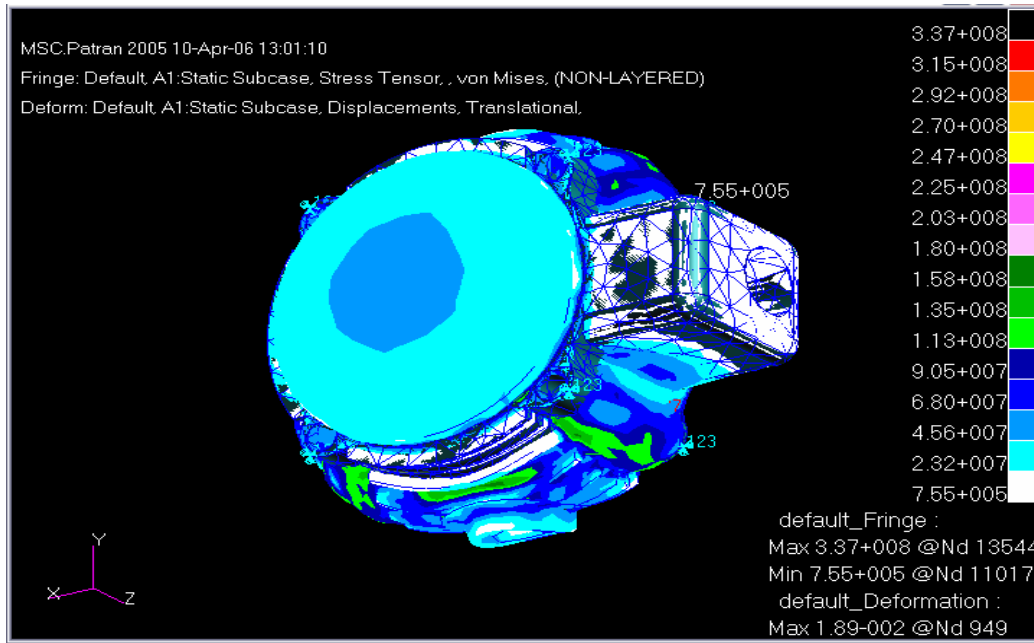


Figure 6.4: Stress Tensor Analysis Result for New Model of Part A Using SS304

For the displacement analysis, as shown in Figure 6.5, the maximum displacement of Part A new model using SS304 is 0.0189 mm. It is showed that the displacement is not critical due to the small distance of node displacement. Thus, the new model with 3.0mm thickness is safe to operate at the applied pressure.

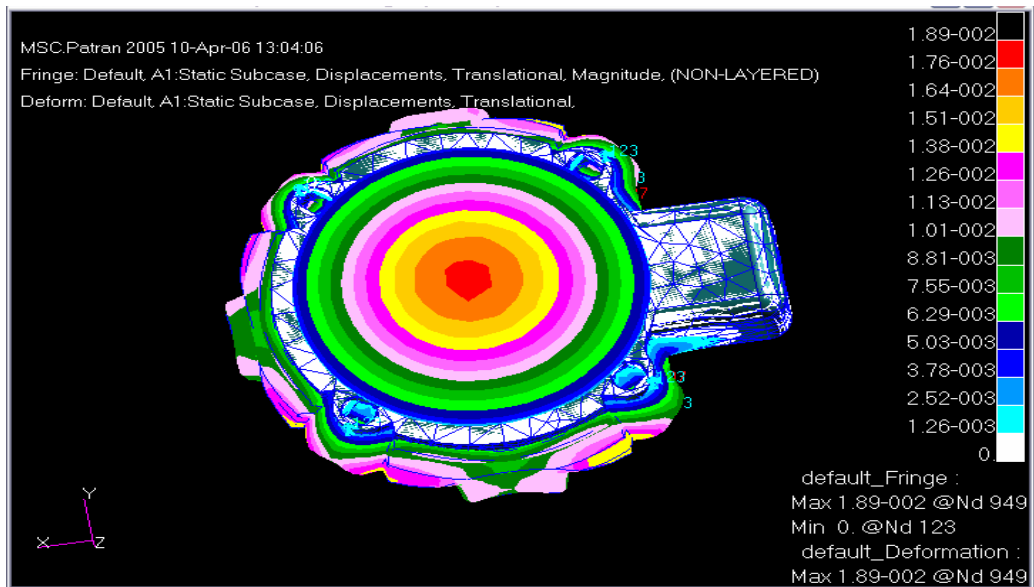


Figure 6.5: Deformation Analysis Result For New Model of Part A Using SS304

The optimized thickness of Brass as material construction is 3.5mm. Stress tensor analysis result for this material shown in Figure 6.6. It is shown that maximum stress is 0.238 GPa, which is 29.38% less than maximum node stress of SS304. Maximum stress of node element occurs on node number 10652. The maximum stress is under the design stress of brass material.

While, the maximum node displacement of this material is 0.0340 mm occurs on node number 11358 as shown in Figure 6.7 below. The maximum displacement of Brass as construction material is 44.41% more than SS304. The analysis shows that the displacement values is less than 1mm, which mean the base regulator body is sufficient to support the maximum operating pressure, 3000psi.

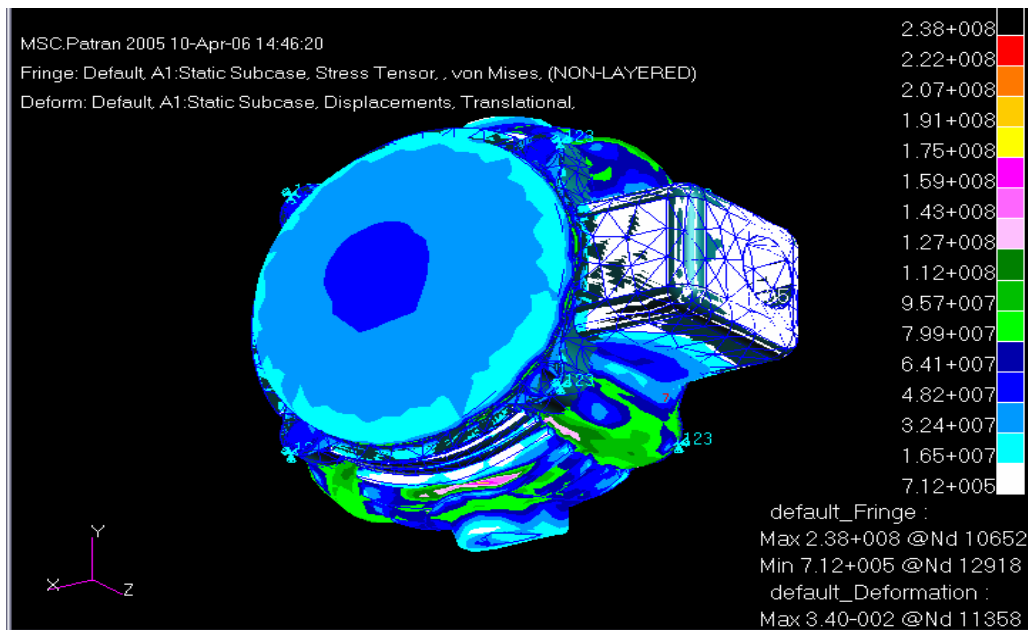


Figure 6.6: Stress Tensor Analysis Result for New Model of Part A Using Brass

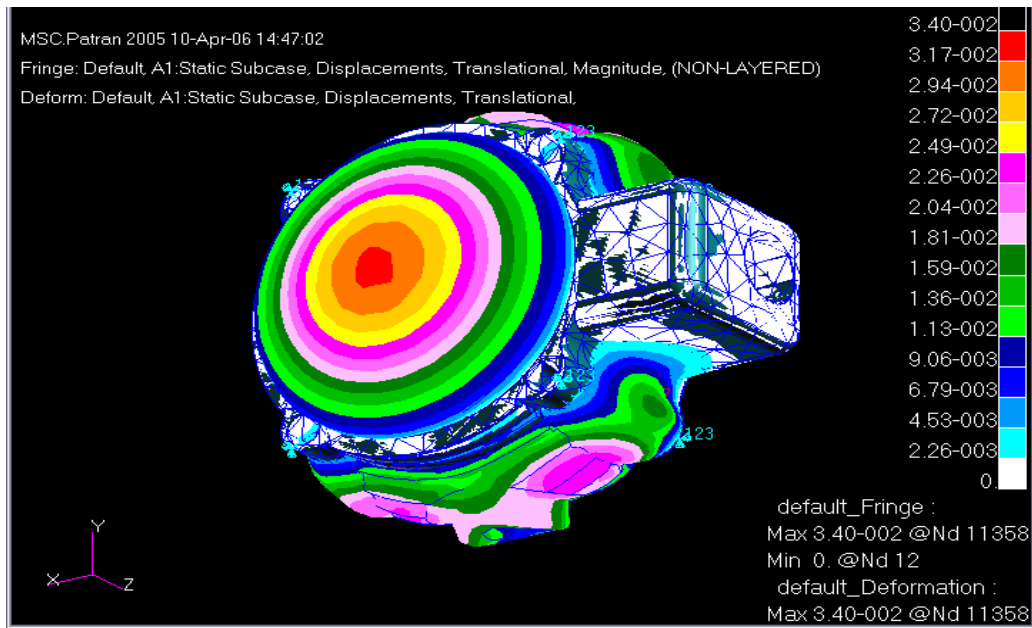


Figure 6.7: Deformation Analysis Result for New Model of Part A Using Brass

While, aluminum cast alloy gives the largest thickness among the material constructions, which is 6.0mm. The optimized thickness of cast aluminum alloy 50% higher than SS304. The maximum stress tensor for this material is 0.104 GPa occurs on node number 4681 as shown in Figure 6.8. The maximum stress tensor of this material is less 69.13% and 56.30% than SS304 and Brass

The maximum node displacement of this material is 0.0338 mm occurs on node number 8431 as shown in Figure 6.9 below. The maximum displacement of cast aluminum alloy as construction material is 44.08% more than SS304.

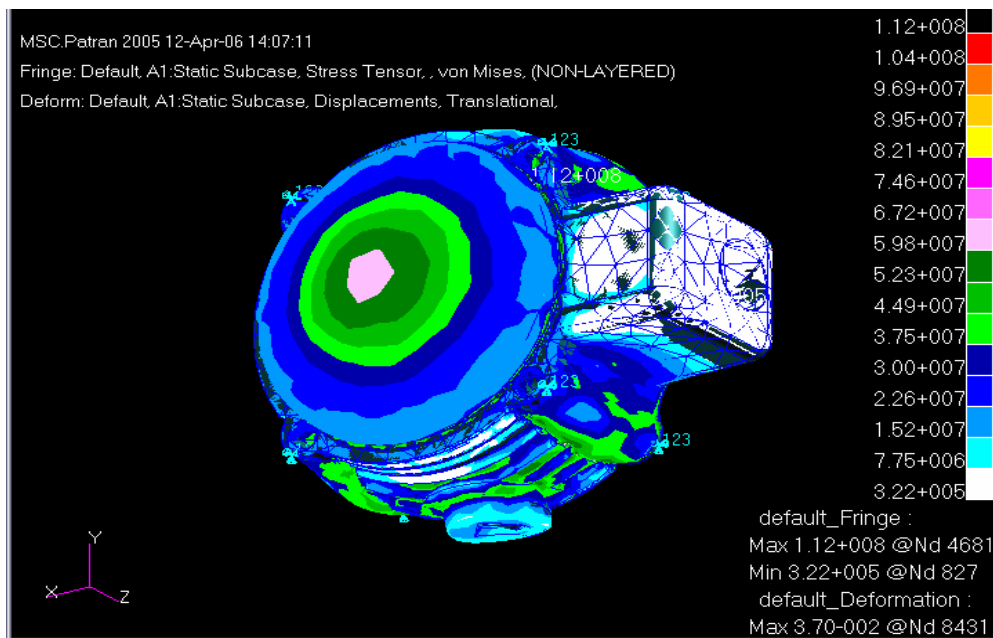


Figure 6.8: Stress Tensor Result for New Model of Part A Using Aluminum Cast Alloy

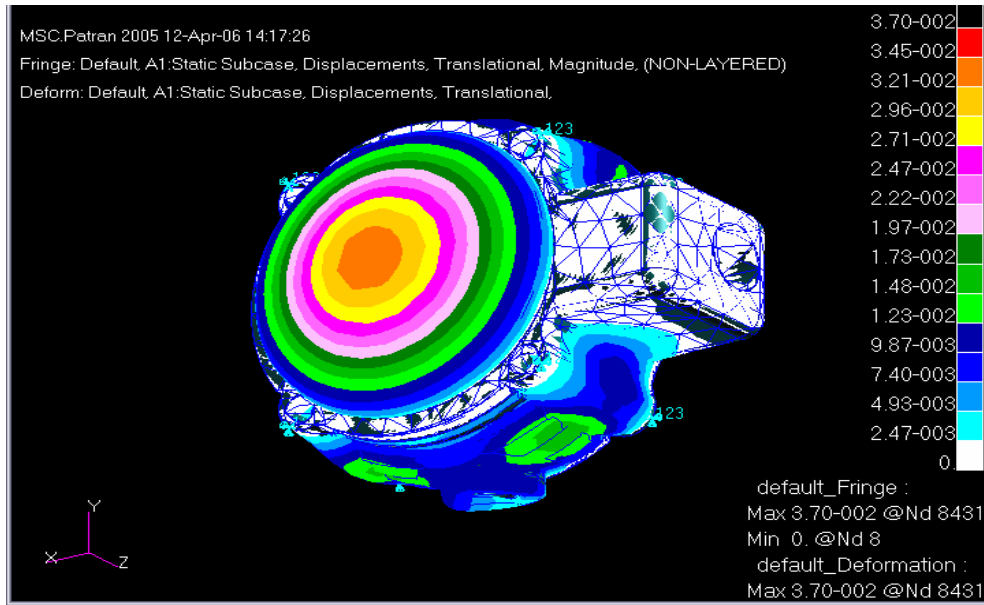


Figure 6.9: Deformation Analysis Result for New Model of Part A Using Aluminum Cast Alloy

Figure 6.10 shows stress tensor for Part B of SS304. After structure modification on the critical region, the maximum stress of Part B reduced to 0.176 GPa, which is under the design stress. The maximum stress occurs on node number 215. The modification is done by adding rib and additional thickness model to the top part. Beside that, fin also added incorporated to the structure of Part B.

For the displacement analysis, it shows that the maximum displacement of new model using SS304 is 0.00504 mm. This is because the deformations associated with these modes are prevented by the stiffener. The displacement is not critical due to the small distance of node displacement. Thus, the new model with 3.0mm thickness is safe to operate at the applied pressure. Figure 6.11 shows detail on the maximum node displacement.

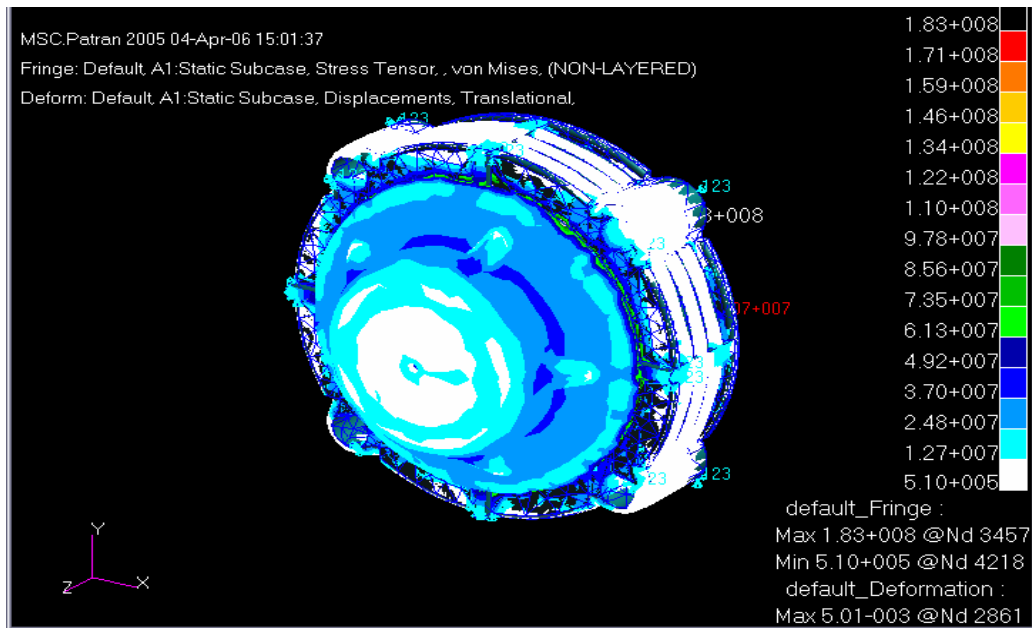


Figure 6.10: Stress Tensor Result for New Model of Part B Using SS304

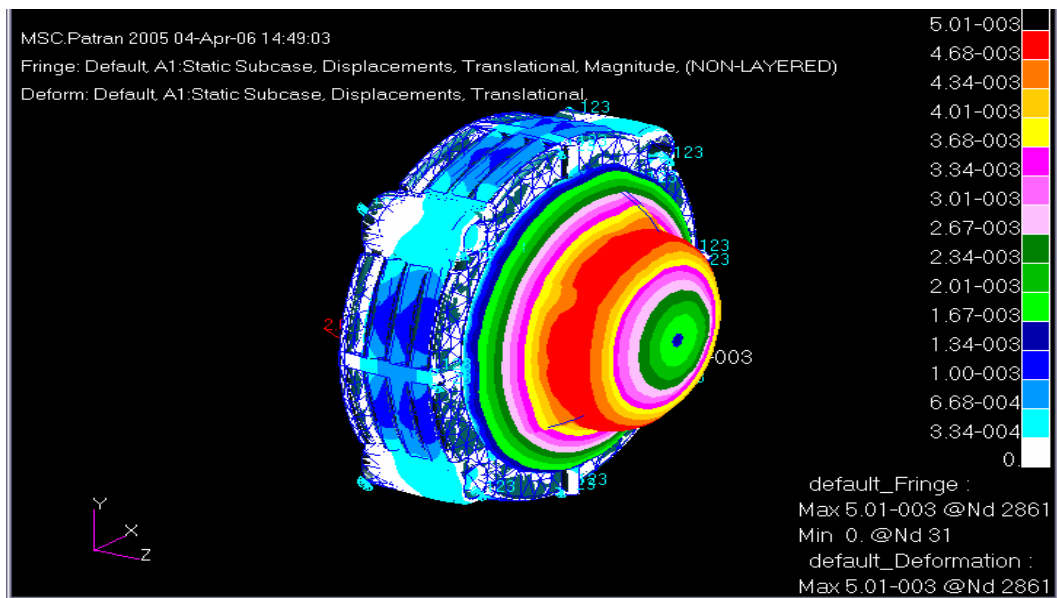


Figure 6.11: Deformation Analysis Result for New Model of Part B Using SS_304

Figure 6.12 shows the maximum stress tensor of Part B for Brass. The maximum stress of new design is 0.143 GPa, occurs on node number 11847. Compared to SS304, the maximum stress of Brass is less 18.75%. While, the maximum node displacement of this material is 0.00876 mm occurs on node number 9210 which is 3.72% more than maximum displacement of SS304.

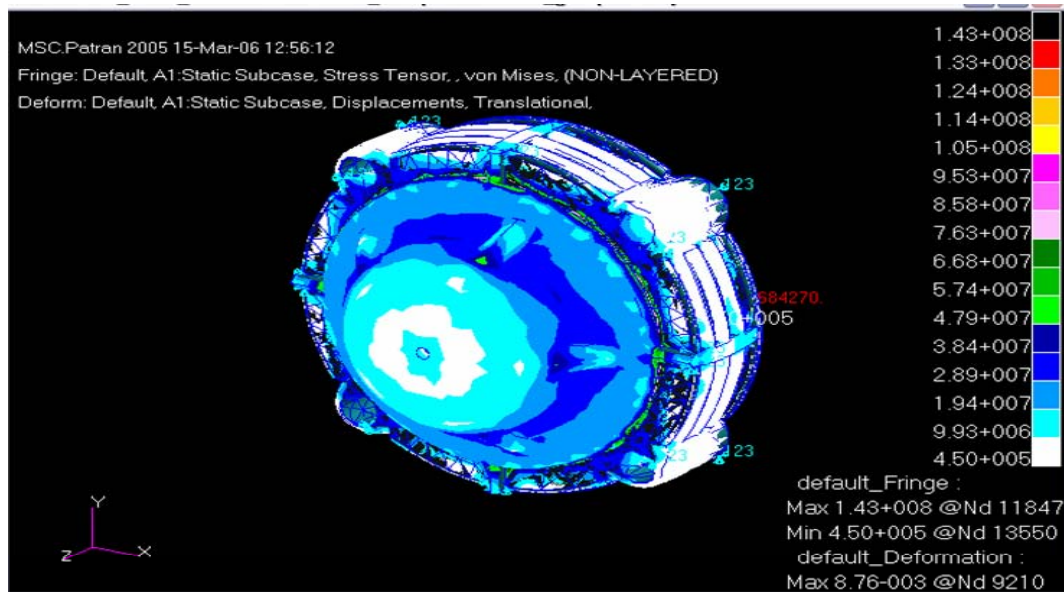


Figure 6.12: Stress Tensor Result for New Model of Part B Using Brass

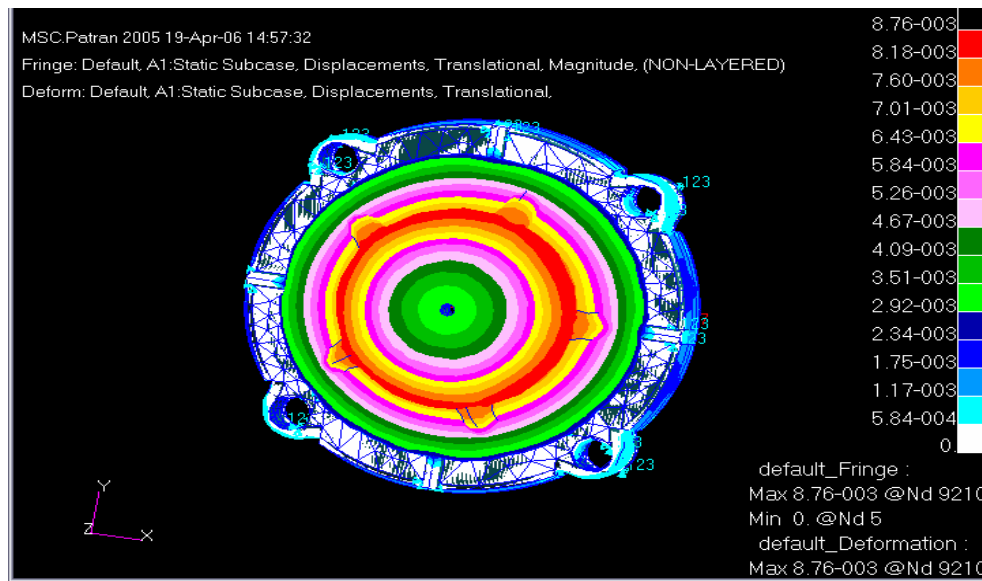


Figure 6.13: Displacement Result for New Model of Part B Using Brass

For aluminum cast alloy, the maximum stress tensor for Part B is 0.0854GPa occur at node number 2660. It is shown in Figure 6.14 below. The maximum stress tensor of this material is less 51.48% and 46.96% than SS34 and Brass. While, maximum node displacement of this material is 0.0108 mm occurs on node number 13271 which is 53.3% and 56.48% more than maximum displacement of SS304 and Brass.

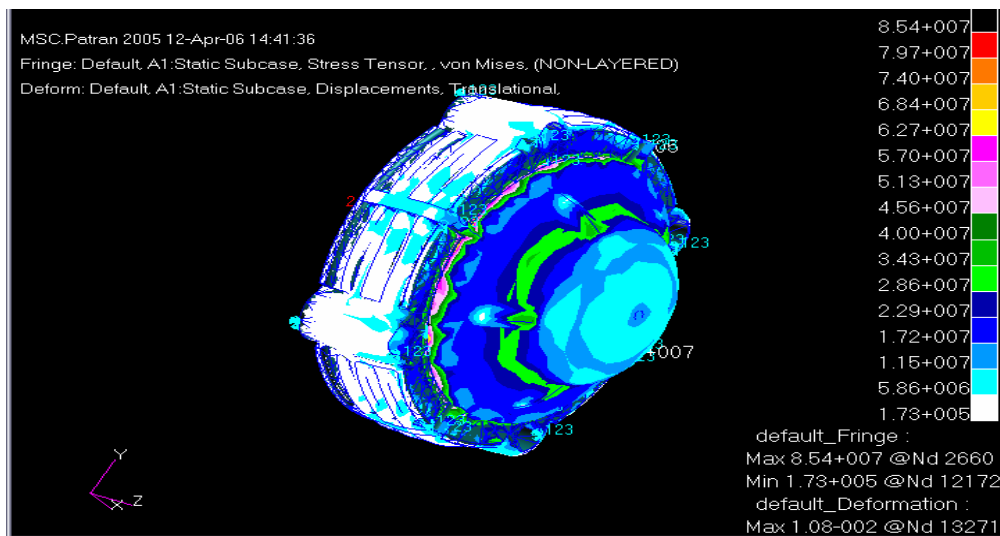


Figure 6.14: Stress Tensor Result for New Model of Part B Using Aluminum Cast Alloy

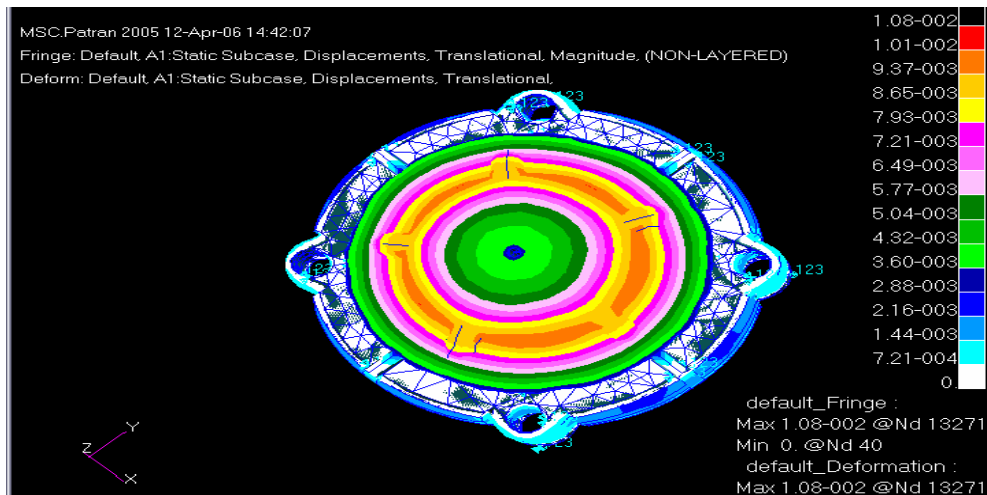


Figure 6.15: Deformation Analysis Result for New Model of Part B Using Aluminum Cast Alloy

6.10 Comparison on Material Selection

The structure of regulator base prototype is also analyzed via their material strength using several of material types. Materials selected for this analysis are Stainless Steel 304 (SS304), Brass (RED; 80% CU, 20% Zn) and Cast Aluminum Alloy. Selection of this material is based on normally materials used to fabricate the regulator base. The analysis is focus on predicting the mass and density of the prototype for different type of material and the changes of the moment of inertia. Table 6.10 and Table 6.12 show the material strength preliminary analysis on the Part A and Part B of the new prototype with thickness 3.0mm.

Table 6.10: Material Strength Preliminary Analysis for Part A

				
Measurement Result		SS_304	Brass	Aluminum Cast Alloy
Thickness (mm)		3.0	3.5	6.0
Surface Area (mm ²)		35666.424	35656.1499	35605.1415
Volume (mm ³)		107766.49	110314.9506	122396.8195
Density (g/mm ³)		0.0080	0.0088	0.0027
Mass (gram)		862.13189	970.7716	330.4714
Center of Mass	x	-8.2260	-8.0208	-7.1635
	y	-0.1614	-0.1578	0.1422
	z	11.2741	11.5619	12.7616
Principle Moments of Inertia	Px	437991.9	498781.8934	175447.5265
	Py	706846.05	795286.7258	267466.6522
	Pz	901954.1	1015976.8296	343300.0918
Moments of Inertia: Taken at the center of mass and aligned with the output coordinate systems	Lxx	442235.25	502947.7866	176197.8519
	Lyx	5355.3962	5922.3690	1857.3851-
	Lzx	-43591.025	-45550.2180	-10908.9248
	Lxy	5355.3962	5922.3690	267428.9471
	Lyy	706737.94	795167.0507	1857.3851
	Lzy	-2685.4951	-1183.4364	-306.7331
	Lxz	43591.025	-45550.2180	-10908.9248
	Lyz	1115.913	-1183.4364	306.7331
	Lzz	956180.28	101193.6115	342587.4716

Table 6.11: Material Strength Preliminary Analysis for Part B

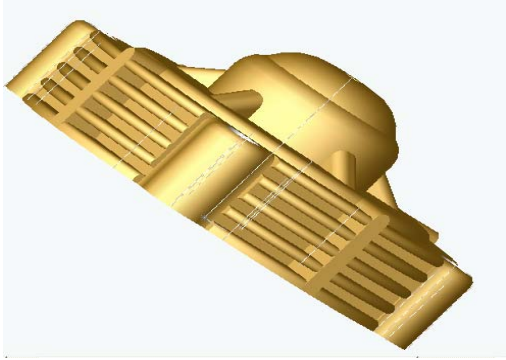
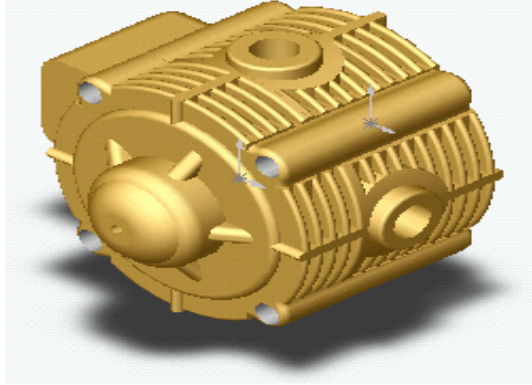
				
Measurement Result		SS_304	Brass	Aluminum Cast Alloy
Thickness (mm)		3.0	3.5	6.0
Surface Area (mm ²)		23206.4723	23179.1566	23219.0106
Volume (mm ³)		60862.2857	61876.7158	65319.9116
Density (g/mm ³)		0.0080	0.0088	0.0027
Mass (gram)		486.8983	535.5881	164.3282
Center of Mass	x	-0.0016	-0.0015	-0.0015
	y	0.0058	0.0057	0.0054
	z	13.1930	13.1406	12.6811
Principle Moments of Inertia	Px	196482.0920	219133.4857	70477.6158
	Py	198886.3836	221778.2067	71289.0645
	Pz	342941.6726	381362.5875	122002.8655
Moments of Inertia: Taken at the center of mass and aligned with the output coordinate systems	Lxx	198886.0400	221777.8287	71288.9485
	Lyx	-28.7423	-31.6166	-9.7006
	Lzx	3.2699	3.5531	0.9724
	Lxy	28.7423	-31.6166	-9.7006
	Lyy	196482.4366	219133.8648	70477.7320
	Lzy	12.2301	-13.2894	-3.6368
	Lxz	3.2699	3.5531	0.9724
	Lyz	-12.2301	-13.2894	-3.6368
	Lzz	342941.6715	381362.5863	122002.8653

Table 6.12: Material Strength Preliminary Analysis for New Prototype Model

			
Measurement Result	SS_304	Brass	Aluminum Cast Alloy
Thickness (mm)	3.0	3.5	6.0
Density (g/mm ³)	0.0080	0.0088	0.0027
Volume (mm ³)	168628.7757	172191.6664	187716.7311
Mass (gram)	1349.0302	1506.3597	494.7996

From Table 6.12 above, it shows that Aluminum Cast Alloy as construction material provide the largest thickness and volume compared to SS304 and Brass which is 6.0mm and 187716.7311 mm³. The thickness of new prototype with aluminum cast alloy is 50% larger than SS304. While, the differential in volume between aluminum cast alloy and SS304 is only 10.17%.

For the mass analysis, it base on the three type of the material selection, which is Stainless Steel (SS304), Brass (RED; 80% CU, 20% Zn) and Aluminum (pure). Even though, aluminum cast alloy give the largest thickness among the selected material construction but this material offer the minimum value of weight which is 63.32% less than SS304.

Decisions on selecting the most preferable material for the fabrication of this regulator also have to take serious consideration on the material market price, in order to gain the mot economic value. Based on the latest market price obtained from

Walsin Precision Technology Sdn. Bhd. Company, Aluminum Cast Alloy gives the lowest market price per kg of material, followed by Brass and Stainless Steel 304 as shown in Table 6.13.

Table 6.13: Gross Material Cost of Regulator New Prototype

Material	Stainless Steel 304	Brass	Cast Aluminum Alloy
Total Weight (gram)	1349.0302	1506.3597	494.80
Price (RM/kg)	33.918	19.80	17.00
Gross Cost (RM)	45.76	29.83	8.41

Therefore the gross cost to fabricate the new regulator base prototype when used Aluminum as the construction material is RM8.41. While, by using Brass and Stainless Steel 304 as construction material the gross cost is RM29.83 and RM45.76. It is 71.81% and 83.9% higher than Aluminum gross cost.

CHAPTER 7

CONCLUSION

The previous chapter vividly shows the performance of the newly developed pressure regulator evaluated by the newly developed pressure regulator test rig. It clearly shows that both the regulator prototype and the regulator test bench has met their objective and has proven to be effective. The performance of the regulator has proven to provide constant pressure at fluctuating flow rates and varying inlet pressure.

Based from the previous research project, a further extend and improvement has been made through the use of finite element analyses; the optimized design of NGVM pressure regulator thickness with the appropriate satisfying material construction is obtained. In the design of pressure regulator structure, it is primarily important to verify that the regulator is able to effectively manage NGV fuel system. This is to ensure the safety and durability of the pressure regulator when it operates at the applied pressure.

Cast Aluminum Alloy as construction material provide minimum amount of stress tensor compared to Brass and Stainless Steel 304, which is 0.104GPa occurs at node number 4681. Though the optimize thickness is 6.0mm, but total weight of base prototype using Cast Aluminum Alloy offer the minimum mass and gross cost. Results has been summarise shown in Table 7.1 below.

Table 7.1: Result Summary

Material Construction	SS304	Brass	Aluminum
Material Design Stress ($\times 10^8$ Pa)	3.510	2.620	0.913
Stress ($\times 10^8$ Pa)	3.37	3.30	2.79
Deformation ($\times 10^{-2}$ mm)	1.89	3.53	5.12
Total Weight (gram)	1349.0302	1506.3597	494.80
Price (RM/kg)	33.918	19.80	17.00
Gross Cost (RM)	45.76	29.83	8.41

This successful pressure regulation would be paired with the intended injector in the second generation fuel system for the NGVM Kriss 110cc.

REFERENCES

- Birky, A., Greene, D., Gross, T., Hamilton, D., Heitner, K., Johnson, L., Maples, J., Moore, J., Patterson, P., Plotkin, S., Stodolsky, F. *Future U.S. Highway Energy Use: A Fifty Year Perspective*. Office of Transportation Technologies Energy Efficiency and Renewable Energy, U.S. Department of Energy. 2001.
- Min, B. H., Bang, K.H., Kim, H. Y., Chung, J. T., Park, S. *Effect of Gas Compositions on the Performance and Hydrocarbon Emissions for CNG Engines*. SAE Technical Paper 981918. 1998.
- Subramaniam, P. K., Yaacob, Z., Amin, N. A. S., Piau, M. P. K. I., Majid, Z. A., *Low Pressure Storage System for Natural Gas Vehicle in Malaysia for Next Millennium*. Malaysian Science & Technology Congress Plaza Hotel, Johor Bharu, 6-8th Dec. 1999.
- Yeap Beng Hi. *Computational Modelling of Air Fuel Mixer for Natural Gas Powered Motorcycle*. Masters Thesis. Universiti Teknologi Malaysia. 2002.
- Wiederkehr, P. *Motor Vehicle Pollution: Reduction Strategies Beyond 2010*. Organisation for Economic Co-operation and Development, Paris. 1995.
- Alternative Fuel Vehicle Report: Fiscal Year 2002. Department of Commerce. 2002.
- U.S. Department of Transportation. *Fuel Options for Reducing Greenhouse Gas Emissions from Motor Vehicles*. Final Report September 2003.
- Department of Energy. *Alternative Fuel News* Vol.5-No.3 U.S.

- Langer, T., Williams, D. *Greener Fleets: Fuel Economy Progress and Prospects*. Report Number T024, American Council for an Energy-Efficient Economy. 2002.
- Tutt, E. *Diesel Engines Emission Reduction: California's Clean Air Strategy*. California Air Resources Board of U.S. 2003.
- Winter, C. *A Green Energy Strategy for Ontario*. The Conservation Council of Ontario. 2002.
- Bleviss, D. L. *Urban Transportation: Challenges Facing Latin America*. 1999.
- Sobti, G. S. *Indian Automotive Industry*. Office of Canadian High Commission, India. 2003.
- Bose, R. K. *Automotive energy use and emissions control: a simulation model to analyse transport strategies for Indian metropolis*. Tata Energy Research Institute, India. 1999.
- Wolf, J.F., Nordheimer, R.K. *BMW's Energy Strategy Promoting the Technical and Political Implementation*. SAE Technical Paper 2000-01-1324. 2000.
- Gustavsson, N. *Alternative Fuels Environmental Care as VCC Core Value*. Volvo Car Corporation. 2003.
- Suga, T., Muraishi, T., Brachmann, T., Yatabe, F. *Potential of a Natural Gas Vehicle as EEV*. SAE Technical Paper 2000-01-1863. 2000.
- Ishak A. *Urban Air Quality Management: Motor Vehicle Emission Control in Malaysia*. Paper No. 18. Clean Air Regional Workshop. 2001.
- PETRONAS NGV Sdn. Bhd. *Natural Gas for Vehicle (NGV)*. Kuala Lumpur. 1996.

- Leong, C.F. “*Instructions for Assembly of Compressed Natural Gas Equipment on a Vehicle*” Tractors Malaysia. 1996.
- Tartarini Automotive. *Instructions for the Assembly of CNG Equipment on a Vehicle*. Italy. 1982.
- Chen, J.L., Chen, G. *Flow and Structural Analysis for Fuel Pressure Regulator Performance*. SAE Technical Paper 950073. 1995.
- Kalam, M. A., Masjuki, H. H, Maleque, M. A., Amalina, M. A., Abdessalem, H. and Mahlia, T.M.I. *Air-Fuel Ratio Calculation for a Natural Gas-Fuelled Spark Ignition Engine*. SAE Technical Paper 2004-01-0640. 2004.
- IMPCO Technologies Inc. *Material Handling & Industrial Engine Gaseous Fuel Training Manual*. 1998.
- Yaacob, Z., Majid, Z. A., Piau, M. P. K. I. A Study on Exhaust Emission, Performance and Lubricating Oil. *Jordan International Chem. Eng. Conference III*. 27-29 Sept. Amman, Jordan. 1999.
- Martin Philip King Ik Piau. *Development of natural gas fuel system for motorcycle with exhaust emission and performance comparison to gasoline*. Masters Thesis. Universiti Teknologi Malaysia. 2001.
- Piau, M. P. K. I. P, Yaacob, Z., Majid, Z. A., Mohsin, R: Development of Natural Gas Motorcycle in Malaysia. *Gasex 2000, Conference and Exhibition*. Pattaya, Thailand, 11-14th September 2000.
- Majid, Z. A., Yaacob, Z., Mohsin, R., Piau, M. P. K. I. Cleaner Emission From Natural Gas Powered Motorcycle. *Malaysian Science & Technology Congress’ 99*. Hilton Kuching, Sarawak, 8-10th Nov. 1999.

- Majid Z. A., Yaacob, Z., Piau, M. P. K. I. Natural Gas Motorcycle- Emission. *International Conference & Exhibition on Natural Gas Vehicle*. Yokohama, Japan, 17-20th October 2000.
- Majid, Z. A., Yaacob, Z., Yahya, M. A. A Comparison Study on Engine Oil Properties for Bi-Fuel Motorcycle. *Second World Engineering Congress 2002*, Sarawak, 22nd-25th July 2002.
- Whitehouse, R.C. *The Valve and Actuator User's Manual*. The British Valve and Actuator Manufacturers Association. Mechanical Engineering Publications Limited. 1993.
- Jury, F. D. *Fundamental of Gas Pressure Regulation*. Technical Monograph 27, Fisher Controls Company. 1972.
- Carlson, H. *Springs: Troubleshooting and Failure Analysis*. Marcel Dekker, Inc. 1980.
- Smith, B. and Vivian, B.E. *An Introductory Guide to Valve Selection*. Mechanical Engineering Publications Limited. 1995.
- Zappe, R.W. *Valve Selection Handbook: Engineering Fundamentals for Selecting Manual Valves Check Valves and Pressure Relief Valves*. Gulf Publishing Company. 1981.
- Lyons, J. L. *Lyons's Valve Designer's Handbook*. Van Nostrand Reinhold Company. 1982.
- Warring, R.H. *Spring Design and Calculation*. Model & Allied Publications Limited. 1973.
- Stanton, V. A. *The Best Spring Material for High Temperature. Spring Design and Application*. McGraw-Hill. Pg 314-318, 1961.

- Jury, F. D. *Fundamental of Three-Mode Controllers*. Technical Monograph 28. Fisher Control Company. 1973.
- Heenan, J.S. *Fuel System Pressure Control Improves NGV Performance*. SAE Technical Paper 960851. 1996.
- International Standard. *Road Vehicles- Compressed Natural Gas (CNG) Fuel System Components – Pressure Regulator*. ISO 15500 -9. 2001.
- Malaysian Standard. *Code of Practice for the Use of CNG Fuels in Internal Combustion Engines*, MS 1096. 1997.
- National Fire Protection Association. *Standard for Compressed Natural Gas (CNG) Vehicular Fuel Systems*. NFPA 52. 1984.
- Sun, X., Aia, A., Hussain, S. *A Dual-Fuel System for Motor Vehicles*. SAE Technical Paper 981356. 1998.
- Pan, C. P., Li, M.C., Hussain, S.F. *Fuel Pressure Control for Gaseous Fuel Injection Systems*. SAE Technical Paper 981397. 1998.
- Oothuizen, P. H. and Carscallen, W. E. *Compressible Fluid Flow*. McGraw Hill Inc. 1997.
- Versteeg, H. K. and Malalasekera, W. *An Introduction to Computational Fluid Dynamics, The Finite Volume Method*. Prentice Hall. 1995.
- Friend, D. G. Ely, J. F., Ingham, H. Thermophysical Properties of Methane. *J. Phys. Chem. Ref. Data* 1989. Vol. 18 No.2.
- Cain, T. *Spring Design & Manufacture. Workshop Practice Series Number 19*. Argus Books Limited. 1988.
- Society of Automotive Engineers. *Manual on Design and Application of Helical and Spiral Springs*. SAE HS 795. 1990.

Carlson, C.R.H. *Properties of Spring Materials and Allowable Working Stresses. Spring Design and Application*. McGraw-Hill. Pg 310-313; 1961.

The American Society of Mechanical Engineers. *ASME Boiler and Pressure Vessel Code, Section VIII Division*. 1977.

Blake, A. *Threaded Fasteners. What Ever Engineer Should Know Series Vol. 18*. Marcel Dekker, Inc. 1986.

Society of Automotive Engineers. *Mechanical and Material Requirements for Metric Externally Threaded Steel Fasteners*. SAE J1199. 2001.

Eakin, C.T. *High Temperature Creep of Coil Springs. Spring Design and Application*. McGraw-Hill. Pg 77-81; 1961.

Beckwith, J.B. *Flat Spring Material – Cost and Stress Factors. Spring Design and Application*: McGraw-Hill. Pg 122; 1961.

Dillon, C.P. *Corrosion Resistance of Stainless Steels*. Marcel Dekker Inc. 1995.

American Society of Testing Materials. *Standard Specification for Carbon and Alloy Steel Nuts [Metric]*. A 563 M. 2003.

Kalpakjian, S. *Manufacturing Engineering and Technology*. Addison Wesley Publishing Company. 1995.

APPENDIX

BI-FUEL ENGINE FUEL CONSUMPTION AND EMISSION RESULTS BASED ON NON-LOADED OPERATION

Rahmat, M., Zulkefli, Y., Shameed, A.

Gas Engineering Department
Faculty of Chemical and Natural Resources Engineering
Universiti Teknologi Malaysia
81310 UTM Skudai, Johor Darul Takzim, Malaysia.

ABSTRACT

Alternative fuels for the internal combustion engines are introduced as an improved fuel over mainstream fuels such as petrol and diesel. Compressed Natural Gas (CNG) is the most successful and widely used alternative fuels that helps mitigate emission problem caused by vehicles. Mainstream fuelled vehicles are fitted with a conversion kit to enable the operation with CNG, these converted vehicles are called Natural Gas Vehicles. A bi-fuel engine test rig was fabricated using a 1500cc 12 Valve engine fitted with a Landi Renzo conversion kit enabling operations on petrol and natural gas. This test rig was used to conduct experiments to obtain the fuel consumption and the corresponding exhaust emission quality. The results obtained were compared with the actual NGV taxi using a Tartarini conversion kit for validation purpose. The findings from this experimental rig form a comparison between the use of petrol and natural gas as fuel for vehicles. The results clearly prove that the use of natural gas provides better exhaust emission at lower cost.

Keywords: NGV, bi-fuel engine, fuel consumption, exhaust emission.

Bahanapi alternative diperkenalkan sebagai bahanapi yang lebih baik untuk menggantikan bahanapi konvensional seperti petrol dan diesel. Gas Asli Termampat merupakan bahanapi alternative yang paling berkesan dan digunakan diseluruh dunia. Pembakaran gas asli yang lebih bersih dari bahanapi utama lain dapat mengurangkan pencemaran udara akibat kenderaan. Kit pengubahsuaian perlu dipasang untuk membolehkan kenderaan untuk berfungsi menggunakan gas asli. Bagi menguatkan pemahaman ke atas system dwi-bahan, rig pengujian engine menggunakan injin 1500 cc 12 Injap yang dilengkapi dengan kit Landi Renzo telah dihasilkan. Rig ujikaji ini digunakan untuk mendapatkan kadar keperluan bahanapi dan pembebasan eksos pada kelajuan injin yang pelbagai. Keputusan yang diperolehi dibandingkan dengan hasil yang diperolehi menggunakan kit tartarini untuk memastikan kesahihan keputusan. Hasil ujikaji ini membuktikan bahawa penggunaan gas asli sebagai bahanapi dapat mengurangkan pencemaran udara dan mengurangkan kos.

Katakunci: NGV, enjin dwi-bahanapi, kadar penggunaan bahanapi, pembebasan Ekzos.

1 INTRODUCTION

The introduction of Compressed Natural Gas (CNG) as an alternative fuel in Malaysia was supported by various factors that include; the abundant local natural gas reserve, the availability of Peninsular Gas Utilization distribution system (PGU) infrastructure, and the clean burning property of natural gas. The typical petrol operated mono-fuel vehicle is fitted with an imported conversion kit enabling bi-fuel capabilities of petrol and CNG. Two authorised conversion kit installers in Malaysia are Tractors Malaysia and OGPP that supply Tartarini NGV and Landi Renzo conversion kits respectively. These imported Natural Gas Vehicle (NGV) conversion kits are exempted from import duty and sales tax to encourage vehicle user to convert the engine into bi-fuel system. Road tax is reduced from the existing level by 50% for Mono-fuel (operating only on one fuel i.e. natural gas) and 25% for bi-fuel (operating on two types of fuel, one at a time) and dual- fuel (operating on both fuels forming a mixture of fuel).

The Petronas is the only fuel retailer that offers CNG to NGV users. There are two types of NGV station called “mother station” and “daughter station”. The “mother station” type has a natural gas pipeline to its premises where the gas is compressed to 3600 psig via three stage compressor system and stored in a cascading storage system. The cascading storage systems are made portable enabling it to be moved to the “daughter station”. The daughter station supplies customers from the cascading storage system charged at the “mother station”. This is done by transferring the CNG from the cascading storage to the vehicle’s onboard storage cylinder thru the CNG dispenser unit.

Petrol is priced at RM 1.36 per litre where as one litre of natural gas is priced at RM 0.585, making it the cheapest commercial fuel available in the market. The litre measurement used to describe the CNG pricing is proven by calculations shown in the appendix that it is actually litres energy equivalent to petrol. Due to the energy equivalent factor, the energy within the natural gas bought for RM 0.565 is the same as the energy content within 1 litre of petrol at RM 1.34. It is known from reference that 1 litre of petrol has approximately 30.676 MJ of energy [1]. The energy content of Malaysian natural gas is 1053 Btu per cubic ft [2] which translates to 0.9574 MJ per mol of natural gas. From experiments conducted, one 55 litre water capacity tank would accommodate approximately RM 7 worth of natural gas. The energy content of this fully charged tank is predicted as 380 MJ by the energy content calculations (shown in appendix A). The value is then divided with the energy content per mol of natural gas to obtain 397 moles of natural gas per charge of a 55 litre cylinder. The petrol cost for similar amount of energy would sum up to RM 16.60, giving savings up to RM 9.60 for every charge of the NGV tank.

The amount of moles within the NGV cylinder as predicted by the energy content calculation is validated using PV relations based on thermodynamic principles. The generalized correlation for gases by Pitzer [3], Benedict/Webb/Rubin [4], and results obtained from Friend *et al* [5] are compared to obtain the best prediction of mol content within the storage cylinder. The findings by Friend *et al*, is comparatively the most accurate method and proves similar value with the Benedict/Webb/Rubin method until the designed CNG operating pressure of 3000

psig. The Pitzer correlation deviates greatly at 353 K and 3000 psig from both friend et al and Benedict/Webb/Rubin methods.

Referring to MS 1096, the cylinder temperature would rise up to 80°C (353 K) during charging [7]. This internal temperature increase during charging depends on the cylinder's material of construction that has different heat dissipation abilities. The storage capacity of a cylinder is inversely related to the internal temperature during fast fill. CNG cylinders constructed primarily from steel (NGV Type 2) employed on the system under study provides the most cost effective storage capabilities [6]. The graph displayed by friend et al and Benedict Webb Rubin clearly shows that 400 moles within the cylinder would generate an internal pressure of 2700 psig at 353 K. This value corresponds to the value obtained during the experimental charging done with an empty cylinder. The storage internal pressure is unable to reach the designed operating pressure of 3000 psig during charging due to the temperature compensating mechanism included in the CNG dispenser. Currently most commercially available CNG dispensers rely on a mathematical model or algorithm utilizing the measured temperature of the gas flowing in the dispenser to determine full charge pressure [6]. This safety mechanism helps avoid extreme internal pressure build up caused by heat within the vehicle during extreme weather.

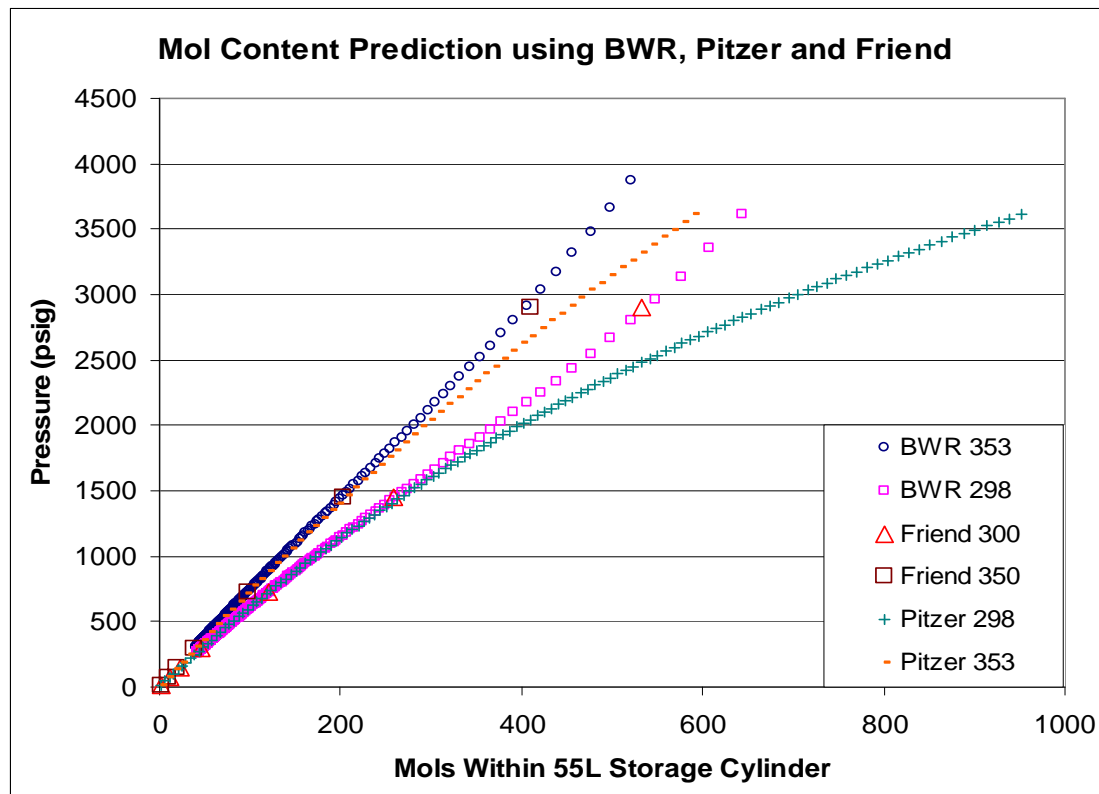


Figure 1.0: Comparison between Mol content of Natural Gas within Storage Cylinder at 298.15 K and 363.15 K internal temperature.

Apart from these calculations conducted to estimate the gas content within the cylinder, the fuel consumption and the corresponding exhaust emission are attained thru experiments conducted on the bi-fuel test rig. A used 1.5 litre 12 Valve Carburettor Proton engine was serviced and fitted with a newly imported Landi Renzo

conversion kit to form the bi-fuel engine test rig. This helps establish a comprehensive understanding on the existing bi-fuel engine fuel system widely implied on local taxis.

2 THE BI-FUEL ENGINE TEST RIG

The engine test rig has three mounting points that are made adjustable in both horizontal and vertical direction to aid the alignment of the engine onboard the rig. These movable mounting points would allow the engine rig to cater for other engines with similar size. The four poles around on the main structure is design to hold the closure panel to ensure safety of operator from the moving parts of the engine. Wheels are attached to the rig to ease manoeuvring and to aid the dampening of the engine vibration during operation. The rig metal structure is coated with epoxy (powder coating) to avoid corrosion caused by extreme working conditions. The installation of the NGV fuel system was based on the MS 1096 and NFPA 52.

Graphical representation of the main structure used to support the engine and other equipments are as shown in Figure 2.0. Two separate skids are made to hold the NGV storage cylinder and the engine respectively. Figure 3.0 displays the control panel used to hold other components such as the petrol tank, the switches and sensors in place. Figure 4.0 depicts the bi-fuel system where the petrol from the tank is drawn and sent to the carburettor through a petrol solenoid valve. The return hose from the petrol pump is used to send access petrol to the storage tank during the NGV operation. The NGV system can be seen where the high pressure CNG is sent to the pressure regulator via high pressure tubing. Low pressure natural gas from the pressure regulator is then sent to the mixer beneath the air filter using a low pressure hose. Figure 5.0 presents the rig setup equipped with closure panels and extended exhaust pipe for operation.

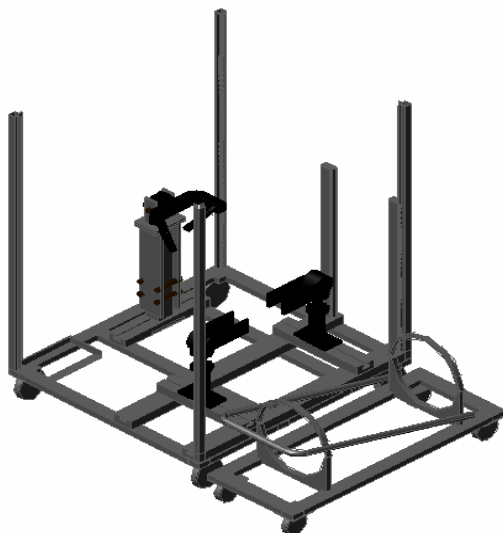


Figure 2.0: Main Engine Mounting Frame

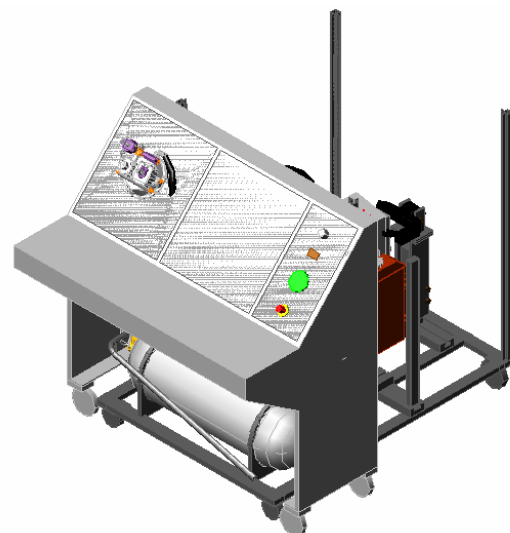


Figure 3.0: Test rig equipped with control panel

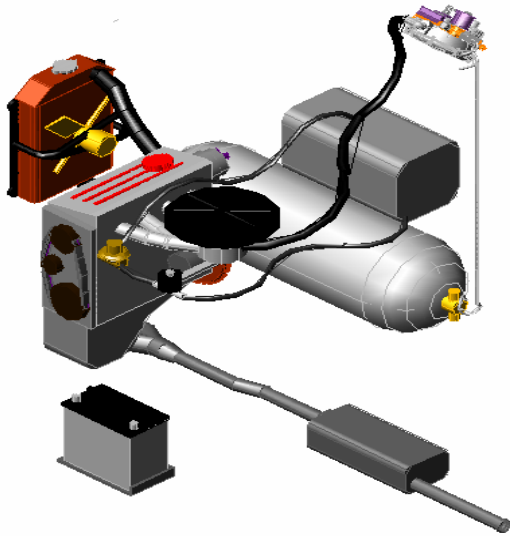


Figure 4.0: Bi-fuel Fuel Systems

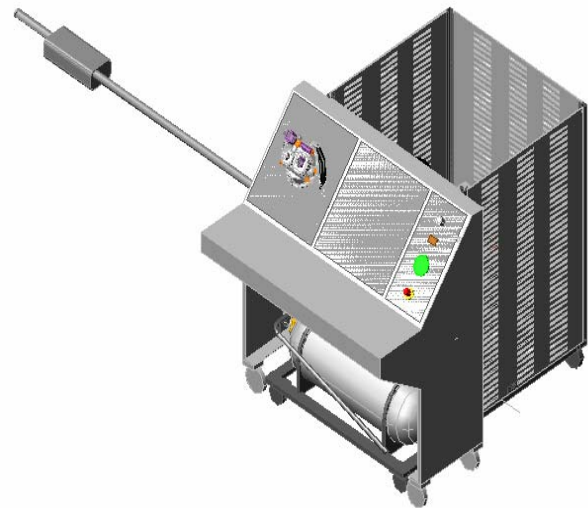
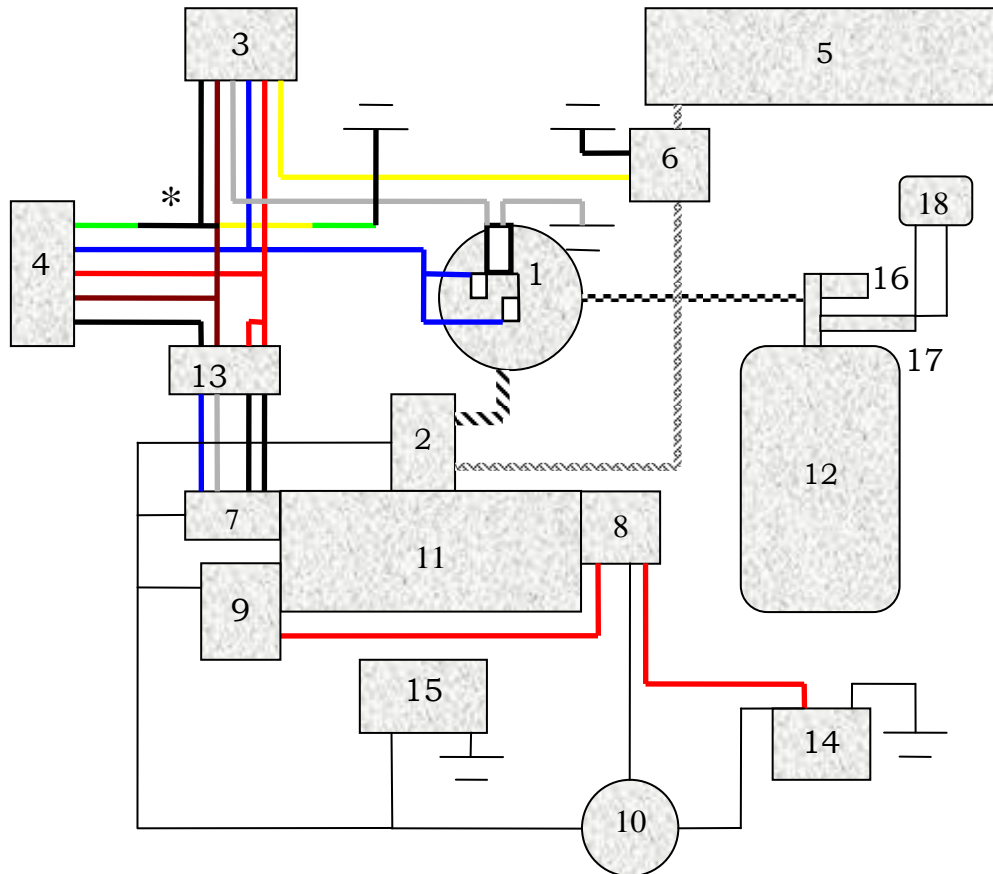


Figure 5.0: Engine Test Rig for Operation

The engine components were assembled and wired according to Figure 6.0. When the ignition key is turned to I.G point (ignition - engine starting position), the current from the battery will be supplied to the various components such as the carburettor, radiator fan, spark distributor, and alternator. The voltage of the current is magnified by the ignition coil at the spark distributor to provide suitable voltage for the operation of spark plug. The distributor provides the spark for the combustion to take place according to the engines preset firing order. Current supplied to the petrol solenoid within the carburettor will allow fuel from the petrol pump to enter the carburettor to form combustible mixture with air. The fuel from the petrol tank is drawn by the petrol pump actuated by the movement of the cam shaft caused by the movement of pistons. Excess petrol from the petrol pump will be sent to the petrol tank thru the fuel return line. The alternator is used to recharge the battery and to supply power to other components on board the car such as car lamp, radio which are not relevant in our study.

When the ignition is turned to start, the current from the battery is supplied to the starter motor which cranks the engine. This will begin the four stroke combustion cycle (intake, compression, power, exhaust) within the engine block which is perpetual depending on the supply of fuel; air and electric current are supplied. The engine is turned off by cutting the current supply from the battery thru the ignition key. The distributor is unable to supply current to form spark within the combustion chamber. This would cause the petrol solenoid to block the petrol from entering the carburettor. The conversion kit employed on this test rig is only suitable for the carburetion type internal combustion engine. The conversion kit produced by Landi Renzo comprises of a fuel selector switch, step 51 (spark advancer), mixer, pressure regulator and petrol solenoid. The electrical wiring for the conversion kit is shown in the Figure 6.0. The completely assembled conversion kit would enable the operator to switch between fuels thru the fuel selector switch with ease.



No	Component	No	Component
1	Pressure Regulator	2	Carburettor
3	Fuel Selector Switch	4	Spark Timing Advancer
5	Petrol Tank	6	Petrol Solenoid
7	Spark Distributor	8	Starter Motor
9	Alternator	10	Ignition Key
11	Engine Block	12	NGV Storage Cylinder
13	Wire Connection block	14	Battery
15	Radiator Fan	16	Refuelling Receptacle
17	Pressure Sensor	18	Pressure Display Unit
	Petrol Line		CNG High Pressure Tubing
	N.G. Low Pressure Tubing		Ground
	Typical Common Wire		High Current Wire
*	All the other coloured wires belong to the NGV fuel system wiring		

Figure 6.0: Bi-fuel Engine Rig Set Up

When this is done, the petrol solenoid will block the flow of the petrol to the carburettor. While this occurs, current is supplied to open the built in NGV solenoid valve on the pressure regulator to permit gas flow from the storage tank. High pressure tubing is used to channel the CNG from the storage cylinder to the pressure

regulator. At the regulator, gas is regulated according to the requirement of the engine and sent to the mixer through the low pressure tubing. The natural gas fuel demand of the engine is sensed using the vacuum pressure generated by the air flow thru the mixer. This vacuum pressure generated by the mixer acts on the 3rd stage diaphragm of the regulator to provide greater fuel flowrate. The spark advancer is activated during engine operation with gas to alter the spark sequence to suit the combustion of CNG which varies from petrol. The mixer placed beneath the air filter not only detects fuel flow but also promotes the mixing between natural gas and air to improve combustion.

3 METHODOLOGY

The engine RPM was gauged using an infrared tachometer installed at the flywheel. The engine RPM was varied by manipulating the throttle opening at the carburettor. The engine RPM was held at a constant value while the fuel consumption and fuel emission was carried out. The petrol consumption was measured by combining a measuring cylinder and a stopwatch that provided the rate of fuel volume consumed by the engine at constant engine RPM. The corresponding exhaust emission of the engine was also acquired simultaneously at the same engine RPM. Several runs were conducted for each engine RPM to ensure the repeatability of the result obtained. The engine RPM was increased by 1000 from 1000 to 5000 in order to obtain the fuel consumption and emission behaviour of the bi-fuel engine.

Similar test was conducted to obtain the natural gas consumption and the emission generated at different engine RPM. The method used to measure the natural gas consumption is based on the fact that the storage cylinder pressure will deplete proportionally to the moles of gas consumed at constant engine RPM. Higher engine RPM would consume more fuel causing greater rate of pressure depletion within storage cylinder. The relation between the storage pressure and mol content of gas within the tank is established using suitable thermodynamic equation incorporating the compressibility factor. The time taken for the pressure drop will be used to calculate the mol flowrate of gas consumed. The fuel consumption and corresponding emission result for both petrol and natural gas are displayed in the following section.

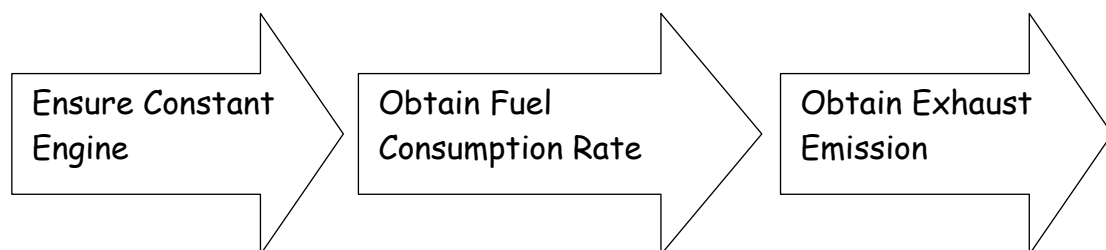


Figure 7.0: Methodology arranged in sequence for each engine RPM.

4 RESULTS & DISCUSSION

4.1 Fuel Consumption Result

The emission results from this bi-fuel test rig operating on natural gas were compared with the results obtained by Tractors Malaysia that carried out tests based on a similar engine fitted with a Tartarini NGV conversion kit. The unburned hydrocarbon values of 50-60 ppm discharged at 2500 RPM by the Tartarini fuel system (shown in the appendix B) is similar to the results obtain using the fuel system understudy (Figure 11.0). The rig understudy releases 0.1 % CO (Figure 12.0) which is much lower then the results from the tartarini fuel system that releases 0.3-0.5% CO (Appendix B). This is caused by the spark advancer employed in the landi renzo kit understudy but not applied in the tartarini system. This comparison between the only two types of NGV fuel system authorised to be installed in similar 1500 cc 12 valve engine taxis proves the validity of the result of the study. Other results obtained from the test engine understudy are displayed and discussed in the following paragraphs.

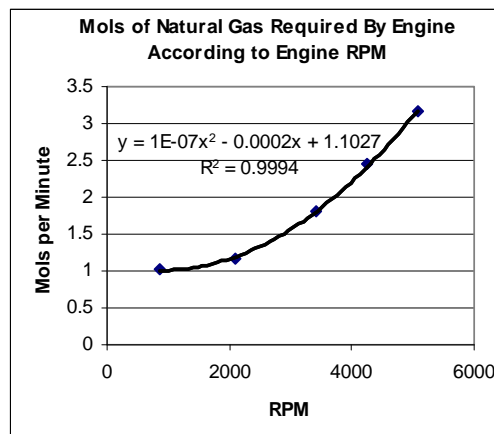


Figure 8.0: Moles of Natural Gas Required By Engine According to Engine RPM

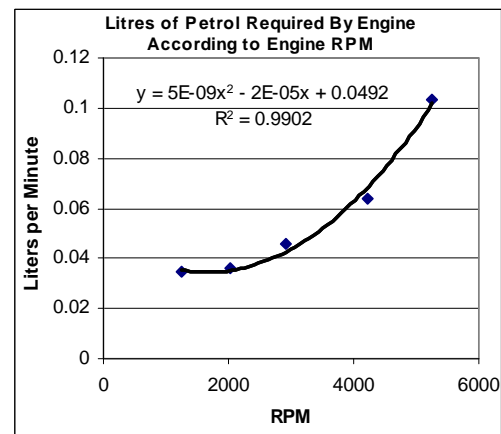


Figure 9.0: Litres of Petrol Required By Engine According to Engine RPM.

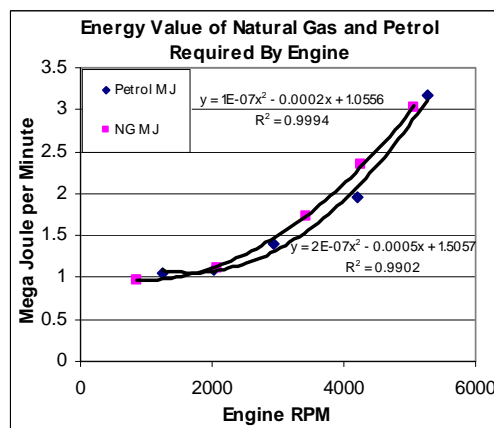


Figure 10.0: Energy Value of Natural Gas and Petrol Required By Engine

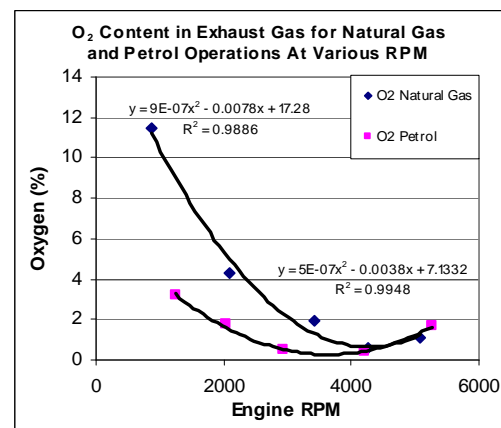


Figure 11.0: Oxygen Content in Exhaust Gas for Natural Gas and Petrol Operations at Various RPM

The natural gas and petrol consumption at the corresponding engine crankshaft revolutions (RPM) are displayed in Figures 8.0 and 9.0 respectively. Both the graphs display similar pattern indicating the engines intrinsic fuel requirement to generate the desired engine RPM. Since the fuel is in different phases, comparisons are done by converting the fuel in terms of energy content (similarly done in appendix A) as shown in Figure 10.0. The average engine energy requirement is obtained between the natural gas energy supply and the petrol energy supply to the engine. This average value may come in handy with future works on alternative fuel system design.

The percentage of oxygen content of the exhaust gas is obtained using the emission analyser and plotted in figure 11. The exhaust oxygen content graph displays the lowest oxygen content within the region of 3500 engine RPM for the natural gas operation and 4200 engine RPM for the petrol operation. The most effective combustion occurs within this the minimal oxygen concentrated regions. This effective combustion would cause very low values of unburned hydrocarbon content in the exhaust gas. Figure 13.0 depicts minimal unburned hydrocarbon values around 3000 RPM for the natural gas operation and 3500 RPM for the petrol operation. This slightly differs from the optimum combustion point described by the exhaust oxygen content in figure. This phenomenon is caused by the intake volumetric efficiency which alters the air to fuel ratio.

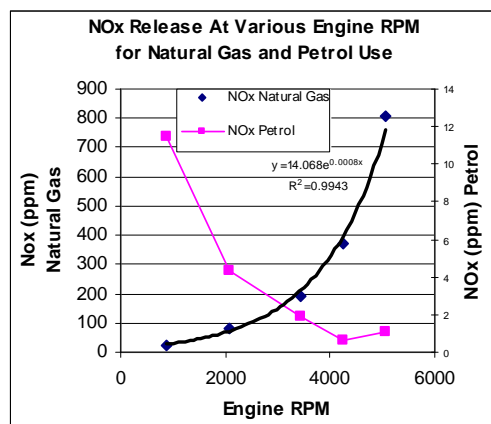


Figure 12: NOx Content in Exhaust Gas at Resulting Engine RPM

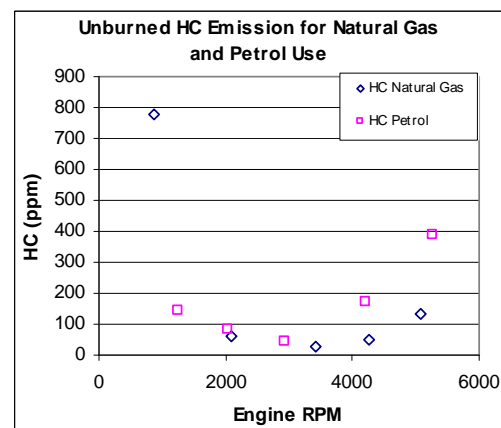


Figure 13: Unburned Hydrocarbon Content in Exhaust Gas at Parallel Engine RPM

The formation of nitrogen oxides are caused either by the combustion itself or the heat of combustion called thermal NOx. Figure 12.0 describes that the formation of NOx during petrol operation decreases with engine RPM. This proves that the NOx is formed due to the poor combustion and mixing factors. As the engine RPM increases, better combustion and mixing causes the NOx formation to decrease. The situation is inversed in the natural gas operation. This occurrence is caused by the formation of thermal NOx, as the operation with natural gas would cause higher exhaust temperature. This temperature increases with the engine RPM as the rate of combustion and exhaust air emission increases.

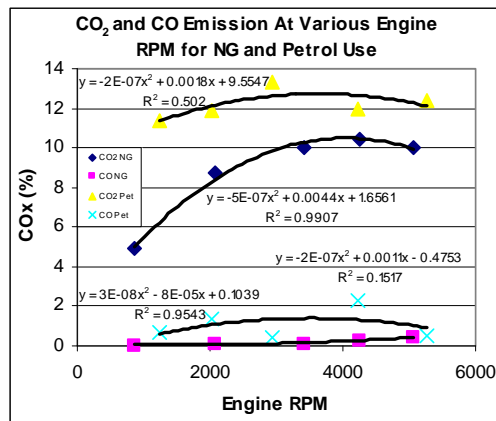


Figure 14.0: CO₂ and CO Content in Exhaust Gas at Relevant Engine RPM

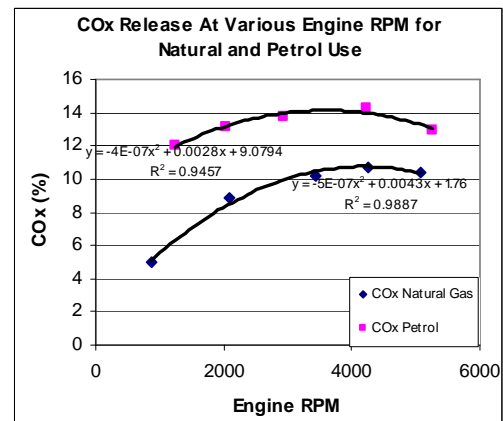


Figure 15.0: CO_x Content in Exhaust Gas at Related Engine RPM

Carbon based emission gases are unavoidable due to the use of carbon based fuels. The formation of carbon monoxide is less favourable compared to carbon dioxide due to its impact on human health. Figure 15.0 portrays that the use of natural gas as fuel decreases the total carbon based emission gas compared with petrol operation. The break down of the carbon based exhaust emission is shown in Figure 14.0 as carbon monoxide and carbon dioxide. Carbon monoxide released by petrol operation is much greater compared to the use of natural gas. The discharge of carbon dioxide is also greater with the use of petrol compared to natural gas.

5 CONCLUSION

The results obtained from the bi-fuel test rig have achieved its objective to provide a comprehensive understanding of the existing bi-fuel system existing in Malaysia. The emission data obtained has clearly proven that the use of natural gas is much more favourable compared to the use of petrol. The fuel cost calculations shown in the introduction has proven that natural gas is not only cleaner burning fuel but also cheaper than the existing mainstream fuels. Most effective combustion occurs at 3500 engine RPM during operation with natural gas and at 4200 engine RPM for the operation with petrol.

6 ACKNOWLEDGEMENT

Authors would like to extend gratitude to the Ministry of Science Technology and Innovation (MOSTI) for the financial support under Vot 74169. Special thanks dedicated to the Research Management Centre (RMC), UTM for the kind assistance and support during the tenure of research. To those involved directly and indirectly to this project, authors are deeply indebted.

7 References

1. "Perry's Chemical Engineers' Handbook" 1997. 7th ed. McGraw-Hill, Inc. 2-195.
2. Gas Malaysia Sdn. Bhd., <http://www.gasmalaysia.com>.
3. Smith, J.M., Van Ness, H.C., Abbott, M.M. 1996. "Introduction to Chemical Engineering Thermodynamics". 5th ed., McGraw-Hill, Inc. 85-93.

4. Cengel, Y. A. & Boles, M.A. "Thermodynamics an Engineering Approach, 3rd ed., McGraw Hill, 1998.
5. Friend, D. G., Ely, J. F., Ingham, H. 1989. "Thermophysical Properties of Methane". *J. Phys. Chem. Ref. Data*. Vol. 18, No.2.
6. Diggins, D.D, "CNG Fuel Cylinder Storage Efficiency and Economy in Fast Fill Operations", SAE Technical Paper 981398, 1998.
7. MS 1096, 1997. "Code of Practice for the Use of CNG in Internal Combustion Engines". Department of Standards Malaysia.
8. MS 1024, 1986. "Specification for Wheel Nuts for Passenger Vehicles". Department of Standards Malaysia.
9. NFPA 52-1984. "Compressed Natural Gas (CNG) Vehicular Fuel Systems". National Fire Protection Association.
10. Leong, C.F., 1997. "Training Manual on NGV", Tractors Malaysia Sdn Bhd.

8 APPENDIXES

Appendix A

- a) From the ideal gas law we know one mole of gas would occupy the following volume at room temperature.

$$v = \frac{RT}{P} = \frac{8.314 \frac{\text{kPa} \cdot \text{Liter}}{\text{mol} \cdot \text{K}} \times 298 \text{K}}{101325 \text{Pa}} = 24.45 \text{Litres}$$

- b) Energy content of Natural Gas

$$1053 \frac{\text{btu}}{\text{cft}} \times \frac{1 \cdot \text{cft}}{28.31684659 \cdot \text{Litre}} \times \frac{24.4 \cdot \text{litre(at298K)}}{1 \cdot \text{mol}} \times \frac{1 \cdot \text{MJ}}{947.8169879 \cdot \text{btu}} = 0.9573 \cdot \frac{\text{MJ}}{\text{mol}}$$

- c) Energy content of 1 Litre of petrol (estimate 1)

$$\frac{0.69 \cdot \text{kg}}{1 \cdot \text{Litre}} \times \frac{1000 \cdot \text{g}}{1 \cdot \text{kg}} \times \frac{1 \cdot \text{mol}}{114.23 \cdot \text{g}} \times \frac{5.07 \times 10^6 \text{ J}}{1 \cdot \text{mol}} \times \frac{1 \cdot \text{MJ}}{1 \times 10^6 \text{ J}} = \frac{30.625 \cdot \text{MJ}}{1 \cdot \text{Litre}}$$

- d) Energy content of 1 Litre of petrol (estimate 2)

$$1 \cdot \text{Litre} \times \frac{1 \cdot \text{mol}}{0.165 \cdot \text{Litre}} \times \frac{5.07 \times 10^6}{1 \cdot \text{mol}} \times \frac{1 \cdot \text{MJ}}{1 \times 10^6} = \frac{30.727 \cdot \text{MJ}}{1 \cdot \text{mol}}$$

- e) Energy within a 55 Litre NGV cylinder charged for RM 7

based on RM 0.565 NGV = RM 1.34 = 30.676 MJ

$$\frac{RM 7}{cylinder} \times \frac{30.625 \cdot MJ}{RM 0.565} = \frac{379.425 \cdot MJ}{cylinder}$$

f) Mol content within a cylinder based on energy per mol of natural gas.

$$\frac{379.425 \cdot MJ}{cylinder} \times \frac{1 \cdot mol}{0.9573 \cdot MJ} = \frac{396.35 \cdot mol}{cylinder}$$

Appendix B

Compiled By Leong Chok Fong
Group Training Manager
11th April 1997

Emission Reference Chart

<u>Gasoline</u>	<u>HC RPM</u>	<u>CO%</u>
Non-Catalyst : Idle	300	2.5-3.0
Catalyst : Idle	30-100	0.2-0.5
Non-catalyst @ 2,500 RPM No Load	100	0.5-1.5
Catalyst @ 2,500 RPM No Load	20-30	0.5-1.5
Non-Catalyst Full Load*	50-70	0.5-1.5
Catalyst Full Load*	10-20	0.1-0.2
<u>Natural Gas</u>	<u>HC RPM</u>	<u>CO%</u>
Non-Catalyst : Idle	100-150	0.5-1.0
Catalyst : Idle	20-50	0.1-0.3
Non-catalyst @ 2500 RPM No Load	50-60	0.3-0.5
Catalyst @ 2500 RPM No Load	20-30	0.1-0.3
Non-catalyst: Full Load*	10-20	0.1-0.2
Catalyst Full Load*	10-20	0.1-0.2

*full throttle @ 80 KMH on Dynamometer:

2 nd gear Automatic	3 or 4 speed
2 nd gear Manual	3 speed
3 rd gear Manual	4 or 5 speed.

Note : The above chart is for reference purpose only.